

The SIAM logo is displayed in a stylized, lowercase font within a dark green horizontal bar at the top of the page.

siam

7th Annual Meeting of the Bulgarian Section of SIAM
December 19-20, 2012
Sofia

BGSIAM⁴12

PROCEEDINGS

HOSTED BY THE INSTITUTE OF MATHEMATICS AND INFORMATICS
BULGARIAN ACADEMY OF SCIENCES



7th Annual Meeting of the Bulgarian Section of SIAM
December 19-20, 2012
Sofia

BGSIAM'12

PROCEEDINGS

HOSTED BY THE INSTITUTE OF MATHEMATICS AND INFORMATICS
BULGARIAN ACADEMY OF SCIENCES

7th Annual Meeting of the Bulgarian Section of SIAM
December 19-20, 2012, Sofia

BGSIAM'12 Proceedings

©BGSIAM'12

ISSN:1314-7145

Printed in Sofia, Bulgaria

PREFACE

The 7th Annual Meeting of Bulgarian Section of SIAM (BGSIAM) took part on December 19 and 20, 2012 and was hosted by the Institute of Mathematics and Informatics, Bulgarian Academy of Sciences, Sofia. The conference support provided by SIAM, as the major international organization for Industrial and Applied Mathematics, is very highly appreciated.

The Bulgarian Section of SIAM was founded on January 18, 2007 and the accepted Rules of Procedure were officially approved by the SIAM Board of Trustees on July 15, 2007. The activities of BGSIAM follow the general objectives of SIAM, as established in its Certificate of Incorporation. The role of SIAM is very important for promotion of interdisciplinary collaboration between applied mathematics and science, engineering and technology in the Republic of Bulgaria.

During the 7th Annual Meeting of BGSIAM (BGSIAM'12) a wide range of problems concerning recent achievements in the field of industrial and applied mathematics were presented. Following the established tradition, the conference provided a forum for exchange of ideas between scientists, who develop and study mathematical methods and algorithms, and researchers, who apply them for solving real life problems.

More than 50 participants from universities, institutes of the Bulgarian Academy of Sciences and also from outside the traditional academic departments took part in BGSIAM'12. They represent most of the strongest Bulgarian research groups in the field of industrial and applied mathematics. We are very glad to report that young researchers and students presented talks during BGSIAM'12. Organization of such sessions for young researchers is the main goal of BGSIAM in our conferences.

LIST OF INVITED LECTURES:

- RAITCHO LAZAROV
Department of Mathematics, Texas A&M University, College Station, USA
ANALYSIS OF FINITE ELEMENT APPROXIMATIONS OF FRACTIONAL
ORDER DIFFERENTIAL EQUATIONS
- TODOR GRAMCHEV
Department of Mathematics, University of Cagliari, Italy
GLOBAL NORMAL FORMS OF PERTURBATIONS OF THE HARMONIC
OSCILLATOR
- VLADIMIR VELIOV
Department of Mathematics, Vienna University of Technology, Austria Vienna,
Austria
METRIC REGULARITY, STABILITY AND APPROXIMATIONS IN OPTI-
MAL CONTROL

- NIKOLAJ KUTEV
Institute of Mathematics and Informatics, Bulgarian Academy of Sciences, Bulgaria
EQUATION OF ANISOTROPIC DIFFUSION AND APPLICATION TO IM-
AGE PROCESSING

The present volume contains proceedings of the conference talks: Invited Lectures (Part A), Contributed Talks (Part B) and List of Participants (Part c).

Angela Slavova
Chair of BGSIAM Section

Geno Nikolov
Vice-Chair of BGSIAM Section

Krassimir Georgiev
Secretary of BGSIAM Section

Sofia, December 2012

CONTENTS

Part A: Invited Lectures

Todor Gramchev, Giorgia Tranquilli

**Global Normal Forms of Perturbations of
the Harmonic Oscillator** 1

B. Jin, J. Pasciak, R. Lazarov, and Z. Zhu

**Analysis of Finite Element Approximations
of Fractional Order Differential Equations** 7

Nikolay Kutev

**Anisotropic Diffusion and Applications to Image
Processing** 9

Vladimir Veliov

**Metric Regularity, Stability and
Approximations in Optimal Control** 15

Part B: Contributed Talks

Gregory Agranovich, Elena Litsyn, Angela Slavova
Stabilizing Effects of Chaotic CNN Models 17

Ana Avdzhieva, Geno Nikolov
**Numerical Computation of Gaussian Quadrature
Formulae for Spaces of Cubic Splines with
Equidistant Knots** 28

Danail Brezov, Clementina Mladenova, Ivailo Mladenov
On the Factorization of Rotations 39

Nina Dobrinkova, Nikodim Lazarov, Valentin Marinov
**Sofia Municipality Features in GOES Project
System Implementation** 49

<i>Stefka Fidanova, Pencho Marinov</i> Influence of the Number of Ants on Mono-Objective Ant Colony Optimization Algorithm for Wireless Sensor Network Layout	59
<i>Vladimir Gerdjikov</i> New Spinor Models in Two Dimensions with Z_2-Reductions	67
<i>Rossen Ivanov, Tony Lyons</i> On the Peakon and Soliton Solutions of an Integrable PDE with Cubic Nonlinearities	78
<i>Stoyan Kapralov, Valentina Dyankova</i> Modelling System with Discrete Events	89
<i>Virginia Kiryakova</i> The Special Functions - Classical and New, and Relations to Fractional Calculus	96
<i>Jordanka Paneva-Konovska</i> Comparison Between the Convergence of Power and Mittag-Leffler Series	111
<i>Maya Markova</i> CNN Computing of the Interaction of Fluxons in Modified sine-Gordon Equation	116
<i>Rosangela Sviercoski</i> Review on Analytical Approximation for the Generalized Laplace's Equation and Applications in Multiscale Modeling	125
<i>Yancho Todorov, Sevil Ahmed and Michail Petrov</i> Application of Fuzzy-Neural Modeling and Quadratic Programming for Model Predictive Control	136

PART A: INVITED LECTURES ¹

¹Arranged alphabetically according to the family name of the first author

GLOBAL NORMAL FORMS OF PERTURBATIONS OF THE HARMONIC OSCILLATOR

Todor Gramchev and Giorgia Tranquilli

Dipartimento di Matematica e Informatica
Università di Cagliari
via Ospedale 72, 09124 Cagliari, Italy
Emails: todor@unica.it, tranquilli@unica.it

Abstract. The main goal of the present work is to outline some recent investigations of some global regularity issues and spectral properties for second order (pseudo)differential operators of Shubin type, generalizing the harmonic oscillator. Our approach is based on the reduction to simpler normal forms by means of conjugations with transformations acting globally in weighted Sobolev spaces and , Gelfand–Shilov spaces.

Mathematics Subject Classification (2000). Primary 35S05; Secondary 47G30, 34M05, 37G05.

Keywords: harmonic oscillator, pseudodifferential operators, normal forms, Gelfand–Shilov spaces

1 Introduction and preliminaries

The main goal of the present work is to study classes of second order Shubin type pseudodifferential operators by global reduction to simpler (normal) forms. Our notion of normal form is based on (and motivated by) ideas in the recent works of M. Ruzhansky and M. Sugimoto [10] and M. Ruzhansky and V. Turunen [11], on the study of the global properties of (pseudo)differential operators in the context of the harmonic analysis and quantization.

We are also able to consider perturbations of non-self adjoint complex harmonic oscillators and to apply our approach for getting generalizations of some previous estimates due to E.B. Davies [5], [6]. In particular, we classify all second order globally elliptic (in the sense of Shubin) linear differential operators on the real line and compute explicitly the spectrum $\sigma(P)$ and the represent explicitly the eigenfunctions in the case $\sigma(P)$ is discrete. In that latter case, we are able to reduce to complex harmonic oscillator by means of transformations acting in the Gelfand–Shilov space $S_\mu^\mu(\mathbb{R})$, $\mu < 1$. Here the crucial ingredient for our approach is the body of the decay and the global regularity estimates in the Gelfand–Shilov spaces of the eigenfunctions of Shubin type operators (cf. Capiello, Gramchev, Rodino [2], [3]) and the fact that for $\mu < 1$ the Gelfand–Shilov spaces consist of restriction of suitable classes of entire functions of exponential type on the real line.

We recall that the Shubin type pseudodifferential operators, cf. M.A. Shubin [], generalize the Schrödinger harmonic oscillator operator

$$H = -\Delta + \|x\|^2, \quad (1)$$

appearing in Quantum Mechanics. The spectrum of H in $L^2(\mathbb{R}^n)$ is discrete with eigenvalues $\lambda = \lambda_k = \sum_{j=1}^n (2k_j + 1)$, $k = (k_1, \dots, k_n) \in \mathbb{Z}_+^n$ while eigenfunctions are the Hermite functions

$$H_k(x) = \prod_{j=1}^n \frac{1}{\sqrt{2\pi k_j!}} P_{k_j}(x_j) \exp(-|x|^2/2), \quad (2)$$

where $P_r(t)$ stands for the r -th Hermite polynomial. The main interest here comes historically from Quantum Mechanics, where the exponential decay of eigenfunctions has been intensively studied, starting from the fundamental work of S. Agmon [1] for $-\Delta + V(x)$ with general potentials or other second order elliptic operators. We point out that in general the results imply pointwise decay estimates for the eigenfunctions but not for their higher order derivatives. Consider the following example: given a positive integer k , the two functions

$$e^{-x^2} \quad \text{and} \quad \theta(x) = \exp(-x^2) (2 + \cos(\exp(\eta x^2))), \quad \eta > 0$$

satisfy the same type of pointwise estimates, both are restrictions of entire functions on the real line, however the k -th derivative of $\theta(x)$ is unbounded on \mathbb{R} provided $k \geq \eta$. Returning to the harmonic oscillator (1), we point out to the fact that the Hermite functions $H_k(x)$, $k \in \mathbb{Z}_+^n$, (2) are not only entire functions, but for every $\gamma \in]0, 1/2[$ there exists $A_\gamma > 0$ such that

$$|\partial_z^\alpha H_k(z)| \leq A_\gamma^{|\alpha|+|k|+1} (\alpha!)^{1/2} e^{-(1/2-\gamma)|z|^2}, \quad z \in \mathbb{C}^n, |\Im z| < \gamma |\Re z|, \alpha \in \mathbb{Z}_+^n, \quad (3)$$

The estimates (3) lead in a natural way to the idea that the appropriate functional framework to study simultaneously the decay and the global analytic Gevrey regularity is given by the spaces of Gelfand–Shilov type (cf. the classical book of Gelfand

and Shilov [7], see also [8]). We recall that $f \in S_\nu^\mu(\mathbb{R}^n)$, $\mu > 0$, $\nu > 0$, $\mu + \nu \geq 1$, iff $f \in C^\infty(\mathbb{R}^n)$ and there exist $C > 0$, $\varepsilon > 0$ such that

$$|\partial_x^\beta f(x)| \leq C^{|\beta|+1}(\beta!)^\mu e^{-\varepsilon|x|^{1/\nu}} \quad (4)$$

for all $x \in \mathbb{R}^n$, $\beta \in \mathbb{Z}_+^n$ or, equivalently, one can find $C > 0$ such that

$$\sup_{x \in \mathbb{R}^n} |x^\beta \partial_x^\alpha f(x)| \leq C^{|\alpha|+|\beta|+1}(\alpha!)^\mu (\beta!)^\nu, \quad \alpha, \beta \in \mathbb{Z}_+^n. \quad (5)$$

The bounds (4), (5) with $\mu < 1$ grant that f extends to \mathbb{C}^n as an entire function, with uniform estimates in neighbourhoods of the real axis, see [7] for precise statements. In particular, the Hermite functions in (2) belong to $S_{1/2}^{1/2}(\mathbb{R}^n)$.

We consider perturbation for 1D harmonic oscillator in the context of the following issue: given a second order globally elliptic linear differential operator, not necessarily self-adjoint, to investigate its spectral properties, the global regularity of the solutions of the resolvent equation $(P - \lambda)u = f$ in the weighted Sobolev spaces

$$Q^s(\mathbb{R}) = \{u \in S'(\mathbb{R}) : (-\Delta + x^2)^{s/2}u \in L^2(\mathbb{R})\}, \quad s \in \mathbb{R}$$

cf. [12], [8], and in the Gelfand–Shilov spaces $S_\nu^\mu(\mathbb{R})$ by reducing to simpler normal forms of perturbations with zero order pseudodifferential operators of Shubin type. Our approach follows ideas in [10] to reduce estimates in function spaces to normal forms.

Another goal of our investigations is to study non-self-adjoint perturbations of the harmonic oscillator on the real line. E.B. Davies has studied the non-self-adjoint harmonic oscillator cf. [5], [6]. The non-self-adjoint harmonic oscillator is the differential operator of the type

$$H_\omega u = -u'' + \omega x^2 u = D_x^2 + \omega x^2 u, \quad x \in \mathbb{R} \quad (6)$$

for some complex $\omega = \omega_1 + \omega_2 i \in \mathbb{C}$, $\omega_2 \neq 0$. The operator has compact resolvent and its eigenvalues are $\lambda_n = \sqrt{\omega}(2k+1)$, $k \in \mathbb{Z}_+$. The corresponding eigenfunctions are written explicitly. It was proved in that although the set of eigenfunctions is complete in the sense that its linear span is dense in $L^2(\mathbb{R})$, it does not form a (Riesz) basis. We propose reduction to normal forms and the study of the spectral properties of some perturbations of (6).

2 Statement of the main results

First we consider second order differential operators on the real line

$$P = D_x^2 + (\alpha x + \gamma)D_x + \beta x^2 + \delta x + r. \quad (7)$$

with $\alpha, \beta, \gamma, \delta \in \mathbb{C}$. We consider also perturbations of P with zero order pseudodifferential operators $b(x, D)$ of Shubin type cf. [12], [8] for more details on the pseudodifferential calculus

$$P_b = P + b(x, D), \quad (8)$$

where

$$b(x, D)u = \int_{\mathbb{R}} e^{ix\xi} b(x, \xi) \hat{u}(\xi) \overline{d\xi}, \quad \overline{d\xi} = (2\pi)^{-1} d\xi \quad (9)$$

$\hat{u}(\xi) = \mathcal{F}_{x \rightarrow \xi} u = \int_{\mathbb{R}} e^{-ix\xi} u(x) dx$ stands for the Fourier transform and the symbol $b(x, \xi) \in C^\infty(\mathbb{R}^2)$ satisfies the following estimates: for every $(k, j) \in \mathbb{Z}_+^2$ one can find $C > 0$ such that

$$|\partial_x^k \partial_\xi^j b(x, \xi)| \leq C \langle (x, \xi) \rangle^{-k-j}, \quad (x, \xi) \in \mathbb{R}^2, \langle z \rangle = \sqrt{1 + \|z\|^2}. \quad (10)$$

cf. [12], [8] for more details. We recall that P is called globally elliptic if the principal symbol satisfies the global ellipticity condition

$$\xi^2 + ax\xi + bx^2 \neq 0 \quad \text{for} \quad (x, \xi) \neq (0, 0). \quad (11)$$

We limit our attention to the standard quantization associating to the operator $b(x, D)$ the symbol $b(x, \xi)$ of order zero, with action of $b(x, D) : Q^s(\mathbb{R}) \mapsto Q^s(\mathbb{R})$, $s \in \mathbb{R}$. The first new assertion is the following one

Theorem 2.1. *The operator P is globally elliptic self-adjoint iff there exists a unitary transformation $M : L^2(\mathbb{R}) \mapsto L^2(\mathbb{R})$, which is isomorphism of $Q^s(\mathbb{R})$, $s \in \mathbb{R}$, $S_\nu^\mu(\mathbb{R})$, $\mu, \nu \geq 1/2$, satisfying*

$$M^* \circ P \circ M = D_x^2 + \omega x^2 + \lambda_0, \quad \omega = b - a^2/4 > 0 \quad (12)$$

for some $\lambda_0 \in \mathbb{R}$. Moreover, E has the following form

$$M = T_\theta \circ E_{-a/4, -b/2}, \quad \theta \in \mathbb{R} \quad (13)$$

$$T_\theta w(x) = w(x + \theta), \quad (14)$$

$$E_{c,d} w(x) = e^{i(\alpha x^2 + \beta x)} v(x) \quad (15)$$

Finally, we have

$$M^* \circ b(x, D) \circ M = \tilde{b}(x, D) \quad (16)$$

where the symbol $\tilde{b}(x, \xi)$ satisfies

$$\tilde{b}(x, \xi) \sim K_0 \sum_{j=0}^{\infty} \frac{\varkappa^j}{j!} D_\xi^{2j} b(x, -a/4x + \xi - b/2) \quad (17)$$

where $K_0, \varkappa \in \mathbb{C}$, can be written explicitly.

Remark 2.2. We point out that the transformation (respectively, the conjugation with) $E_{c,d}$ can be written as the FIO

$$E_{c,d} w(x) = \int_{\mathbb{R}} e^{i(\alpha x^2 + \beta x + x\xi)} \hat{v}(\xi) \overline{d\xi} \quad (18)$$

(respectively,

$$E_{\alpha,\beta} \circ b(x, D) \circ E_{\alpha,\beta}^* v(x) = \int_{\mathbb{R}^2} e^{i(\alpha(x^2-y^2)+\beta(x-y)+(x-y)\xi)} b(x, \xi) v(y) dy \, d\xi \quad (19)$$

with the phase function $\phi = \alpha x^2 + \beta x + x\xi$ (respectively, $\Phi = \alpha(x^2 - y^2) + \beta(x - y) + (x - y)\xi$) having quadratic growth with respect to space variable but satisfying, in view of the separation of variables, the sharp conditions on $L^2(\mathbb{R})$ boundedness in [9] for the phase function $\alpha x^2 + \beta x + x\xi$ having quadratic growth. Concerning the multidimensional Shubin operators, we stress that the study of the normal forms becomes more involved. For example, rotation terms of the type $x_2 D_{x_1} - x_1 D_{x_2}$ might appear. We address the multidimensional case in another work.

Next, we consider perturbations of non-self-adjoint harmonic oscillator (6)

$$L = D_x^2 + i\varepsilon x D_x + \omega x^2 + p D_x u + q x u, \quad (20)$$

where $\varepsilon \in \mathbb{R}$, $p, q \in \mathbb{C}$, $\omega = \omega_1 + \omega_2 i \in \mathbb{C}$.

First we propose reduction to a normal form of L by conjugation with automorphism of the Gelfand–Shilov spaces $S_\mu^\mu(\mathbb{R})$ provided $\mu < 1$.

Proposition 2.3. *Suppose that $\varepsilon = 0$. Then there exist a transformation L which is an automorphism of $S_\mu^\mu(\mathbb{R})$, $172 \leq \mu < 1$, such that*

$$E^{-1} \circ L \circ E = D_x^2 + \omega x^2 + r, \quad r \in \mathbb{C} \quad (21)$$

The transformation E has the form

$$Ew(x) = e^{a(x+b)} w(x+b) \quad (22)$$

for some $a, b \in \mathbb{C}$.

Remark 2.4. *We note that if $\Re a \neq 0$ or $\Re b \neq 0$ the transformation E is not defined on $L^2(\mathbb{R}^n)$ or $S_\mu^\mu(\mathbb{R})$ for $\mu \geq 1$. The crucial point for the requirement $\mu < 1$ is the fact that the all $f \in S_\mu^\mu(\mathbb{R})$ are restrictions on \mathbb{R} of entire functions and E acts continuously in $S_\mu^\mu(\mathbb{R})$ using equivalent topology for entire functions cf. [7].*

Finally, we propose a classification of the spectral properties of L in the case $\varepsilon \neq 0$.

Theorem 2.5. *The operator L (20) is globally elliptic if and only if*

$$\omega_2^2 + \omega_1 \varepsilon \neq 0, \quad \text{if } \omega_1 \leq 0. \quad (23)$$

Next, suppose that $\omega_1 > 0$. Then the operator L has discrete spectrum for all $\varepsilon \in \mathbb{R}$, $p, q \in \mathbb{C}$ and the eigenfunctions can be written explicitly.

Finally, let $\omega_1 \leq 0$. Then there exists $\varepsilon_0 > 0$ such that if $|\varepsilon| < \varepsilon_0$ the spectrum of L is discrete while for $|\varepsilon| > \varepsilon_0$ the spectrum of L coincides with \mathbb{C} .

The proofs rely on techniques for the study of Shubin (pseudo)differential operators in Gelfand–Shilov spaces and the complex analytic JWKB method. For more details cf. [4].

References

- [1] S. Agmon, *Lectures on exponential decay of second-order elliptic equations: bounds on eigenfunctions of N -body Schrödinger operators*. Math. Notes **29**, Princeton University Press, 1982.
- [2] M. Capiello, T. Gramchev, and L. Rodino, *Super-exponential decay and holomorphic extensions for semilinear equations with polynomial coefficients*. J. Funct. Anal. **237** (2006), 634–654.
- [3] M. Capiello, T. Gramchev, and L. Rodino, *Entire extensions and exponential decay for semilinear elliptic equations*. J. Anal. Math. **111** (2010), 339–367.
- [4] T. Gramchev and G. Tranquilli, Discrete representations and global properties in function spaces of Shubin type pseudodifferential operators, preprint, 2012.
- [5] E.B. Davies, Pseudo-spectra, the harmonic oscillator and complex resonances. R. Soc. Lond. Proc. Ser. A Math. Phys. Eng. Sci. **455** (1999), 585–599.
- [6] E.B. Davies and A.B.J. Kuijlaars, *Spectral asymptotics of the non-self adjoint harmonic oscillator oscillators*. Bull. London Math. Soc. **70** (2004), 420–426.
- [7] I.M. Gel'fand and G.E. Shilov, *Generalized functions, II*. Academic Press, New York, 1968.
- [8] F. Nicola, and L. Rodino, *Global pseudo-differential calculus on Euclidean spaces*, Birkhauser, Basel, 2010.
- [9] M. Ruzhansky and M. Sugimoto, *Global L^2 -boundedness theorems for a class of Fourier integral operators*. Comm. Partial Differential Equations **31** (2006), 547–569.
- [10] M. Ruzhansky and M. Sugimoto, *Smoothing estimates of evolution equations via canonical transforms and comparison*. Proc. London Math. Soc. **105** (2012), 393–423.
- [11] M. Ruzhansky and V. Turunen, *Pseudo-differential Operators and Symmetries. Background Analysis and Advanced Topics*. Birkhäuser, Basel 2010.
- [12] M. Shubin, *Pseudodifferential operators and spectral theory*, Springer Series in Soviet Mathematics, Springer Verlag, Berlin 1987.

ANALYSIS OF FINITE ELEMENT APPROXIMATIONS OF FRACTIONAL ORDER DIFFERENTIAL EQUATIONS

B. Jin, J. Pasciak, R. Lazarov, and Z. Zhu

Department of Mathematics, Texas A&M University,
College Station, TX-77843, USA, and
Institute of Mathematics and Informatics, Bulgarian Academy of
Sciences,
Sofia, Bulgaria
lazarov@math.tamu.edu

We consider the following two sets of problems of fractional order differential equations:

(1) Initial-boundary value problem for the fractional order parabolic equation for $u(x, t)$ for $T \geq t > 0$:

$$D_t^\alpha u - \Delta u = f, \quad \text{in } \Omega \quad u = 0 \quad \text{on } \partial\Omega \quad u(x, 0) = v(x) \quad \text{in } \Omega \quad (1)$$

where $0 < \alpha < 1$, Ω is a bounded polygonal domain in \mathbb{R}^d ($d = 1, 2, 3$) and $D_t^\alpha u$ is the left-sided Caputo fractional derivative.

(2) The eigenvalue problem: find u and $\lambda \in \mathbb{C}$ such that

$$-D_x^\alpha u(x) + qu = \lambda u, \quad x \in \Omega = (0, 1) \quad u(0) = u(1) = 0 \quad (2)$$

with $D_x^\alpha u$ the left-sided Caputo or Riemann-Liouville fractional derivative of order $1 < \alpha < 2$ and $q \in L_\infty(0, 1)$ is a given potential.

For a family $\{\mathcal{T}_h\}_{0 < h < 1}$ of regular partitions of the domain Ω into d -simplexes we will seek a Galerkin approximation u_h to u in the finite element space $X_h \equiv X_h(\Omega)$ of continuous piecewise linear functions over \mathcal{T}_h .

In this talk we present an error analysis of the finite element method under minimal smoothness of the solution of the problems and express the corresponding error bounds in terms of the data.

Here are two representative results from the talk:

Theorem 1. *Let u and u_h be correspondingly the solutions of (1) and the solution of the semidiscrete finite element approximation with $v_h = P_h v$, P_h the orthogonal L_2 -projection. Then with for $t > 0$*

$$\|u_h(t) - u(t)\| + h\|\nabla(u_h(t) - u(t))\| \leq Ch^2 |\log h| t^{-\alpha} \|v\|. \quad (3)$$

Theorem 2. *Let (u, λ) be a fixed eigenpair of the eigenvalue problem (2). The finite element approximation λ_h of λ satisfies*

$$|\lambda - \lambda_h| \leq C(\lambda_j)h^s, \quad s = \begin{cases} \alpha & \text{for Caputo fractional derivative} \\ \alpha - \frac{1}{2} & \text{Riemann-Liouville FD} \end{cases} \quad (4)$$

We present also a number of numerical example that fully confirm the theoretical finding and motivate us for further study.

EQUATION OF ANISOTROPIC DIFFUSION AND APPLICATION TO IMAGE PROCESSING

Nikolai Kutev

Institute of Mathematics and Informatics
Bulgarian Academy of Sciences
Sofia 1113, Bulgaria
kutev@math.bas.bg

1 Introduction and motivation

Consider the initial boundary value problem

$$(1.1) \quad \begin{aligned} u_t - \operatorname{div}(a|\nabla u|^2 \nabla u) &= 0 && \text{in } \Omega \times (0, T), \\ (a|\nabla u|^2) \frac{\partial u}{\partial \nu} &= 0 && \text{on } \partial\Omega \times (0, T), \\ u(x, 0) &= u_0(x) && \text{on } \Omega, \end{aligned}$$

where $\Omega \subset \mathbb{R}$ is a bounded domain with boundary of class C^1 and ν is the exterior normal to $\partial\Omega$. The structural assumptions on a are

$$(1.2) \quad \begin{aligned} a &\in C^1([0, \infty)), && a(s) > 0, \\ \text{the ellipticity function} &&& b(s) := a(s) + 2sa'(s) \end{aligned}$$

is positive for s near 0 and changes sign exactly once at $s_0^2 > 0$.

Moreover, since we consider C^1 solutions, we implicitly assume the compatibility condition

$$\frac{\partial u_0}{\partial \nu} = 0 \quad \text{on } \partial\Omega$$

Typical examples of such diffusion functions a are $a(s) = e^{-s}$ or $a(s) = (1 + s)^{-1}$.

The function $u_0(x)$ represent the brightness of a picture in image enhancement processes. Often images are noisy and one wants to enhance them and to detect edges or discontinuities of the true gray values which led to u_0 . To get a sharper image out of u_0 several approaches have been suggested in the last years. The above model of Perona and Malik leads to an evolution type equation. Numerical computations have shown that this equation can produce desired effect that $u(x, T)$ provides a sharper image than $u(x, 0) = u_0(x)$.

The aim of this paper is the mathematical investigation of the anisotropic diffusion approach in image process equation and the qualitative properties of the solutions, as maximum and comparison principle, uniqueness, preservation of the shapes, nonexistence of global solutions and others.

The motivation for these investigations come from the applications. For example, sending a TV program by satellite one has to enhance the picture. On the tomography, in the case of a concern in the brain, it is important the precise localizations of the tumor. Unfortunately the pictures in the tomography are noisy and one has to enhance them to get a sharper image and sharper contrast in brightness. The same problem appear in the criminology to detect the criminal by means of the finger prints or pictures from the protective, panoramic cameras, or in the scientific experiments, as the robot in Mars (pitfander), sending pictures from so million miles.

To get a sharper image several approach have been suggested in the last years. For example, in the level set method of Chen, Giga and Goto, the singular parabolic equation

$$u_t - |\nabla u| \operatorname{div} \left(\frac{\nabla u}{|\nabla u|} \right) = 0$$

should be solved in the class of continuous viscosity solutions. In the paper of Huisken, Angenent and Giga the mean curvature flow

$$u_t - \sqrt{1 + |\nabla u|^2} \operatorname{div} \left(\frac{\nabla u}{\sqrt{1 + |\nabla u|^2}} \right) = 0$$

was investigated. In fact, the above equations are better models for the process of cristalization.

In the fundamental paper of Alvarez, F. Guichard, P.-L. Lions and Morel was suggested the method of viscosity solutions for fully, nonlinear parabolic equations

$$u_t - F(x, u, Du, Du^2) = 0$$

where F is an invariant function under rotation and translation, For example, the Gaus curvature flow, i.e. F is the Monge Ampere operator, $F = \operatorname{def}(D^2u)$,

$$u_t - \operatorname{def}(D^2u) = 0$$

has the desired invariants. This equation was investigated in the papers of Evans, Sprick and Evans, Soner, Songanidis.

However, the most important models are the Mumford and Shah variational and Perona-Malik diffusion equation model. In 1989 Mumford and Shah suggested studying of the variational problem

$$J(u) = \alpha \int_{\Omega} |u - u_0|^2 dx + \beta \int_{\Omega \setminus S} A(|\nabla u|^2) dx + \gamma H^{n-1}(S)$$

in the class of functions with bounded variations. Here α, β, γ are nonnegative constants, S is a singular set in which edges occur. The function $A(S) = S$, $A(S) = \sqrt{1 + S}$, $A(S) = S^{p/2}$, $1 \leq p < \infty$, or $A(S) = \frac{S}{1 + d_0 S}$, $d_0 = \text{const} > 0$ due to Chipot. The aim of this paper is the diffusion equation model (1.1) of Perona-Malik. This equation in the case of two space dimensions is evolution elliptic-hyperbolic equation. For convenience let us assume for a moment that Ω is a plane domain, that u is continuously differentiable and that $|\nabla u|^2 = u_{x_1}^2 + u_{x_2}^2 \neq 0$ a.e. in $\Omega \times (0, T)$. Then we can rewrite partial derivatives in terms of directional derivatives $v = -\nabla u / |\nabla u|$ (in direction of steepest descent of u), and τ in direction tangent to ∇u . Under such a change of coordinates one knows that $\Delta u = u_{vv} + u_{\tau\tau}$. If we rewrite equation (1.1), it reads

$$u_t - a(s)\Delta u - 2a'(s)su_{vv} = 0$$

or

$$u_t - b(|\nabla u|^2)u_{vv} - a(|\nabla u|^2)u_{\tau\tau} = 0.$$

So the diffusion in direction v can be thought of as a backward diffusion for large values of $|\nabla u|^2$, while the diffusion in direction τ is always smoothing. That is why we speak of anisotropic diffusion. The parameter s_0 is a control parameter. Larger values of s_0 guarantee sharper image and more contrast in brightness.

2 Nonexistence of global C^1 solutions

Our first result is L^∞ estimates for the Lipschitz continuous (weak) solutions of (1.1). The main part of the results are obtained jointly with B. Kawohl (see [6]).

Theorem 2.1. Maximum principle. *Suppose that u is a Lipschitz continuous (weak) solution to (1.1). Then for every $p \in [2, \infty]$ the following inequality holds*

$$\|u(x, t)\|_{L^p(\Omega)} \leq \|u_0(x)\|_{L^p(\Omega)}.$$

From now on we shall restrict ourselves to one space dimension. (1.1) is rewritten as

$$(2.1) \quad \begin{aligned} u_t - (a(u_x^2)u_x)_x &= 0 & \text{in } Q := (-1, 1) \times \mathbb{R}^+, \\ u_x(\pm 1, t) &= 0 & \text{for } t \in \mathbb{R}^+, \\ u(x, 0) &= u_0(x) \text{ on } (-1, 1) & \text{and } u'_0(\pm 1) = 0. \end{aligned}$$

We expect solutions to develop a larger and larger gradient; and we assuming that the initial data have their slope

$$u'_0(x) > s_0 \text{ in } (x_0, y_0) \subset \subset (-1, 1), \quad |u'_0(x)| < s_0 \text{ in } (-1, x_0) \cup (y_0, 1).$$

It seems that the natural class of weak solutions of problem (2.1) is the class of Lipschitz functions. Unfortunately, from the nonexistence result of K. Höllig, for piece wise linear function $a(s)$, problem (2.1) has infinitely many Lipschitz continuous solutions. The idea of Höllig is very tricky. In fact, the space derivative of the initial moment $t = 0$, eliminating the large values of the gradient, i.e. the contours disappear. The careful analysis of the counterexample of Höllig shows that the reason for the nonuniqueness is not the lack of the smoothness of the solution, but the change of the backward regime of the equation with forward regime.

That is why, further on we will consider only C^1 weak solutions of (2.1). In this class of functions equation (2.1) preserves its initial forward or backward regime, i.e. the contours do not disappear.

Assuming that a global C^1 -solution exist we denote with $Q^+ := \{(x, t) \in Q \text{ with } |u_x(x, t)| < s_0\}$ the forward (subsonic) set of equation (3.1), with $Q^- := \{(x, t) \in Q \text{ with } |u_x(x, t)| > s_0\}$ the backward (supersonic) regime and with $Q^0 := \{(x, t) \in Q \text{ with } |u_x(x, t)| = s_0\}$ the (sonic) set where (3.1) degenerates to a first order equation. This notion is borrowed from the theory of transonic flow for an ideal gas, which is modelled by an elliptic-hyperbolic operator of divergence type.

Theorem 2.2. Nonexistence of global C^1 solutions. *Suppose that $a(s)$ and $u_0(x)$ are functions satisfying (1.2). Then (2.1) has no global weak solution in $C^1(Q)$.* From Th. 2.1 we know that the amplitude of the gradient of the weak solution does not blow up for a finite time. Since the gradient explosion occurs only in the backward regime Q_- of the equation, this means that the enhancement process is finished for a finite time.

3 Comparison principle and counterexample

In this section we shall prove a comparison principle for weak C^1 solutions of (2.1) under at least one of two special assumptions on the initial data $u_0(x)$ and $v_0(x)$. One of them says that not only are the initial data ordered, i.e. $u_0(x) \leq v_0(x)$ in $(-1, 1)$, but they can be separated by a subsonic profile $w_0(x)$:

$$(3.1) \quad \exists w_0(x) \in C^{2,\alpha} \text{ such that } u_0(x) \leq w_0(x) \leq v_0(x), \\ |w'_0(x)| < s_0 \text{ in } (-1, 1) \text{ and } w'_0(\pm 1) = 0.$$

The other assumption on the initial data under which we can state a comparison principle is that

$$(3.2) \quad \{x \in (-1, 1) \text{ with } |u'_0(x)| \geq s_0\} \cap \{x \in (-1, 1) \text{ with } |v'_0(x)| \geq s_0\} = \emptyset.$$

Loosely speaking (3.2) says that the closures of the supersonic regimes of u_0 and v_0 do not intersect.

Theorem 3.1. Comparison principle. *Suppose that $u(x, t)$ and $v(x, t)$ are weak C^1 solutions of (2.1) in $Q_T := (-1, 1) \times (0, T)$ with C^1 initial data $u_0(x) \leq v_0(x)$ satisfying (3.1) or (3.2) and with a satisfying (1.2). Then $u(x, t) \leq v(x, t)$ in Q_T .*

The result in Th. 3.1 is sharp as the following example shows

Example. Suppose that there exist weak C^1 solutions $u(x, t)$ and $v(x, t)$ of (2.1) with initial data

$$\begin{aligned} u_0(x) &= 3bx + 2cx^2 - bx^3 - cx^4, \\ v_0(x) &= 3bx - 2dx^2 - bx^3 + dx^4, \end{aligned}$$

where b, c, d with $b > s_0/3$ are arbitrary positive constants. Then u and v violate the comparison principle, because $u_0 \geq v_0$ but for every $t > 0$ we have $u(0, t) < v(0, t)$. The following theorem says that through the time evolution the image becomes sharper.

Theorem 3.3. Shrinking of supersonic regimes. *Suppose that $u(x, t)$ is a weak C^1 solution of (2.1) and that (1.2) holds. Then the union of supersonic and sonic regimes of $u(x, t)$ shrinks in time, i.e. $Q_\tau^- \cup Q_\tau^0 := (Q^- \cup Q^0)\{t = \tau\}$ satisfies the inclusion $Q_\tau^- \cup Q_\tau^0 \subset (Q_s^- \cup Q_s^0)$ for every $0 \leq s \leq \tau$.*

4 Uniqueness of C^1 solutions

Theorem 4.1. Uniqueness. *Suppose that u and v are weak C^1 solution of (2.1) in $Q_T := (-1, 1) \times (0, T)$ with identical and analytic initial data u_0 . Moreover assume that $(u_0)_x^2 - s_0^2$ has only simple zeroes and that the diffusion coefficient a is analytic and satisfies (1.2). Then $u(x, t) \equiv v(x, t)$ in Q_T .*

In image enhancement we want to preserve edges and shapes. No new edges should be generated as the image evolves, nor do we want edges to disappear. If we call each component of $Q^-(u) \cap \{t = t_0\}$ an edge at time t_0 , then we can classify shapes of u according to their number of edges. The following theorem states roughly speaking, that this number is invariant in time.

Theorem 4.2. Preservation of Shapes. *Under the same assumption as in Theorem 4.1*

- i) *the number of the connected components of $Q^+(u) \cap \{t = s\}$ and of $(Q^-(u) \cup Q^0(u)) \cap \{t = s\}$ is invariant in s , and*
- ii) *in particular, no component of $Q^0(u)$ can originate in $Q^+(u)$.*

Reference

- [1] Alvarez, L., Guichard, F., Lions, P. L., Morel, S. M.: Axioms and fundamental equations of image processing. Arch. Rational Mech. Anal. **123** (1993), 199–257.
- [2] Alvarez, L., Lions, P. L., Morel, S. M.: Image selective smoothing and edge detection by nonlinear diffusion II. SIAM J. Numer. Anal. **29** (1992), 845–866.
- [3] Evans, L. C., Spruck, J.: Motion of level sets by mean curvature: I. J. Diff. Geometry **33** (1991), 635–681; II. J. Transactions Amer. Math. Soc. **330** (1992), 321–332.
- [4] Höllig, K.: Existence of infinitely many solutions for a forward-backward heat equation. Trans. Amer. Math. Soc. **278** (1983), 299–316.
- [5] Janenko, N. N., Novikov, V. A.: On some model of fluid with variable viscosity. Cisl. Metody Meh. Splošnoj Sredi **4** (1973), 142–147 (in Russian).

- [6] Kawohl, B., Kutev, N.: Global behaviour of solutions to a parabolic mean curvature equation. *Differ. Integral Equations* **8** (1995), 1923–1946.
- [7] Kawohl, B.: From Mumford-Shah to Perona-Malik in image processing. *Math. Meh. Appl. Sci.* **27** (2004), 1803–1814.
- [8] Kawohl, B., Kutev, N.: Maximum and comparison principle for one-dimensional anisotropic diffusion, *Math. Ann.*, **311** (1998), 107–123.
- [9] Kepinski, S.: Über die Differentialgleichung $Z_{xx} + \frac{m+1}{x}Z_x - \frac{n}{x}Z_t = 0$. *Math. Ann.* **61** (1905), 397–405.
- [10] Kichenassamy, S.: The Perona-Malik paradox, *SIAM J. Appl. Math.* **57** (1997), 1328–1342.
- [11] Ladyženskaja, O. A., Solonnikov, V. A., Ural'ceva, N. N.: Linear and quasilinear equations of parabolic type. Nauka, Moscow, 1967.
- [12] Larkin, P. A., Solonnikov, V. A., Janenko, N. N.: Nonlinear equations of variable type. Nauka, Novosibirsk, 1983 (in Russian).
- [13] Mumford D., Shah, J.: Optimal approximations by piecewise smooth functions and associated variational problems. *Comm. Pure Appl. Math.* **42** (1989), 577–685.
- [14] Perona, P., Malik, J.: Scale space and edge detection using anisotropic diffusion. *IEEE Trans. Pattern Anal. Mach. Intell.* **12** (1990), 629–638.
- [15] Protter, M., Weinberger, H.: Maximum Principle in differential equations. Prentice Hall, Englewood Cliffs, N. J. (1967).
- [16] Tersenov, C. A.: Parabolic equations with variable time. Nauka, Novosibirsk, 1985 (in Russian).
- [17] Vragov, V. N., Podgaev, A. G.: On well-posed problems for some equations of variable type. *Soviet. Math. Doklady* **24** (1981), 253–257.
- [18] Weickert, J.: Anisotropic diffusion in image processing. Dissertation, Kaiserslautern (1996).
- [19] Weickert, J.: Applications of nonlinear diffusion in image processing and computer vision, *Acta Mathematica Univ. Comen.* **70** (2001), 33–50.
- [20] Zelenjak, T. I., Novikov, V. A., Janenko, N. N.: On the properties of the solutions of nonlinear equations of variable type. *Čisl. Metody Meh. Splošnoj Sredi* **5** (1974), 35–47.

METRIC REGULARITY, STABILITY AND APPROXIMATIONS IN OPTIMAL CONTROL

Vladimir M. Veliov

Institute of Mathematical Methods in Economics,
Vienna University of Technology

Abstract

The talk will consist of the following parts.

1. *An informal introduction.* General problems that have led to the concept of metric regularity will be briefly discussed.
2. *Basic definitions and theory* (following A. Dontchev and T. Rockafellar [3]). Some elements of the concept of metric regularity that are relevant to the rest of the talk will be “dressed” in formal terms. The main operational tool—a Lyusternik-Graves-type theorem—will be formulated, following A. Dontchev and V.V. [4]. Then two extensions from M. Quincampoix and V.V. [5] will be presented: *bi-metric regularity* and *Hölder metric regularity*.
3. *Metric regularity of optimal control problems.* In this part the metric regularity will be translated in the terms of optimal control problems. An error estimate for the Euler discretization scheme will be presented as an illustration (A. Dontchev and V.V.[4]).
4. *Bi-metric Hölder regularity of bang-bang optimal control problems.* Although the theory of linear optimal control problems was developed some half a century ago, the “stability” and the error analyses for discretization schemes of such problems is a subject of intensive recent investigation. A new result by M. Quincampoix and V.V. [5] in this area, that involves the material from part 2 will be presented.
5. *Metric regularity and approximations of infinite-horizon optimal control problems.* The approximation of infinite-horizon optimal control problems that arise in economics is an

open and rather challenging issue. Thanks to some recently obtained optimality conditions for such problems (S. Aseev and V.V. [1, 2]) it become possible to apply the metric regularity theory and obtain conditions for approximation and stability analysis of infinite-horizon problems. These will be presented in the final part of the talk.

References

- [1] S. Aseev and V.M. Veliov. Maximum principle for problems with dominating discount. *Dynamics of Continuous, Discrete and Impulsive Systems, Series B*, **19**(1-2b):43–63, 2012.
- [2] S. Aseev and V.M. Veliov. Needle variations in infinite-horizon optimal control. To appear in *Contemporary Mathematics*, 2013.
- [3] A. L. Dontchev, R. T. Rockafellar. *Implicit Functions and Solution Mappings*, Springer Mathematics Monographs, Springer, Dordrecht 2009.
- [4] A.L Dontchev and V.M. Veliov. Metric regularity under approximations. *Control and Cybernetics*, **38**(4):1283–1303 , 2009.
- [5] M. Quincampoix and V.M. Veliov. Metric regularity of linear optimal control problems. Paper in preparation.

PART B:

CONTRIBUTED TALKS ¹

¹Arranged alphabetically according to the family name of the first author

STABILIZING EFFECTS OF CHAOTIC CNN MODELS ¹

G.Agranovich, E.Litsyn, A.Slavova

Dept. of Electrical and Electronic Engineering,
Ariel University Center of Samaria, 44837 Ariel, Israel
agr@ariel.ac.il

Department of Mathematics, Ben-Gurion University of the Negev,
Beer-Sheva, Israel
elena.litsyn@weizmann.ac.il

Institute of Mathematics, Bulgarian Academy of Sciences
Sofia 1113, Bulgaria
slavova@math.bas.bg

1 Introduction

The first model which we shall consider in this paper concerns mathematical modelling of pattern formation. Partial differential equations of diffusion type have long served as models for regulatory feedbacks and pattern formation in aggregates of living cells. We propose new receptor-based models for pattern formation and regulation in multicellular biological systems [1]. The main aim of this work is to check which aspects of self-organization and regeneration can be explained within the framework of CNNs. A reaction-diffusion model involving a hysteretic functional was proposed by Hopfenstead and Jäger [7]. They assumed that the cell's growth had a hysteretic dependence on the amount of nutrients and acid present. Pattern formation in this model is caused by the initial instability of the ordinary differential equations (ODEs).

¹This paper is partially supported by the bilateral joint research project between Bulgarian Academy of Sciences and Israel Academy of Sciences

We consider one-dimensional epithelial sheet of length L . We denote the density of ligands by $v(x, t)$, where x and t are space and time coordinates, with x increasing from 0 to L along the body column. The density of free receptors is denoted by $u(x, t)$. Consider a system of one reaction-diffusion equation and one ordinary differential equation (ODE):

$$\begin{cases} u_t = \Delta u + f(u, v) \\ v_t = g(u, v), \end{cases} \quad (1)$$

where the functions $f(u, v)$ and $g(u, v)$ present the rate of production of new free receptors and ligands, respectively and they are given by:

$$\begin{cases} f(u, v) = -c_1 \frac{u}{1+u^2} + \frac{b_1 u}{(1+u^2-u)(1+v)} \\ g(u, v) = -c_2 \frac{v}{1+v^2} + \frac{b_2 v}{(1+v^2-v)(1+u)}, \end{cases} \quad (2)$$

c_1 is the rate of decay of free receptors, c_2 is the rate of decay of ligands, $b_i > 0$, $i = 1, 2$ are constants.

The systems composed of both diffusion-type and ordinary differential equations cause some difficulties, since both existence and behaviour of the solutions are more difficult to establish. Many aspects of qualitative behaviour have to be investigated numerically. For this purpose we shall apply Cellular Neural Network (CNN) approach for studying system (1),(2). It is known [10,11] that some autonomous CNNs represent an excellent approximation to nonlinear partial differential equations (PDEs).

The famous Hodgkin-Huxley neuron model [6] is the first mathematical model describing neural excitation transmission derived from the angle of physics and lays the basis of electrical neurophysiology. FitzHugh-Nagumo equation [5,8], which is a simplification of Hodgkin-Huxley model, describes the generation and propagation of the nerve impulse along the giant axon of the squid. The FitzHugh-Nagumo systems are of fundamental importance for understanding the qualitative nature of nerve impulse propagation. Based on the finite propagating speed in the signal transmission between the neurons, the following coupled FitzHugh-Nagumo neural system is proposed as second model:

$$\begin{cases} \dot{u}_1 = -u_1(u_1 - 1)(u_1 - a) - u_2 + cf(u_3) \\ \dot{u}_2 = b(u_1 - \gamma u_2) \\ \dot{u}_3 = -u_3(u_3 - 1)(u_3 - a) - u_4 + cf(u_1) \\ \dot{u}_4 = b(u_3 - \gamma u_4), \end{cases} \quad (3)$$

where a, b, γ are positive constants, $u_{1,2}$ represent transmission variables, and $u_{3,4}$ are receiving variables; c measures the coupling strength, $f \in C^3$, $f(0) = 0$, $f'(0) = 1$. We shall take $f(x) = \tanh(x)$ in our investigation. System (3) is symmetric. Thus, considering the existence, spatio-temporal patterns and stability of its Hopf bifurcating periodic solutions is interesting.

In this paper we shall study dynamical behaviour of the CNN models of (1), (2) and (3) and the emergence or complexity of the model will be proved. The edge

of chaos phenomena will be presented. Then we shall design a discrete-continuous regulator of the CNN models in order to stabilize the chaotic motion to an admissible solution which is connected in some way to the original behaviour of the system (1),(2) and (3).

2 Cellular Neural Network models. Edge of chaos in the chaotic CNN models

CNN is simply an analogue dynamic processor array, made of cells, which contain linear capacitors, linear resistors, linear and nonlinear controlled sources. Let us consider a two-dimensional grid with 3×3 neighborhood system as it is shown on Fig.1.

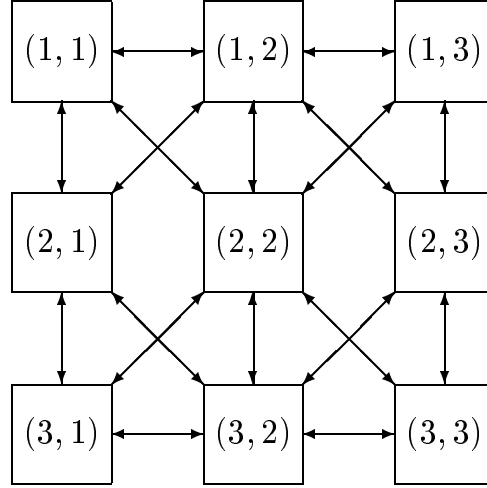


Fig.1. 3×3 neighborhood CNN.

The squares are the circuit units - cells, and the links between the cells indicate that there are interactions between linked cells. One of the key features of a CNN is that the individual cells are nonlinear dynamical systems, but that the coupling between them is linear. Roughly speaking, one could say that these arrays are nonlinear but have a linear spatial structure, which makes the use of techniques for their investigation common in engineering or physics attractive.

We will give the general definition of a CNN which follows the original one [2]:

Definition 1 *The CNN is a*

- a). 2-, 3-, or n - dimensional array of
- b). mainly identical dynamical systems, called cells, which satisfies two properties:

- c). most interactions are local within a finite radius r , and
- d). all state variables are continuous valued signals.

Definition 2 An $M \times M$ cellular neural network is defined mathematically by four specifications:

- 1). CNN cell dynamics;
- 2). CNN synaptic law which represents the interactions (spatial coupling) within the neighbor cells;
- 3). Boundary conditions;
- 4). Initial conditions.

Suppose for simplicity that the processing elements of a CNN are arranged on a 2-dimensional (2-D) grid (Fig.1). Then the dynamics of a CNN, in general, can be described by:

$$\begin{aligned} \dot{x}_{ij}(t) = & -x_{ij}(t) + \sum_{C(k,l) \in N_r(i,j)} \tilde{A}_{ij,kl}(y_{kl}(t), y_{ij}(t)) + \\ & + \sum_{C(k,l) \in N_r(i,j)} \tilde{B}_{ij,kl}(u_{kl}, u_{ij}) + I_{ij}, \end{aligned} \quad (4)$$

$$y_{ij}(t) = f(x_{ij}), \quad (5)$$

$$1 \leq i \leq M, 1 \leq j \leq M,$$

x_{ij}, y_{ij}, u_{ij} refer to the state, output and input voltage of a cell $C(i, j)$; $C(i, j)$ refers to a grid point associated with a cell on the 2-D grid, $C(k, l) \in N_r(i, j)$ is a grid point (cell) in the neighborhood within a radius r of the cell $C(i, j)$, I_{ij} is an independent current source. \tilde{A} and \tilde{B} are nonlinear cloning templates, which specify the interactions between each cell and all its neighbor cells in terms of their input, state, and output variables. Moreover, as we mentioned above the cloning template has geometrical meanings which can be exploited to provide us with geometric insights and simpler design methods.

Now in terms of definition 2 we can present the dynamical systems describing CNNs. For a general CNN whose cells are made of time-invariant circuit elements, each cell $C(ij)$ is characterized by its CNN cell dynamics :

$$\dot{x}_{ij} = -g(x_{ij}, u_{ij}, I_{ij}^s), \quad (6)$$

where $x_{ij} \in \mathbf{R}^m$, u_{ij} is usually a scalar. In most cases, the interactions (spatial coupling) with the neighbor cell $C(i+k, j+l)$ are specified by a CNN synaptic law:

$$\begin{aligned} I_{ij}^s = & A_{ij,kl}x_{i+k,j+l} + \\ & + \tilde{A}_{ij,kl} * f_{kl}(x_{ij}, x_{i+k,j+l}) + \\ & + \tilde{B}_{ij,kl} * u_{i+k,j+l}(t). \end{aligned} \quad (7)$$

The first term $A_{ij,kl}x_{i+k,j+l}$ of (5) is simply a linear feedback of the states of the neighborhood nodes. The second term provides an arbitrary nonlinear coupling, and the third term accounts for the contributions from the external inputs of each neighbor cell that is located in the N_r neighborhood.

In this paper we will present the chaotic models (1),(2) and (3) by a reaction-diffusion CNNs. The intrinsic space distributed topology makes the CNN able to produce real-time solutions of nonlinear PDEs. The theory of local activity provides a definitive answer to the fundamental question: what are the values of the cell parameter for which the interconnected system may exhibit complexity? The answer is given in [3,4] - the necessary condition for a nonconservative system to exhibit complexity is to have its cell locally active. The theory which will be presented below and which follows [4] offers a constructive analytical method for uncovering local activity. We apply the following constructive algorithm:

1. Map chaotic models (1), (2) and (3) into the following associated discrete-space models which we shall call reaction-diffusion CNN models, respectively:

$$\begin{aligned}\frac{du_j}{dt} &= (u_{j-1} - 2u_j + u_{j+1}) + \\ &+ f(u_j, v_j) = U + f \\ \frac{dv_j}{dt} &= g(u_j, v_j) = g, 1 \leq j \leq N.\end{aligned}\tag{8}$$

$$\left\{ \begin{aligned} \frac{du_j^1}{dt} &= -u_j^1(u_j^1 - 1)(u_j^1 - a) - u_j^2 + cf(u_j^3) \\ \frac{du_j^2}{dt} &= b(u_j^1 - \gamma u_j^2) \\ \frac{du_j^3}{dt} &= -u_j^3(u_j^3 - 1)(u_j^3 - a) - u_j^4 + cf(u_j^1) \\ \frac{du_j^4}{dt} &= b(u_j^3 - \gamma u_j^4), j = 1, \dots, n. \end{aligned} \right.\tag{9}$$

2. Find the equilibrium points of (8) and (9). According to the theory of dynamical systems the equilibrium points of (8) and (9) are these for which :

$$\begin{aligned}U - c_1 \frac{u^e}{1 + (u^e)^2} + \frac{b_1 u^e}{(1 + (u^e)^2 - u^e)(1 + v^e)} &= 0 \\ -c_2 \frac{v}{1 + (v^e)^2} + \frac{b_2 v^e}{(1 + (v^e)^2 - v^e)(1 + u^e)} &= 0.\end{aligned}\tag{10}$$

$$\left\{ \begin{aligned} -u_j^1(u_j^1 - 1)(u_j^1 - a) - u_j^2 + c \tanh(u_j^3) &= 0 \\ b(u_j^1 - \gamma u_j^2) &= 0 \\ -u_j^3(u_j^3 - 1)(u_j^3 - a) - u_j^4 + c \tanh(u_j^1) &= 0 \\ b(u_j^3 - \gamma u_j^4) &= 0. \end{aligned} \right.\tag{11}$$

3. Calculate the cell coefficients of the Jacobian matrix of (10) and (11) about each system equilibrium point E_i .

4. Calculate the trace $Tr(E_i)$ and the determinant $\Delta(E_i)$ of the Jacobian matrix for each equilibrium point.

Definition 3 A diffusion cell is locally active at an equilibrium point E_i , iff the matrix:

$$L_{E_i} = \begin{bmatrix} -2f_1^e & -(f_2^e + g_1^e) \\ -(f_2^e + g_1^e) & -2g_2^e \end{bmatrix} \quad (12)$$

is not positive semi-definite at the equilibrium point E_i .

Remark 1 A matrix M is called positive semi-definite if $x^*MX \geq 0$ for all $x \in \mathbf{R}^n$, where x^* denotes the conjugate transpose of x .

Definition 4 Local activity region $LAR(E_i)$ is defined as follows:

$$LAR(E_i) : g_2^e > 0 \quad 4f_1^e g_2^e < (f_2^e + g_1^e)^2. \quad (13)$$

Definition 5 Stable and locally active region $SLAR(E_i)$ at the equilibrium point E_i for the reaction-diffusion CNN model is such that $Tr < 0$ and $\Delta > 0$.

5. Edge of chaos

In the literature [4], the so-called edge of chaos (EC) means a region in the parameter space of a dynamical system where complex phenomena and information processing can emerge. We shall try to define more precisely this phenomena till now known only via empirical examples. Moreover, we shall present an algorithm for determining the edge of chaos for diffusion CNN models as our CNN models (8) and (9).

Definition 6 Reaction-diffusion CNN is said to be operating on the edge of chaos EC iff there is at least one equilibrium point E_i , which is both locally active and stable.

For our CNN models (8) and (9) the following theorems hold, respectively:

Theorem 1 Reaction-diffusion CNN model for the system (1), (2) is operating in the edge of chaos regime iff $c_1 > b_1 > 0$, $c_2 > b_2 > 0$. For this parameter values, there is at least one equilibrium point which is both locally active and stable.

Theorem 2 CNN model of coupled FitzHugh-Nagumo system (3) is operating in the edge of chaos regime for all a , b and γ positive. For this parameter values there is at least one equilibrium point which belongs to $SLAR(E)$.

Here in this paper we shall perform simulations for the reaction-diffusion CNN models (8) and (9). We obtain the following figures:

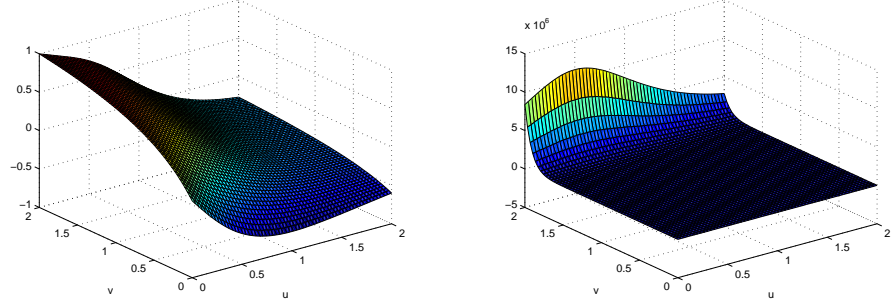


Fig.1. Stationary wave solution of the receptor-based CNN model for the following parameter set: $c_i, b_i \in [1, 2], i = 1, 2$.

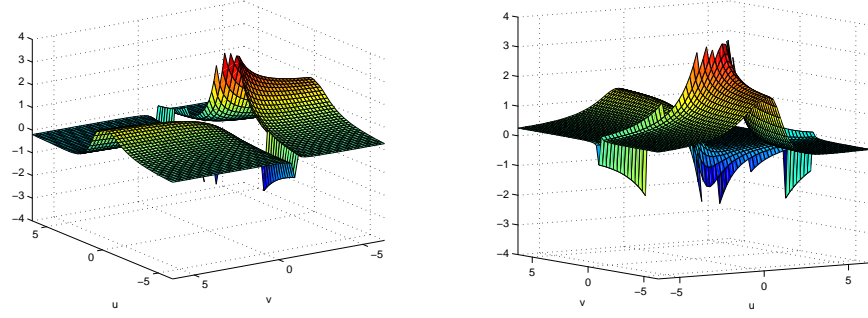
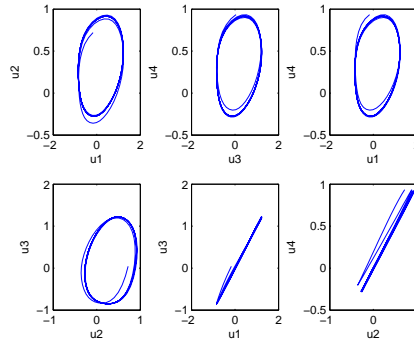


Fig.2. Spatio-temporal solution of the receptor-based CNN model for the following parameter set: $c_i, b_i \in [1, 2], i = 1, 2$.



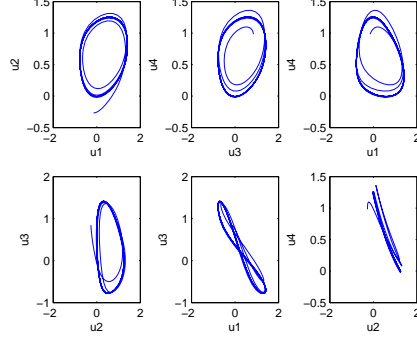


Fig.3. EC phenomena for CNN model (9).

3 Continuous feedback control of the CNN models

We propose the following algorithm for the continuous feedback control of our CNN models (8) and (9).

1. Rewrite the CNN models (8) and (9) by the simultaneous $2 * N$ ordinary differential equations:

2. Numbers of cells N lies in bounds $1 \leq N \leq 25$. Constant coefficients

$$c_j \in [0, 1], b_j \in [1, 2]. \quad (14)$$

3. Boundary conditions are

$$u(t, -1) = u(t, N + 1) = 0$$

and initial conditions are in the intervals

$$u(0, j) \in [0, 2], v(0, j) \in [0, 2].$$

4. The matrix form of the CNN models with continuous feedback control is

$$\begin{aligned} \frac{dU}{dt} &= F(U, V) + Z_U, \\ \frac{dV}{dt} &= G(U, V) + Z_V \end{aligned} \quad (15)$$

5. The nonlinear state model of (15) is in the following matrix form

$$\frac{dX}{dt} = F_e(X) + Z \quad (16)$$

in which the block matrices are

$$X = \begin{bmatrix} U \\ V \end{bmatrix}, F_e = \begin{bmatrix} F \\ G \end{bmatrix}, Z = \begin{bmatrix} Z_U \\ Z_V \end{bmatrix}. \quad (17)$$

6. Linearized model of (16) in the neighborhood of the equilibrium point X_s is

$$\frac{dX}{dt} = (F_{Xe}(X_s))X + Z, \quad (18)$$

where

$$F_{Xe}(X_s) = \frac{\partial F_e(X_s)}{\partial X} = \begin{bmatrix} \frac{\partial F(X_s)}{\partial U} & \frac{\partial F(X_s)}{\partial V} \\ \frac{\partial G(X_s)}{\partial U} & \frac{\partial G(X_s)}{\partial V} \end{bmatrix}. \quad (19)$$

7. At the equilibrium point $E_1 = (0, 0)$ the coefficient matrix of linearized system (18) takes the form

$$F_{Xe}(X_s) = \begin{bmatrix} (b_1 - c_1)E & 0_{N \times N} \\ 0_{N \times N} & (b_2 - c_2)E \end{bmatrix}. \quad (20)$$

8. Express the eigenvalues $\{\lambda_j^0, j = 1 \dots 2N\}$ of the linearized system (18) in the following way:

$$\begin{aligned} \lambda_j^0 &= b_1 - c_1, \quad j = 1 \dots N; \\ \lambda_{N+1}^0 &= \dots = \lambda_{2N}^0 = \mu^0 = b_2 - c_2. \end{aligned} \quad (21)$$

9. We shall seek stabilized controls for (18), (20) as follows

$$Z_U = k_u V, \quad Z_V = k_v U + k_w V, \quad (22)$$

where the values of the scalar control coefficients k_u, k_v, k_w are to be found.

10. The close-loop system (18), (20), (22) have the matrix representation

$$\frac{dX}{dt} = (F_{Xe}(X_s) + R)X, \quad (23)$$

where

$$R = \begin{bmatrix} 0_{N \times N} & k_u E \\ k_v E & k_w E \end{bmatrix}.$$

11. We obtain the following close-loop system's dynamical matrix

$$A_{cl} = \begin{bmatrix} (b_1 - c_1)E & k_u E \\ k_v E & (k_w - b_2 - c_2)E \end{bmatrix} \quad (24)$$

Then the following theorem holds:

Theorem 3 *If the parameters of the close-loop system (23) with open-loop eigenvalues (21) satisfy the following inequalities*

$$\begin{aligned} k_w &\leq -2\sigma - \mu^0 - \max_j(\lambda_j^0) \\ k_u k_v &\leq \sigma^2 + \sigma(k_w + \mu^0) + \min_j \lambda_j^0(\sigma + k_w + \mu^0) \end{aligned} \quad (25)$$

for some $\sigma \geq 0$, then eigenvalues of the close-loop system satisfy the inequality $\lambda_j^{cl} \leq -\sigma$. For each value of $\sigma \geq 0$ exist values of control feedback parameters (22), for which the inequalities (25) are satisfied.

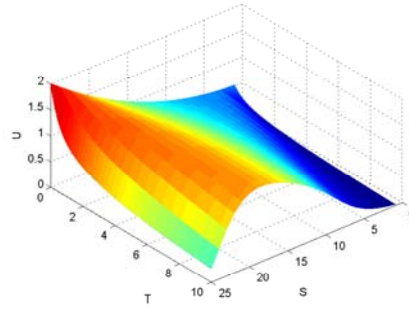


Fig.3. Spatio-temporal solution of the unstabilized receptor-based CNN model.

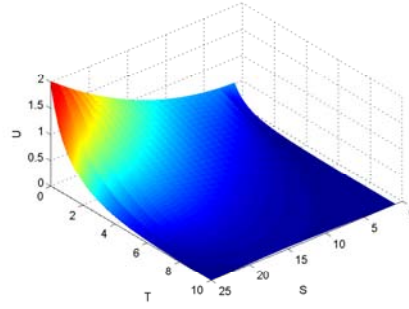


Fig.4. Spatio-temporal solution of the stabilized receptor-based CNN model, $\sigma = 0.5$.

As in can be seen from figures 3 and 4, the proposed method allows so to stabilize the system's dynamics so to assign its rate of convergence.

References

- [1] N.F.Britton, *Reaction-Diffusion Equations and Their Applications to Biology*, New York: Academic, 1986.

- [2] L.O.Chua, L.Yang, "Cellular Neural Network: Theory and Applications", *IEEE Trans. CAS*, vol. 35, pp. 1257-1290, Oct. 1988.
- [3] L.O. Chua, CNN:A Paradigm for Complexity, World Scientific Series on Nonlinear Science, Series A, vol. 31, World Scientific, Singapore, 1988.
- [4] L.O.Chua,Local activity in the origin of complexity, *Int.J.Bifurcations and Chaos*, 2005.
- [5] R.FitzHugh, Impulses and physiological states in theoretical models of nerve membrane, *Biophys.J.*, 1, 1961, pp.445-466.
- [6] A.L.Hodgkin, The local electric changes associated with repetitive action in a non-modulated axon, *J.Physiol.*, 107, 1948, 165-181
- [7] F.Hoppensteadt, W.Jäger, "Pattern formation by bacteria". In S.Levin, editor, *Lecture Notes in Biomathematics:Biological Growth and Spread*, pp. 69-81, Heidelberg, Springer-Verlag,1980.
- [8] J.Nagumo, S.Arimoto, S.Yoshizawa, An active pulse transmission line simulating nerve axon, *Proc.IRE* 50, 1962, 2061-2070
- [9] J.Rinzel, G.B.Ermentrout, Analysis of Neural Excitability and Oscillations, *Methods in Neuronal Modeling*, MIT, Cambridge, 1989.
- [10] T.Roska,L.O. Chua, D.Wolf, T.Kozek,R. Tetzlaff,F. Puffer, Simulating nonlinear waves and partial differential equations via CNN- Part I: Basic techniques, *IEEE Trans. CAS-I*, vol. 42, N 10, 1995, 807-815.
- [11] A.Slavova, Applications of some mathematical methods in the analysis of Cellular Neural Networks, *J.Comp.Appl.Math.*, 114, 2000, 387-404.
- [12] A.Slavova, P.Zecca, CNN model for studying dynamics and travelling wave solutions of FitzHugh-Nagumo equation, *Journ. Comp. and Appl. Math.*, 151, 2003, 13-24.

NUMERICAL COMPUTATION OF GAUSSIAN QUADRATURE FORMULAE FOR SPACES OF CUBIC SPLINES WITH EQUIDISTANT KNOTS

Ana Avdzhieva, Geno Nikolov

Department of Mathematics, University of Sofia,
5 James Bourchier Boulevard, 1164 Sofia, Bulgaria
aavdzheva@fmi.uni-sofia.bg, geno@fmi.uni-sofia.bg

1 Introduction

Throughout this paper π_k will stand for the set of algebraic polynomials of degree not exceeding k . For a fixed natural $n \geq 5$, we set

$$x_k = \frac{k}{N}, \quad k = 0, 1, \dots, N, \quad \text{where } N = 2n - 3. \quad (1)$$

Denote by S the linear space of cubic splines with $N - 1$ knots $\{x_k\}_{k=1}^{N-1}$

$$S := \{f \in C^2[0, 1] : f|_{(x_k, x_{k+1})} \in \pi_3, \quad k = 0, 1, \dots, N - 1\}. \quad (2)$$

The space S of splines with equidistant knots (considered as functions defined in the interval $[0, 1]$) has dimension $2n$, and a basis for S is given by

$$1, x, x^2, x^3, (x - x_1)_+^3, (x - x_2)_+^3, \dots, (x - x_{N-1})_+^3, \quad (3)$$

where $(\cdot)_+$ stands for the truncated power function, i.e.,

$$u_+ := \max\{u, 0\}. \quad (4)$$

Associated with S there exists a unique n -point quadrature formula

$$Q_n^G[f] = \sum_{k=1}^n a_k f(\tau_k), \quad 0 < \tau_1 < \tau_2 < \dots < \tau_n < 1, \quad (5)$$

for approximate calculation of

$$I[f] := \int_0^1 f(x) dx,$$

with the property

$$R[Q_n^G; f] := I[f] - Q_n^G[f] = 0 \quad \text{whenever } f \in S. \quad (6)$$

Q_n^G is called Gaussian quadrature formula associated with the space S , by analogy with the classical Gaussian quadrature formulae, which use n point evaluations and are exact for the functions from the space π_{2n-1} , which has dimension $2n$. In a similar manner one defines Radau- and Lobatto-type quadrature formulae associated with appropriate linear spaces of spline functions. The general problem of existence and uniqueness of Gauss-type quadrature formulae for spaces of polynomial splines is settled by the fundamental theorem of algebra for monosplines, see [5]. Similarly to their classical analogues, these Gauss-type quadrature formulae enjoy the property of positive weights.

Our interest in the Gauss-type quadrature formulae associated with spaces of splines with equidistant knots is inspired by the results in [6], where it has been shown their asymptotical optimality in appropriate Sobolev classes of functions. Let us briefly explain what this mean. For $r \in \mathbb{N}$, set

$$\widetilde{W}_p^r := \{f \in C^{r-1}[0, 1], f - 1\text{-periodic}, f^{(r-1)} \text{ abs. cont.}, \|f\|_p < \infty\},$$

$$W_p^r := \{f \in C^{r-1}[0, 1], f^{(r-1)} \text{ abs. cont.}, \|f\|_p < \infty\},$$

where

$$\|f\|_p := \left(\int_0^1 |f(t)|^p dt \right)^{1/p}, \quad \text{if } 1 \leq p < \infty, \quad \text{and} \quad \|f\|_\infty = \sup_{t \in (0,1)} |f(t)|.$$

It has been shown in [6] that the Gauss-type quadrature formulae associated with spaces of splines of degree $r - 1$ with equidistant knots are asymptotically optimal in W_∞^r for all r , and, for odd r , in W_p^r , for all $p \in [1, \infty]$. For the error of the quadrature formula (5) it was proved in [6] that

$$|R[Q_n^G; f]| \leq c_{4,\infty}(Q_n^G) \|f^{(4)}\|_\infty \quad \text{for every } f \in W_\infty^4, \quad (7)$$

where the error constant $c_{4,\infty}(Q_n^G)$ satisfies

$$c_{4,\infty}(Q_n^G) \leq \frac{5}{384} \frac{1}{(2n-3)^4} \left(1 - \frac{7}{75(2n-3)} \right). \quad (8)$$

It is well-known that in all periodic Sobolev classes \widetilde{W}_p^r there is an universal optimal n -point quadrature formula, namely the rectangles quadrature formula

$$Q_n^*[f] = \frac{1}{n} \sum_{k=1}^n f\left(\frac{2k-1}{2n}\right).$$

The optimality of Q_n^* in \widetilde{W}_p^r means that the infimum

$$\mathcal{E}_n(\widetilde{W}_p^r) := \inf_{Q_n} \sup\{|R[Q_n; f]| : f \in \widetilde{W}_p^r, \|f^{(r)}\|_p \leq 1\}$$

is attained for, and only for $Q_n = Q_n^*$. Obviously, the analogously defined quantities $\mathcal{E}_n(W_p^r) := \inf_{Q_n} \sup\{|R[Q_n; f]| : f \in W_p^r, \|f^{(r)}\|_p \leq 1\}$ satisfy $\mathcal{E}_n(W_p^r) \geq \mathcal{E}_n(\widetilde{W}_p^r)$, since $\widetilde{W}_p^r \subset W_p^r$. From

$$\mathcal{E}_n(\widetilde{W}_\infty^4) = \frac{5}{384} \frac{1}{(2n)^4}$$

and (8) we obtain

$$1 \leq \lim_{n \rightarrow \infty} \frac{\mathcal{E}_n(W_p^r)}{\mathcal{E}_n(\widetilde{W}_p^r)} \leq \lim_{n \rightarrow \infty} \frac{c_{4,\infty}(Q_n^G)}{\mathcal{E}_n(\widetilde{W}_p^r)} \leq 1,$$

whence

$$\lim_{n \rightarrow \infty} \frac{c_{4,\infty}(Q_n^G)}{\mathcal{E}_n(W_p^r)} = 1.$$

This is the claimed asymptotical optimality of the Gaussian quadrature formulae $\{Q_n^G\}$ in the Sobolev class W_∞^4 . The existence and uniqueness of optimal quadrature formulae in the Sobolev spaces W_p^r are equivalent to existence and uniqueness of monosplines of minimal L_q deviation from zero, where q is the conjugate to p , i.e., $1/p + 1/q = 1$. Though the existence and uniqueness of such monosplines (and hence existence and uniqueness of optimal quadrature formulae) is known, see Bojanov [1], [2], [3], only in a few special cases the optimal quadrature formulae are known explicitly. This is the reason for studying quadrature formulae, which are asymptotically optimal.

Another fact motivating our study of quadrature formulae exact for cubic splines is the extensive use of cubic splines, in particular with equidistant knots, in numerical procedures.

Let us mention that algorithms for construction and error estimates of Gauss-type quadrature formulae associated with spaces of linear and parabolic spline functions are proposed in [7], [9] (see also [8] for the case of cubic splines with double equidistant knots).

2 Equations for Derivation of Q_n^G

Clearly, the quadrature formula (5) will satisfy $I[f] = Q_n^G[f]$ for every $f \in S$ if and only if $I[f] = Q_n^G[f]$ for the basis functions (3). According to Peano's theorem, if $f \in W_1^4$, then the remainder of Q_n^G can be represented (see, e.g., [4]) as

$$R[Q_n^G; f] = \int_0^1 K(t) f^{(4)}(t) dt, \quad \text{with } K(t) = \frac{1}{3!} R[Q_n^G; (\cdot - t)_+^3].$$

Explicit representations of the Peano kernel $K(t)$ for $t \in [0, 1]$ are

$$K(t) = \frac{(1-t)^4}{24} - \frac{1}{6} \sum_{k=1}^n a_k (\tau_k - t)_+^3 \quad (9)$$

and

$$K(t) = \frac{t^4}{24} - \frac{1}{6} \sum_{k=1}^n a_k (t - \tau_k)_+^3. \quad (10)$$

In view of the definition $K(t)$, Q_n^G will be exact for $f(x) = (x-u)_+^3$, $u \in (0, 1)$ if and only if $K(u) = 0$. Similarly, the condition that Q_n^G is exact for $f(x) = x^3, x^2, x, 1$ can be interpreted as $K(t)$ has a zero of multiplicity four at $x = 0$. Thus, the problem for construction of Q_n^G is equivalent to finding a monospline $K(t)$ of the form (9) with prescribed zeros $\{x_k\}_{k=1}^{m-1}$ and a zero of multiplicity four at $x = 0$:

$$\begin{aligned} K(x_j) &= 0, \quad j = 1, 2, \dots, N-1, \\ K(0) &= K'(0) = K''(0) = K'''(0) = 0. \end{aligned} \quad (11)$$

Since the Gaussian quadrature formula Q_n^G associated with S is unique, and S is invariant with respect to reflection $x \rightarrow 1-x$, it follows that Q_n^G is symmetric, i.e., $a_k = a_{n+1-k}$ and $\tau_{n+1-k} = 1 - \tau_k$ for $k = 1, 2, \dots, n$. Therefore, Q_n^G is of the form

$$Q_n^G[f] = \sum_{k=1}^{\lfloor \frac{n+1}{2} \rfloor} a_k (f(\tau_k) + f(1 - \tau_k)), \quad 0 < \tau_1 < \tau_2 < \dots < \tau_{\lfloor \frac{n+1}{2} \rfloor} \leq \frac{1}{2}, \quad (12)$$

and $\tau_{\lfloor \frac{n+1}{2} \rfloor} = \frac{1}{2}$ only when n is odd number. Accordingly, equations (11) simplify to

$$\begin{aligned} K(x_j) &= 0, \quad j = 1, 2, \dots, n-2, \\ \sum_{k=1}^{\lfloor \frac{n+1}{2} \rfloor'} a_k &= \frac{1}{2}, \\ \sum_{k=1}^{\lfloor \frac{n+1}{2} \rfloor'} a_k (\tau_k^2 + (1 - \tau_k)^2) &= \frac{1}{3} \end{aligned} \quad (13)$$

(here and henceforth, \sum' means that in the case of odd n the last summand is to be halved).

A principle difficulty in the construction of Q_n^G is to determine the location of the nodes $\{\tau_k\}_{k=1}^n$ relative to the spline knots $\{x_j\}_{j=1}^{2n-4}$. Based on some numerical experiments performed with MATHEMATICA we are led to the validity of the following

Proposition 1. *The nodes of Q_n^G in the interval $[0, \frac{1}{2}]$ are located as follows:*

$$\tau_1 \in (x_0, x_1), \quad \tau_k \in (x_{2k-3}, x_{2k}) \quad \text{for } k = 2, \dots, \left\lfloor \frac{n+1}{2} \right\rfloor.$$

Moreover, if n is odd, then $\tau_{\frac{n+1}{2}} = \frac{1}{2}$.

2.1 The case $n = 2m$

In this case $N = 2n - 3 = 4m - 3$. For the sake of convenience, we set

$$\tau_1 = \frac{\theta_1}{N}, \quad \tau_j = \frac{2j - 3 + \theta_j}{N}, \quad j = 2, \dots, m, \quad (14)$$

where, in agreement with Proposition 1, $\theta_j \in (0, 1)$, $j = 1, \dots, m$. For the weights of Q_n^G we substitute

$$a_j = \frac{\delta_j}{N}, \quad j = 1, \dots, m, \quad \text{where } \delta_j > 0.$$

With the above notation, the equations $K(x_j) = 0$, $j = 1, \dots, 2m - 2$ in (13) become

$$\delta_1(1 - \theta_1)^3 = \frac{1}{4}, \quad (15)$$

$$\begin{aligned} \delta_1(2 - \theta_1)^3 + \delta_2(1 - \theta_2)^3 &= \frac{2^4}{4}, \\ \delta_1(3 - \theta_1)^3 + \delta_2(2 - \theta_2)^3 &= \frac{3^4}{4}, \end{aligned} \quad (16)$$

$$\begin{aligned} \delta_1(2k - 2 - \theta_1)^3 + \delta_2(2k - 3 - \theta_2)^3 + \delta_3(2k - 5 - \theta_3)^3 + \dots + \delta_k(1 - \theta_k)^3 &= \frac{(2k - 2)^4}{4}, \\ \delta_1(2k - 1 - \theta_1)^3 + \delta_2(2k - 2 - \theta_2)^3 + \delta_3(2k - 4 - \theta_3)^3 + \dots + \delta_k(2 - \theta_k)^3 &= \frac{(2k - 1)^4}{4}, \end{aligned} \quad (17)$$

for $k = 3, \dots, m - 1$, and

$$\delta_1(2m - 2 - \theta_1)^3 + \delta_2(2m - 3 - \theta_2)^3 + \delta_3(2m - 5 - \theta_3)^3 + \dots + \delta_m(1 - \theta_m)^3 = \frac{(2m - 2)^4}{4}. \quad (18)$$

The last two equations in (13) transform to

$$\sum_{k=1}^m \delta_k = \frac{4m - 3}{2}, \quad (19)$$

$$\delta_1\theta_1(4m - 3 - \theta_1) + \sum_{k=2}^m \delta_k(2k - 3 + \theta_k)(4m - 2k - \theta_k) = \frac{(4m - 3)^3}{12}. \quad (20)$$

2.2 The case $n = 2m + 1$

In this case $N = 4m - 1$, and we set $\{\theta_j\}_{j=1}^m$ as in (14), with $\theta_j \in (0, 1)$; furthermore, $\theta_{m+1} = \frac{1}{2}$ and $a_j = \delta_j/N$ for $j = 1, \dots, m + 1$. The equations $K(x_j) = 0$, $j =$

$1, \dots, 2m-1$ in (13) in this case are equations (15), (16) and (17), the latter for $k = 3, \dots, m$. The last two equations in (13) in this case are

$$\sum_{k=1}^{m+1} \delta_k = \frac{4m-1}{2}, \quad (19')$$

$$\delta_1 \theta_1 (4m-1-\theta_1) + \sum_{k=2}^m \delta_k (2k-3+\theta_k) (4m+2-2k-\theta_k) + \frac{1}{8} \delta_{m+1} (4m-1)^2 = \frac{(4m-1)^3}{12}. \quad (20')$$

3 Shooting Method for Numerical Calculation of Q_n^G

The non-linear system of equations for $\{\theta_k\}$ and $\{\delta_k\}$ is suitable for application of the shooting method. Namely, starting from an initial value θ_1 , one can find δ_1 from (15), and then to calculate from the subsequent pairs of equations consecutively (θ_2, δ_2) , $(\theta_3, \delta_3), \dots$, ending up with two equations to be satisfied by the last undetermined parameter or three equations to be satisfied by the last two undetermined parameters. These two, respectively three equations are satisfied if θ_1 is properly chosen. The algorithm differs slightly in the cases of odd and even n .

3.1 Algorithm for the case $n = 2m + 1$

The unknowns $\{\theta_k\}_{k=1}^m$ and $\{\delta_k\}_{k=1}^{m+1}$ satisfy equations (15), (16), (17), (19') and (20'). We start with some initial value of θ_1 in $(0, 1)$.

Step 1: Find δ_1 from (15):

$$\delta_1 = \frac{1}{4(1-\theta_1)^3}.$$

Step 2: Find θ_2 and δ_2 from (16):

$$\alpha_2 = \sqrt[3]{\frac{3^4 - 4\delta_1(3-\theta_1)^3}{2^4 - 4\delta_1(2-\theta_1)^3}}; \quad \theta_2 = \frac{\alpha_2 - 2}{\alpha_2 - 1}; \quad \delta_2 = \frac{3^4 - 4\delta_1(3-\theta_1)^3}{4(2-\theta_1)^3}.$$

Step 3: For $k = 3, \dots, m$, find θ_k and δ_k from (17):

$$\alpha_k = \sqrt[3]{\frac{(2k-1)^4 - 4\delta_1(2k-1-\theta_1)^3 - 4\sum_{i=2}^{k-1} \delta_i(2k+2-2i-\theta_i)^3}{(2k-2)^4 - 4\delta_1(2k-2-\theta_1)^3 - 4\sum_{i=2}^{k-1} \delta_i(2k+1-2i-\theta_i)^3}};$$

$$\theta_k = \frac{\alpha_k - 2}{\alpha_k - 1};$$

$$\delta_k = \frac{(2k-1)^4 - 4\delta_1(2k-1-\theta_1)^3 - 4\sum_{i=2}^{k-1} \delta_i(2k+2-2i-\theta_i)^3}{4(2-\theta_k)^3}.$$

The unknown θ_{m+1} must satisfy equations (19') and (20').

Step 4: Find δ_{m+1} from (20'):

$$\delta_{m+1} = \frac{2(4m-1)}{3} - \frac{8}{(4m-1)^2} \left(\delta_1 \theta_1 (4m-1-\theta_1) + \sum_{k=2}^m \delta_k (2k-3+\theta_k)(4m+2-2k-\theta_k) \right);$$

Step 5: With the so found $\{\delta_k\}_{k=1}^{m+1}$ verify if equation (19')

$$\sum_{k=1}^m \delta_k + \frac{1}{2} \delta_{m+1} = \frac{4m-1}{2}$$

is satisfied (with a suitable tolerance). If instead of " $=$ " some of relations " $>$ " or " $<$ " holds, modify appropriately θ_1 and go to *Step 1*, otherwise *Stop*.

3.2 Algorithm for the case $n = 2m$

The unknowns $\{\theta_k\}_{k=1}^m$ and $\{\delta_k\}_{k=1}^m$ satisfy equations (15), (16), (17), (18), (19) and (20). Again, we choose initial value of θ_1 in $(0, 1)$.

Step 1: Same as in the case $n = 2m + 1$;

Step 2: Same as in the case $n = 2m + 1$;

Step 3: As in the case $n = 2m + 1$, but for $k = 3, \dots, m - 1$;

The unknown θ_m and δ_m must satisfy equations (18), (19) and (20).

Step 4: Find θ_m and δ_m from equations (18) and (20) as follows:

$$c_m = \frac{(2m-2)^4 - 4\delta_1(2m-2-\theta_1)^3 - 4 \sum_{i=2}^{m-1} \delta_i(2m+1-2i-\theta_i)^3}{(4m-3)^3/3 - 4\delta_1\theta_1(4m-3-\theta_1) - 4 \sum_{i=2}^{m-1} \delta_i(2i-3+\theta_i)(4m-2i-\theta_i)};$$

θ_m is the only real root of the cubic equation

$$\theta^3 - (c_m + 3)\theta^2 + 3(c_m + 1)\theta + 2m(2m - 3)c_m - 1 = 0;$$

$$\delta_m = \frac{4(m-1)^4 - \delta_1(2m-2-\theta_1)^3 - \sum_{i=2}^{m-1} \delta_i(2m+1-2i-\theta_i)^3}{(1-\theta_m)^3}.$$

Step 5: With the so found $\{\delta_k\}_{k=1}^m$ verify if equation (19)

$$\sum_{k=1}^m \delta_k = \frac{4m-3}{2}$$

is satisfied (with a suitable tolerance). If instead of " $=$ " some of relations " $>$ " or " $<$ " holds, modify appropriately θ_1 and go to *Step 1*, otherwise *Stop*.

4 Numerical Results and Conclusions

The proposed algorithm has been applied for numerical computation of the knots and weights of the Gaussian quadrature formulae Q_n^G . The numerical experiments show that both "generating parameters" $\theta_1(n)$ and $\delta_1(n)$ increase monotonically with n , tending to some limit values (see Table 1). In fact, in the implementation of the shooting method described above we have used the numerically found value $\theta_1(n)$ as initial value for $\theta_1(n+1)$. Another observation from our numerical experiments is that the sequence $\{\theta_k(n)\}_{k=3}^{\lfloor \frac{n+1}{2} \rfloor}$ is monotonically decreasing to the limit value $\frac{1}{2}$, while the sequence $\{\delta_k(n)\}_{k=1}^{\lfloor \frac{n+1}{2} \rfloor}$ is monotonically increasing to the limit value 2.

Table 1: Numerical values of $\theta_1(n)$ and $\delta_1(n)$, $3 \leq n \leq 16$.

n	$\theta_1(n)$	$\delta_1(n)$
3	0.325879311204089	0.81606930150704
4	0.334789459371097	0.84930296833471
5	0.335431675462501	0.85176756049067
6	0.335481776200068	0.85196022970102
7	0.335485747325945	0.85197550369182
8	0.335486062735084	0.85197671685368
9	0.335486087792330	0.85197681323175
10	0.335486089783014	0.85197682088855
11	0.335486089941165	0.85197682149685
12	0.335486089953730	0.85197682154518
13	0.335486089954728	0.85197682154902
14	0.335486089954807	0.85197682154932
15	0.335486089954813	0.85197682154935
16	0.335486089954814	0.85197682154935

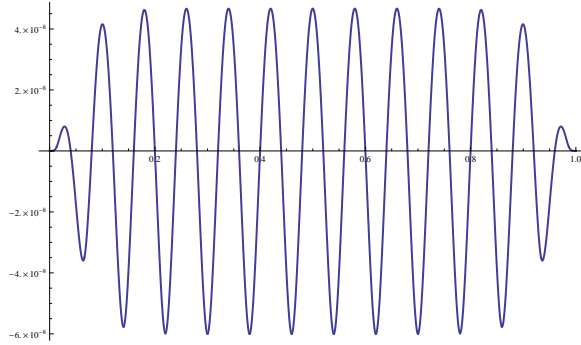


Figure 1: Graph of the Peano kernel $K(Q_{14}^G; t)$.

Figure 1 depicts the graph of $K(Q_{14}^G; t)$. Typically, except for small neighborhoods of the end-points, the graphs of Peano kernels of Q_n^G have nearly equioscillating behavior.

In Table 2 we give the numerically computed weights and nodes of Q_n^G , $3 \leq n \leq 16$.

Table 2: Numerical values of $a_{k,n}$ and $\tau_{k,n}$, $3 \leq n \leq 16$.

$n = 3$			$n = 4$		
k	$a_{k,n}$	$\tau_{k,n}$	k	$a_{k,n}$	$\tau_{k,n}$
1	0.272023100502	0.108626437068	1	0.169860593667	0.066957891874
2	0.455953798995	0.5	2	0.330139406333	0.327589851637
$n = 5$			$n = 6$		
k	$a_{k,n}$	$\tau_{k,n}$	k	$a_{k,n}$	$\tau_{k,n}$
1	0.121681080070	0.047918810780	1	0.094662247744	0.037275752911
2	0.240818518494	0.235892149497	2	0.187625219419	0.183590462413
3	0.275000802872	0.5	3	0.217712532836	0.390423386607
$n = 7$			$n = 8$		
k	$a_{k,n}$	$\tau_{k,n}$	k	$a_{k,n}$	$\tau_{k,n}$
1	0.077452318517	0.030498704302	1	0.065536670527	0.025806620210
2	0.153532519291	0.150218100952	2	0.129913541965	0.127108142991
3	0.178389487078	0.319539393216	3	0.150962568586	0.270386360944
4	0.181251350226	0.5	4	0.153587218922	0.423163380281
$n = 9$			$n = 10$		
k	$a_{k,n}$	$\tau_{k,n}$	k	$a_{k,n}$	$\tau_{k,n}$
1	0.056798454215	0.022365739186	1	0.050116283582	0.019734475870
2	0.112591833470	0.110160426334	2	0.099345742221	0.097200378683
3	0.130835439531	0.234335319538	3	0.115443119942	0.206766491600
4	0.133124180172	0.366747560705	4	0.117463581772	0.323601207025
5	0.133300185222	0.5	5	0.117631272483	0.441181733408
$n = 11$			$n = 12$		
k	$a_{k,n}$	$\tau_{k,n}$	k	$a_{k,n}$	$\tau_{k,n}$
1	0.044840885342	0.017657162628	1	0.040570324835	0.015975528093
2	0.088888296156	0.086968760052	2	0.080422744176	0.078686021012
3	0.103291218626	0.185001600106	3	0.093453960144	0.167382400266
4	0.105099070267	0.289537951780	4	0.095089640470	0.261962910908
5	0.105249990501	0.394741925098	5	0.095226250692	0.357147482937
6	0.105261078217	0.5	6	0.095237079683	0.452381290909
$n = 13$			$n = 14$		
k	$a_{k,n}$	$\tau_{k,n}$	k	$a_{k,n}$	$\tau_{k,n}$
1	0.037042470502	0.014586351737	1	0.034079072862	0.013419443598
2	0.073429462076	0.071843758317	2	0.067555105110	0.066096257651
3	0.085327528859	0.152827408950	3	0.078501326552	0.140601216235
4	0.086820976478	0.239183527506	4	0.079875298389	0.220048845317
5	0.086945712143	0.326091182023	5	0.079990055537	0.300003887604
6	0.086955657318	0.413043811901	6	0.079999209332	0.380000308747
7	0.086956385250	0.5	7	0.079999932217	0.460000022620

$n = 15$			$n = 16$		
k	$a_{k,n}$	$\tau_{k,n}$	k	$a_{k,n}$	$\tau_{k,n}$
1	0.031554697094	0.012425410739	1	0.029378511088	0.011568485861
2	0.062551023250	0.061200238566	2	0.058237159578	0.056979532458
3	0.072686413475	0.130186311329	3	0.067673557373	0.121207945030
4	0.073958609621	0.203748930850	4	0.068858015854	0.189697280446
5	0.074064866264	0.277781377422	5	0.068956944455	0.258624041049
6	0.074073342303	0.351852137857	6	0.068964835967	0.327586473189
7	0.074074015543	0.425925948494	7	0.068965463124	0.396551745297
8	0.074074064900	0.5	8	0.068965512559	0.465517243060

Acknowledgments.

The authors are supported by Sofia University Research Foundation through Contract 181/2012.

References

- [1] Bojanov, B. D.: Uniqueness of the monosplines of least deviation. In: "Numerische Integration" (G. Hämmerlin, Ed.), ISNM 45, Birkhäuser, Basel, 1979, 67–97.
- [2] Bojanov, B. D.: Existence and characterization of monosplines of least L_p deviation. In: "Constructive Function Theory '77" (Bl. Sendov and D. Vačov, Eds), Sofia, BAN, 1980, 249–268.
- [3] Bojanov, B. D.: Uniqueness of the optimal nodes of quadrature formulae, Math. Comput. 36 (1981), 525–546.
- [4] Braß, H.: Quadraturverfahren. Vandenhoeck & Ruprecht, Göttingen (1977).
- [5] Karlin, S., Micchelli, C. A.: The fundamental theorem of algebra for monosplines satisfying boundary conditions. Israel J. Math. 11 (1972), 405–451.
- [6] Köhler, P., Nikolov, G. P.: Error bounds for Gauss type quadrature formulae related to spaces of splines with equidistant knots. J. Approx. Theory 81, no. 3 (1995), 368–388.
- [7] Nikolov, G.: Gaussian quadrature formulae for splines. In: Numerische Integration, IV, (G. Hämmerlin and H. Brass, Eds.), ISNM Vol. 112, Birkhäuser, Basel, 1993, 267–281.
- [8] Nikolov, G.: On certain definite quadrature formulae. J. Comput. Appl. Math. 75 (1996), 329–343.
- [9] Nikolov, G., Simian, C.: Gauss-type quadrature formulae for parabolic splines with equidistant knots. In: Approximation and Computation - In Honor of Gradimir V. Milovanovic (W. Gautschi, G. Mastroianni, Th. M. Rassias, eds.),

Springer Optimization and its Applications, Springer Verlag, Berlin - Heidelberg
- New York, 2010, 207–229.

ON THE FACTORIZATION OF ROTATIONS

Danail S. Brezov, Clementina D.Mladenova, Ivailo
M.Mladenov

University of Architecture, Civil Engineering and Geodesy
1 Hristo Smirnenski Blvd., Sofia 1046, Bulgaria
e-mail: danail.brezov@gmail.com

Institute of Mechanics, Bulgarian Academy of Sciences
Acad. G. Bonchev Str., Bl. 4, Sofia 1113, Bulgaria
e-mail: clem@imbm.bas.bg

Institute of Biophysics, Bulgarian Academy of Sciences
Acad. G. Bonchev Str., Bl. 21, Sofia 1113, Bulgaria
e-mail: mladenov@obzor.bio21.bas.bg

1 Introduction

The orthogonal group in \mathbb{R}^3 is somewhat special not only due to its various physical applications, but also because for $n = 3$ we have an isomorphism between one-forms and two-forms given by the *Hodge* duality $*$: $\Lambda^k(\mathbb{R}^n) \rightarrow \Lambda^{n-k}(\mathbb{R}^n)$, which in this particular case can be interpreted as a one-to-one correspondence between vectors and skew-symmetric matrices in \mathbb{R}^3 . Since the latter constitute the Lie algebra $\mathfrak{so}(3)$, this allows the standard representation of the rotation generators to be given by the exceptional formula $*$: $\mathbf{c} \rightarrow \mathcal{A}(\mathbf{c}) = \mathbf{c}^\times$, or in components $\mathbf{c}_{ij}^\times = \varepsilon_{ilj}c_l$, where ε_{ilj} are the entries of the *Levi-Civita* symbol and the summation is performed over repeated indices following *Einstein* convention. In this way any skew-symmetrical matrix \mathcal{A} can be easily written in the form

$$\mathcal{A}(\mathbf{c}) = \begin{pmatrix} 0 & -c_3 & c_2 \\ c_3 & 0 & -c_1 \\ -c_2 & c_1 & 0 \end{pmatrix}. \quad (1)$$

Geometrically the so-called *vector-parameter* \mathbf{c} determines the axis of rotation and its magnitude is connected to the angle of rotation φ by the simple formula

$$\mathbf{c}^2 = \tan^2 \frac{\varphi}{2}. \quad (2)$$

Then the actual matrix of the corresponding orthogonal operator can be obtained in the standard way as $\mathcal{R} = \exp \mathcal{A}$, or alternatively, using *Cayley* representation

$$\mathcal{R} = \frac{\mathcal{I} + \mathcal{A}}{\mathcal{I} - \mathcal{A}} \quad (3)$$

where \mathcal{I} is the identity operator. The above can be expanded in geometric-type series, which is easily reduced to a polynomial, due to *Hamilton-Cayley* theorem. As a consequence we have

$$\mathcal{R}(\mathbf{c}) = \frac{(1 - \mathbf{c}^2) \mathcal{I} + 2 \mathbf{c} \otimes \mathbf{c}^t + 2 \mathbf{c}^\times}{1 + \mathbf{c}^2} \quad (4)$$

which is the main formula we rely on for the derivation of our result. The procedure of obtaining it, however, involves a couple of more tricks besides using the characteristic equation of \mathcal{A} and is explained in detail in [4, 7, 10]. We use it without proof and let the reader catch up with the technicalities. Here and bellow $\mathbf{c} \otimes \mathbf{c}^t$ stands for the usual tensor product of vectors used for the construction of projectors that is in components $(\mathbf{c} \otimes \mathbf{c}^t)_{ij} = c_i c_j$.

Expression (4) can also be written as

$$\mathcal{R}(\mathbf{c}) = \frac{2}{1 + \mathbf{c}^2} \begin{pmatrix} 1 + c_1^2 & c_1 c_2 - c_3 & c_1 c_3 + c_2 \\ c_1 c_2 + c_3 & 1 + c_2^2 & c_2 c_3 - c_1 \\ c_3 c_1 - c_2 & c_3 c_2 + c_1 & 1 + c_3^2 \end{pmatrix} - \mathcal{I}. \quad (5)$$

There is a composition law for the vector parameters that comes quite handy for our considerations. Namely, from the group properties of the $\text{SO}(3)$ matrices it can be derived that the vector parameter of the composition $\mathcal{R}(\mathbf{a}) \mathcal{R}(\mathbf{c}) = \mathcal{R}(\langle \mathbf{a}, \mathbf{c} \rangle)$ can be written as

$$\langle \mathbf{a}, \mathbf{c} \rangle = \frac{\mathbf{a} + \mathbf{c} + \mathbf{a} \times \mathbf{c}}{1 - (\mathbf{a}, \mathbf{c})}. \quad (6)$$

One more time we refer to [4] for the details. It is not so difficult to write a similar formula for a composition of three rotations. In that case it can be shown that the vector parameter of $\mathcal{R}(\mathbf{a}) \mathcal{R}(\mathbf{b}) \mathcal{R}(\mathbf{c})$ is just

$$\langle \langle \mathbf{a}, \mathbf{b} \rangle, \mathbf{c} \rangle = \frac{\mathbf{a} + \mathbf{b} + \mathbf{c} + \mathbf{a} \times \mathbf{b} + \mathbf{a} \times \mathbf{c} + \mathbf{b} \times \mathbf{c} + (\mathbf{a} \times \mathbf{b}) \times \mathbf{c} - (\mathbf{a}, \mathbf{b}) \mathbf{c}}{1 - (\mathbf{a}, \mathbf{b}) - (\mathbf{a}, \mathbf{c}) - (\mathbf{b}, \mathbf{c}) - (\mathbf{a}, \mathbf{b} \times \mathbf{c})}. \quad (7)$$

Note that this operation is associative, but not commutative unless the vectors are parallel.

It should be mentioned that the vector-parameter is known also as the Gibbs' or Rodrigues' vector. Some authors call it also a vector of finite rotations. The vector

representation of rotations in three-dimensional space \mathbb{R}^3 is a principal subject of consideration in many papers and a far from exhaustive list includes [1], [7], [13], and references therein. Actually, Fedorov [4] explores the vector-parametrization mainly in the context of problems related to the Lorentz group while two of the present authors are among the first who make use of it in the classical [8] and quantum mechanics [6].

2 The Generic Case

Suppose we are given a special orthogonal matrix \mathcal{R} - either by Gram-Schmidt procedure, or due to the axis-angle representation of rotations (i.e., the Rodrigues' formula [12])

$$\mathcal{R}(\mathbf{n}, \varphi) = \cos \varphi \mathcal{I} + (1 - \cos \varphi) \hat{\mathbf{n}} \otimes \hat{\mathbf{n}}^t + \sin \varphi \hat{\mathbf{n}}^\times \quad (8)$$

Let us choose three unit vectors $\hat{\mathbf{c}}_k$, possibly coplanar, but such that $\hat{\mathbf{c}}_2$ is not parallel to any of the other two. These will play the role of axes of rotations in our decomposition

$$\mathcal{R}(\mathbf{c}) = \mathcal{R}_3(w\hat{\mathbf{c}}_3)\mathcal{R}_2(v\hat{\mathbf{c}}_2)\mathcal{R}_1(u\hat{\mathbf{c}}_1) \quad (9)$$

where $\mathbf{c} = \tan \frac{\varphi}{2} \hat{\mathbf{c}}$, $|\hat{\mathbf{c}}| = 1$ and the scalar parameters u, v, w play the role of vector magnitudes so construction (5) becomes

$$\mathcal{R}(c\hat{\mathbf{c}}) = \frac{2}{1+c^2} \begin{pmatrix} 1+c^2\hat{c}_1^2 & c^2\hat{c}_1\hat{c}_2 - c\hat{c}_3 & c^2\hat{c}_1\hat{c}_3 + c\hat{c}_2 \\ c^2\hat{c}_1\hat{c}_2 + c\hat{c}_3 & 1+c^2\hat{c}_2^2 & c^2\hat{c}_2\hat{c}_3 - c\hat{c}_1 \\ c^2\hat{c}_1\hat{c}_3 - c\hat{c}_2 & c^2\hat{c}_2\hat{c}_3 + c\hat{c}_1 & 1+c^2\hat{c}_3^2 \end{pmatrix} - \mathcal{I} \quad (10)$$

with $c = |\mathbf{c}|$.

This formula will be used repeatedly for specifying the matrix entries of \mathcal{R}_k once the corresponding scalar parameter is calculated.

In order to find the equations for u, v and w we use (9) and suitably chosen scalar products (see also [9]). Let us start with

$$(\hat{\mathbf{c}}_3, \mathcal{R}(\mathbf{c}) \hat{\mathbf{c}}_1) = (\hat{\mathbf{c}}_3, \mathcal{R}_3(w\hat{\mathbf{c}}_3)\mathcal{R}_2(v\hat{\mathbf{c}}_2)\mathcal{R}_1(u\hat{\mathbf{c}}_1) \hat{\mathbf{c}}_1) = (\hat{\mathbf{c}}_3, \mathcal{R}_2(v\hat{\mathbf{c}}_2) \hat{\mathbf{c}}_1) \quad (11)$$

where we use the fact that $\hat{\mathbf{c}}_1$ is an eigenvector for \mathcal{R}_1 with eigenvalue equal to one and so is $\hat{\mathbf{c}}_3$ for \mathcal{R}_3 for any value of their scalar parameters. In combination with (4) this leads to a quadratic equation for v in the form

$$(\sigma_{31} + \kappa_{31} - 2\kappa_{12}\kappa_{23})v^2 + 2\omega v + \sigma_{31} - \kappa_{31} = 0 \quad (12)$$

in which for simplicity we use the notation $\kappa_{ij} = (\hat{\mathbf{c}}_i, \hat{\mathbf{c}}_j)$, $\sigma_{ij} = (\hat{\mathbf{c}}_i, \mathcal{R}(\mathbf{c})\hat{\mathbf{c}}_j)$ and $\omega = (\hat{\mathbf{c}}_1, \hat{\mathbf{c}}_2 \times \hat{\mathbf{c}}_3)$. This equation has real solutions whenever its discriminant is non-negative, that is

$$\omega^2 = \det(\kappa) \geq \sigma_{31}^2 - \kappa_{31}^2 - 2\kappa_{12}\kappa_{23}(\sigma_{31} - \kappa_{31}). \quad (13)$$

Taking into account that κ is symmetric with diagonal elements equal to one, we may easily write its determinant as

$$\det(\kappa) = 1 + 2\kappa_{12}\kappa_{23}\kappa_{13} - \kappa_{12}^2 - \kappa_{13}^2 - \kappa_{23}^2$$

which allows for expressing the above inequality as

$$\begin{vmatrix} 1 & \kappa_{12} & \sigma_{31} \\ \kappa_{21} & 1 & \kappa_{23} \\ \sigma_{31} & \kappa_{32} & 1 \end{vmatrix} \geq 0. \quad (14)$$

Thus we recover the condition

$$(\hat{\mathbf{c}}_1, (\mathcal{R}(\mathbf{c}) - \hat{\mathbf{c}}_2 \otimes \hat{\mathbf{c}}_2^t) \hat{\mathbf{c}}_3)^2 \leq \left(1 - (\hat{\mathbf{c}}_1, \hat{\mathbf{c}}_2)^2\right) \left(1 - (\hat{\mathbf{c}}_3, \hat{\mathbf{c}}_2)^2\right) \quad (15)$$

given in [11]. We encourage the reader to go through the article for the authors' derivation of this formula and a detailed proof why it should be considered as a necessary and sufficient condition (provided $\hat{\mathbf{c}}_2$ is not parallel to either $\hat{\mathbf{c}}_1$ or $\hat{\mathbf{c}}_3$) for the existence of the decomposition (9). We use it to test whether or not certain choice of the rotational axes is appropriate for a given orthogonal matrix.

If it is, we may solve the above equation for v and use the two roots v_{\pm} for the computation of the respective matrix entries of \mathcal{R}_1 in the same way

$$(\hat{\mathbf{c}}_3, \mathcal{R}(\mathbf{c}) \hat{\mathbf{c}}_2) = (\hat{\mathbf{c}}_3, \mathcal{R}_3(w \hat{\mathbf{c}}_3) \mathcal{R}_2(v_{\pm} \hat{\mathbf{c}}_2) \mathcal{R}_1(u \hat{\mathbf{c}}_1) \hat{\mathbf{c}}_2) = (\hat{\mathbf{c}}_3, \mathcal{R}_2(v_{\pm} \hat{\mathbf{c}}_2) \mathcal{R}_1(u \hat{\mathbf{c}}_2) \hat{\mathbf{c}}_2)$$

and this leads to a pair of quadratic equations for the scalar parameter u

$$((\sigma_{32} + \kappa_{32})(1 + v_{\pm}^2) + 2\kappa_{12}\nu_{\pm}) u^2 + 2\mu_{\pm}u + (\sigma_{32} - \kappa_{32})(1 + v_{\pm}^2) = 0 \quad (16)$$

where

$$\begin{aligned} \nu_{\pm} &= \kappa_{13}(v_{\pm}^2 - 1) - 2\kappa_{12}\kappa_{23}v_{\pm}^2 + 2\omega v_{\pm} \\ \mu_{\pm} &= \omega(v_{\pm}^2 - 1) + 2(\kappa_{12}\kappa_{23} - \kappa_{13})v_{\pm}. \end{aligned} \quad (17)$$

Hence we have four solutions for u . Now it remains to determine the value of w by exploiting the equality

$$\begin{aligned} (\hat{\mathbf{c}}_2, \mathcal{R}(\mathbf{c}) \hat{\mathbf{c}}_1) &= (\hat{\mathbf{c}}_2, \mathcal{R}_3(w \hat{\mathbf{c}}_3) \mathcal{R}_2(v_{\pm} \hat{\mathbf{c}}_2) \mathcal{R}_1(u \hat{\mathbf{c}}_1) \hat{\mathbf{c}}_1) \\ &= (\hat{\mathbf{c}}_2, \mathcal{R}_3(w \hat{\mathbf{c}}_3) \mathcal{R}_2(v_{\pm} \hat{\mathbf{c}}_2) \hat{\mathbf{c}}_1) \end{aligned}$$

from which we derive the corresponding quadratic equations

$$((\sigma_{21} + \kappa_{21})(v_{\pm}^2 + 1) + 2\kappa_{23}\nu_{\pm}) w^2 + 2\mu_{\pm}w + (\sigma_{21} - \kappa_{21})(v_{\pm}^2 + 1) = 0. \quad (18)$$

In this way we end up with eight candidates for *Euler* decomposition, since each of the three quadratic equations has two solutions in the generic case. To choose the actual solution or solutions to the problem among these eight possibilities one may simply compare their matrix entries with the corresponding entries of $\mathcal{R}(\mathbf{c})$ or evaluate the norm of the matrix difference.

On the other hand, using representation (10) and the composition law for the vector parameters (7), we can start with the defining relation

$$\langle \mathbf{c}_3, \langle \mathbf{c}_2, \mathbf{c}_1 \rangle \rangle = \mathbf{c}$$

in order to derive one more condition. This can be achieved by multiplying both sides of the equality with $\hat{\mathbf{c}}_k$, $k = 1, 2, 3$ and in this way to obtain the following system of relations for the scalar parameters

$$\begin{aligned} (\omega\xi_1+\kappa_{23})uvw + (\omega-\kappa_{23}\xi_1)vw - \kappa_{12}\xi_1uv - \kappa_{13}\xi_1uw + \xi_1 &= u + \kappa_{12}v + \kappa_{13}w \\ (\omega\xi_2-\kappa_{13})uvw - (\omega+\kappa_{13}\xi_2)uw - \kappa_{12}\xi_1uv - \kappa_{23}\xi_1vw + \xi_2 &= v + \kappa_{12}u + \kappa_{23}w \\ (\omega\xi_3+\kappa_{12})uvw + (\omega-\kappa_{12}\xi_3)vw - \kappa_{13}\xi_3uw - \kappa_{23}\xi_3vw + \xi_3 &= w + \kappa_{13}u + \kappa_{23}v \end{aligned}$$

where we make use of the notation $\xi_k = (\mathbf{c}, \hat{\mathbf{c}}_k) = (\hat{\mathbf{c}}, \hat{\mathbf{c}}_k) \tan \frac{\varphi}{2}$.

The above formulae might be used as a base for an alternative algorithm and we encourage the reader to give it a try. However, our approach, described in detail below, is based on (12), (16) and (18).

3 The Symmetric Case

We consider the particular case of a symmetric orthogonal matrix

$$\mathcal{O}(\hat{\mathbf{n}}) = 2\hat{\mathbf{n}} \otimes \hat{\mathbf{n}} - \mathcal{I} = \mathcal{R}(\hat{\mathbf{n}}, \pi) \quad (19)$$

that is basically a rotation by an angle π about the axis specified by the unit vector $\hat{\mathbf{n}}$. It is easy to see that $-\mathcal{O}(\hat{\mathbf{n}})$ is a mirror reflection with respect to the plane normal to $\hat{\mathbf{n}}$.

Applying directly the ideas from the previous section we find the analogue of (12) to be

$$(\tau_1\tau_3 - \kappa_{12}\kappa_{23})v^2 + \omega v + \tau_1\tau_3 - \kappa_{13} = 0 \quad (20)$$

where $\tau_i = (\hat{\mathbf{n}}, \hat{\mathbf{c}}_i)$, with the condition for the discriminant

$$\omega^2 = \det(\kappa) \geq 4(\tau_1\tau_3 - \kappa_{12}\kappa_{23})(\tau_1\tau_3 - \kappa_{13}) \quad (21)$$

which can also be written as

$$4(\tau_1\tau_3 - \kappa_{12}\kappa_{23} - \kappa_{13})\tau_1\tau_3 \leq 1 - 2\kappa_{12}\kappa_{23}\kappa_{13} - \kappa_{12}^2 - \kappa_{13}^2 - \kappa_{23}^2. \quad (22)$$

Similarly from (16) and (18) we get

$$(\tau_2\tau_3(v_{\pm}^2 + 1) + \kappa_{12}\nu_{\pm})u^2 + \mu_{\pm}u + (\tau_2\tau_3 - \kappa_{23})(v_{\pm}^2 + 1) = 0 \quad (23)$$

from which we derive u and for w

$$(\tau_1\tau_2(v_{\pm}^2 + 1) + \kappa_{23}\nu_{\pm})w^2 + \mu_{\pm}w + (\tau_1\tau_2 - \kappa_{12})(v_{\pm}^2 + 1) = 0. \quad (24)$$

All the considerations in the previous section are applicable here except for the relations derived from the composition law for the vector parameters as the denominator of (7) vanishes in the symmetric case. This can be concluded directly from (10). One

way to make it symmetric is to set the scalar parameter equal to zero, but then one gets the identity matrix. The other possibility is to take the limit $c \rightarrow \infty$ in (10). And this is the only way to end up with a half turn of the type (19). Since this limiting procedure yields a vanishing denominator for the composed vector parameters in (7), we have another independent condition that in our notation reads

$$(\mathbf{c}_1, \mathbf{c}_2) + (\mathbf{c}_1, \mathbf{c}_3) + (\mathbf{c}_2, \mathbf{c}_3) + (\mathbf{c}_1, \mathbf{c}_2 \times \mathbf{c}_3) = 1.$$

In terms of the scalar parameters it can be rewritten as

$$\kappa_{12}uv + \kappa_{13}uw + \kappa_{23}vw + \omega uvw = 1. \quad (25)$$

One should be careful though when applying the above formula - there is a simple geometrical condition to decide whether it can be written as an explicit function for certain variable. For example one can solve for $w = w(u, v)$ if the vector $\mathbf{c}_1 + \mathbf{c}_2 + \mathbf{c}_1 \times \mathbf{c}_2$ does not lie in the plane normal to \mathbf{c}_3 , or equivalently $(\mathbf{c}_1, \mathbf{c}_2) \neq 1$. In a similar way one may write it as an explicit function $u = u(v, w)$ whenever $\mathbf{c}_2 + \mathbf{c}_3 + \mathbf{c}_2 \times \mathbf{c}_3$ is not parallel to \mathbf{c}_1 , or in other words $(\mathbf{c}_2, \mathbf{c}_3) \neq 1$. It can be easily shown that in the *Euler* case (25) is reduced to $uw = 1$, while we will have $uvw + 1 = 0$ for the so-called *Bryan* decomposition. Both cases are exemplified in full detail in [2].

4 Decomposition Into Two Rotations

There is one more question that can be discussed in the present context. Namely, in certain cases one can ask if it is possible to write the vector decomposition for two, rather than three, rotational matrices, i.e.,

$$\mathcal{R}(\mathbf{c}) = \mathcal{R}_2(\mathbf{c}_2) \mathcal{R}_1(\mathbf{c}_1). \quad (26)$$

Then we have to specify only two parameters, but accordingly much less relations to work with. Generally speaking, it is not clear whether such a representation is possible at all, and a consistent treatment of the problem should clarify what conditions have to be fulfilled in order to allow it. If we apply the same approach as we did in the generic case, we end up with a much simplified relations for the parameters

$$\begin{aligned} (\hat{\mathbf{c}}_2, \mathcal{R}(\mathbf{c}) \hat{\mathbf{c}}_1) &= (\hat{\mathbf{c}}_2, \mathcal{R}_2(v \hat{\mathbf{c}}_2) \mathcal{R}_1(u \hat{\mathbf{c}}_1) \hat{\mathbf{c}}_1) = (\hat{\mathbf{c}}_2, \hat{\mathbf{c}}_1) \\ (\hat{\mathbf{c}}_2, \mathcal{R}(\mathbf{c}) \hat{\mathbf{c}}_2) &= (\hat{\mathbf{c}}_2, \mathcal{R}_2(v \hat{\mathbf{c}}_2) \mathcal{R}_1(u \hat{\mathbf{c}}_1) \hat{\mathbf{c}}_2) = (\hat{\mathbf{c}}_2, \mathcal{R}_1(u \hat{\mathbf{c}}_1) \hat{\mathbf{c}}_2) \\ (\hat{\mathbf{c}}_1, \mathcal{R}(\mathbf{c}) \hat{\mathbf{c}}_1) &= (\hat{\mathbf{c}}_1, \mathcal{R}_2(v \hat{\mathbf{c}}_2) \mathcal{R}_1(u \hat{\mathbf{c}}_1) \hat{\mathbf{c}}_1) = (\hat{\mathbf{c}}_1, \mathcal{R}_2(v \hat{\mathbf{c}}_2) \hat{\mathbf{c}}_1). \end{aligned}$$

From the first equation we have $\sigma_{21} = \kappa_{21}$ which can be considered as a necessary condition for the existence of the decomposition (26). In [11] it is shown that this condition is also sufficient provided that $\kappa_{12} \neq \pm 1$ (as in this case we have parallel axes and there is nothing to do). Then from the second and the third we easily get the solutions for the scalar parameters u and v in the form

$$u_{\pm} = \pm \sqrt{\frac{1 + \sigma_{22} - 2\kappa_{12}^2}{1 - \sigma_{22}}} = \pm \frac{\sqrt{\cos^2 \frac{\theta_2}{2} - \cos^2 \frac{\gamma}{2}}}{\sin \frac{\theta_2}{2}} \quad (27)$$

$$v_{\pm} = \pm \sqrt{\frac{1 + \sigma_{11} - 2\kappa_{12}^2}{1 - \sigma_{11}}} = \pm \frac{\sqrt{\cos^2 \frac{\theta_1}{2} - \cos^2 \frac{\gamma}{2}}}{\sin \frac{\theta_1}{2}} \quad (28)$$

where γ is the angle between $\hat{\mathbf{c}}_1$ and $\hat{\mathbf{c}}_2$, and θ_k - those by which $\mathcal{R}(\mathbf{c})$ rotates $\hat{\mathbf{c}}_k$. A simple geometrical argument shows that the denominators cannot vanish unless $\mathbf{c}_1 \parallel \mathbf{c}_2$ or $\mathbf{c} \perp \mathbf{c}_{1,2}$ which needs to be discussed separately. Note that in the particular case of perpendicular axes, we have

$$u_{\pm} = \pm \cot \frac{\theta_2}{2}, \quad v_{\pm} = \pm \cot \frac{\theta_1}{2}$$

which gives a direct expression for the angular parameters $\psi_1^{\pm} = 2 \arctan u_{\pm}$, $\psi_2^{\pm} = 2 \arctan v_{\pm}$ in terms of the angles ψ_k and hence, in terms of φ - the angular parameter in $\mathcal{R}(\mathbf{c})$. Namely, we have in this case

$$\psi_1^{\pm} = \pm |\pi - \theta_2|, \quad \psi_2^{\pm} = \pm |\pi - \theta_1|$$

and the connection between the angles ψ_k and φ becomes apparent from Rodrigues' formula (8) because after taking the appropriate scalar products one ends up with

$$\cos \theta_k = \cos \varphi + (1 - \cos \varphi) \cos^2 \beta_k, \quad \beta_k = \angle(\mathbf{c}, \hat{\mathbf{c}}_k). \quad (29)$$

Also note that (27) demands an additional pair of conditions

$$1 + \sigma_{kk}^2 \geq 2\sigma_{21}^2, \quad k = 1, 2$$

to be fulfilled in order to guarantee real solutions.

Written as a condition for the angles, the latter inequality becomes $|\theta_k| \leq 2|\gamma|$ which can be shown to follow directly from the condition $\sigma_{21} = \kappa_{21}$.

Here we can easily add also a couple of relations if we take into account that by the very construction and $\mathcal{R}_1^{-1}(\mathbf{c}_1) = \mathcal{R}_1(-\mathbf{c}_1)$, $\mathcal{R}_2^{-1}(\mathbf{c}_2) = \mathcal{R}_2(-\mathbf{c}_2)$ we have

$$\langle \mathbf{c}, -\mathbf{c}_1 \rangle = \mathbf{c}_2, \quad \langle -\mathbf{c}_2, \mathbf{c} \rangle = \mathbf{c}_1$$

which produce directly

$$u = \frac{\xi_1 - \kappa_{12}}{1 - \kappa_{12}\xi_1}, \quad v = \frac{\xi_2 - \kappa_{12}}{1 - \xi_2\kappa_{12}}. \quad (30)$$

The easiest solution once more appears to be the case of perpendicular axes $\kappa_{12} = 0$. Then we have $u = \xi_1$ and $v = \xi_2$. Since these solutions are bound to coincide with the obtained above, we have

$$\tan \frac{\psi_1}{2} = \tan \frac{\varphi}{2} \cos \beta_1, \quad \tan \frac{\psi_2}{2} = \tan \frac{\varphi}{2} \cos \beta_2. \quad (31)$$

It is time to discuss the problem of vanishing denominators in our equations (27), (28) or (30). This phenomenon is quite natural to appear since the scalar parameters

are allowed to take infinite values in the symmetric case. In particular $\mathcal{R}(\mathbf{c})$ can be symmetric as well - for example a half turn about OZ that is being decomposed into a product of two half turns (about OX and OY respectively) or two mirror reflections with respect to perpendicular lines, as basic geometry teaches us. We can still come up with a solution: whenever $\sigma_{kk} = 1$ it is clear that $\psi_k = \pi$ (we exclude the trivial case $\mathcal{R}(\mathbf{c}) = \mathcal{I}$) and although the corresponding scalar parameter diverges, we can construct the matrix \mathcal{R}_k using the standard representation (19).

5 The Algorithm

The input data at the start consist of a rotational matrix \mathcal{R} and the vectors $\mathbf{c}_1, \mathbf{c}_2, \mathbf{c}_3$ along the prescribed axes. At the first stage the calculations produce either the vector \mathbf{c} or $\hat{\mathbf{n}}$. First we make all vectors with unit length by a simple re-scaling $\mathbf{v} \rightarrow \hat{\mathbf{v}} = \frac{\mathbf{v}}{|\mathbf{v}|}$.

After that we make an attempt to factorize \mathcal{R} into a product of rotations about two of the given axes and this will be successful provided that the conditions mentioned above are satisfied. The procedure is based on the equations (27), (28) and (30). If this is not possible, we apply the scheme for decomposition into three rotational matrices. To start with, we calculate all scalar products and other coefficients involved in the equations (12), (16) and (18) - that is ω , κ_{ij} , σ_{ij} and ξ_i as well as $v_{\pm}^2 \pm 1$, ν_{\pm} and μ_{\pm} , so that these expressions do not have to be computed repeatedly. Next we construct a procedure to calculate the matrices $\mathcal{R}_1(u \hat{\mathbf{c}}_1)$, $\mathcal{R}_2(v \hat{\mathbf{c}}_2)$ and $\mathcal{R}_3(w \hat{\mathbf{c}}_3)$ based on formula (10).

Before moving on we need to check whether the necessary and sufficient conditions for the existence of a generalized *Euler* representation are fulfilled, namely that the vector \mathbf{c}_2 is not parallel to any of the other two vectors \mathbf{c}_1 and \mathbf{c}_3 together with the inequality for the discriminant (15). If so, we proceed to solving equation (12), then substitute its roots v_{\pm} in (16) and (18) and solve them for u and w . Having all these solutions, we calculate each of the matrices \mathcal{R}_k using the previously designed for this procedure based on (10), obtain the product $\mathcal{R}_3 \mathcal{R}_2 \mathcal{R}_1$ and check whether it has the same matrix entries as $\mathcal{R}(\mathbf{c})$ or, as we did in our programme, if the norm of $\mathcal{R} - \mathcal{R}_3 \mathcal{R}_2 \mathcal{R}_1$ vanishes (within the machine precision as far as numerical operations are involved). If not, we continue searching for a true solution up to exhausting all possibilities. Since the solution may not be unique, and in fact in most cases there are two corresponding respectively to v_+ and v_- , we have to choose the most “economic” one from the practical point of view. As a measure of “effectiveness” we can use the cost or penalty function $\mathcal{C}(u, v, w)$ defined as the sum of squares $u^2 + v^2 + w^2$ of the computed scalar parameters.

6 Numerical Tests

Our first example is from [13]. Namely, we consider the rotation by an angle $\varphi = 30^\circ$ about an axis, given by the vector $\hat{\mathbf{c}}$ with coordinates on the unit sphere¹ $(\theta, \phi) = (50^\circ, 25^\circ)$. The three axes of rotation are chosen as follows: the first one is OX , the second one is OY , rotated by 60° clockwise in the XOY plane, and finally again OX . As a result for the angular variables our scheme produces (with five digits precision)

$$\begin{aligned}(\psi_1^+, \psi_2^+, \psi_3^+) &= (178.50326, -108.73792, -40.54766) \\(\psi_1^-, \psi_2^-, \psi_3^-) &= (-102.27231, 108.73792, 38.67676)\end{aligned}$$

which is in complete accordance with the results presented in [13].

If we choose for the third rotation the axis given by a vector with coordinates $(\theta, \phi) = (80^\circ, 45^\circ)$ on the unit sphere and keep everything else as it was before, the results becomes

$$\begin{aligned}(\psi_1^+, \psi_2^+, \psi_3^+) &= (-139.78921, 179.27102, -12.20974) \\(\psi_1^-, \psi_2^-, \psi_3^-) &= (33.72840, -4.496982, 48.63548)\end{aligned}$$

which again agrees with those presented in [13] and [9].

For the scalar parameters we have respectively

$$\begin{aligned}(u_+, v_+, w_+) &= (-2.73183, 157.19197, -0.10695) \\(u_-, v_-, w_-) &= (0.30314, -0.03926, 0.45189)\end{aligned}$$

for the first rotation and

$$\begin{aligned}(u_+, v_+, w_+) &= (76.55670, -1.39519, -0.36939) \\(u_-, v_-, w_-) &= (-1.24092, 1.39519, 0.350947)\end{aligned}$$

for the second one.

These same numbers are obtained in [9] as well, but in order to comply with notation there they are given in the reverse order.

The algorithm we have described here is realized as a MAPLE routine which is freely available and can be downloaded by visiting the web address http://www.bio21.bas.bg/ibf/dpb_files/mfiles/FactorizationRot.mws.

Литература

- [1] M. Borri, L. Trainelli and C. Bottaso: On Representations and Parameterizations of Motion, *Multibody System Dynamics* **4** (2000) 129-193.

¹the convention we use for the azimuthal angle $\theta \in [-\frac{\pi}{2}, \frac{\pi}{2}]$, also adopted from [13], is zero at the equator and 90° at the North Pole.

- [2] D. Brezov, C. Mladenova, I. Mladenov. Vector Decomposition of Half Turns, *To appear in the Proceedings of the IVII-nd Spring Conference of the Union of Bulgarian Mathematicians*, Sofia 2013, pp xxx-zzz.
- [3] P. Davenport. Rotations About Nonorthogonal Axes, *AIAA Journal* **11** (1973) 853-857.
- [4] F. Fedorov. *The Lorentz Group* (in Russian), Science, Moscow 1979.
- [5] L. Fraiture. A History of the Description of the Three-Dimensional Finite Rotation, *J. Astronautical Sciences* **57** (2009) 207-232.
- [6] I. Mladenov and J. Vassileva: A Note on Hibridization, *Commun. Math. Chem.* **11** (1991) 69-73.
- [7] C. Mladenova: Group Theory in the Problems of Modeling and Control of Multi-Body Systems, *J. Geom. Symmetry Phys.* **8** (2006) 17-121.
- [8] C. Mladenova: An Approach to Description of a Rigid Body Motion, *C. R. Acad. Sci. Bulg.* **38** (1985) 1657-1660.
- [9] C. Mladenova, I. Mladenov. Vector Decomposition of Finite Rotations, *Rep. Math. Phys.* **68** (2011) 107-117.
- [10] A. Müller: Group Theoretical Approaches to Vector Parameterization of Rotations, *J. Geom. Symmetry Phys.* **19** (2010) 43-72.
- [11] G. Piovan, F. Bullo. On Coordinate-Free Rotation Decomposition Euler Angles About Arbitrary Axes, *IEEE Transactions on Robotics* **28** (2012) 728-733.
- [12] O. Rodrigues. Des lois géométriques qui regissent les déplacements d'un système solide dans l'espace, et de la variation des coordonnées provenant de ses déplacements considérés indépendamment des causes qui peuvent les produire, *J. Math. Pures Appl.* **5** (1840) 380-440.
- [13] K. Wohlhart: Decomposition of a Finite Rotation into Three Consecutive Rotations About Given Axes, In: *Proc. VI-th Int Conf. on Theory of Machines and Mechanisms*, Czechoslovakia, Liberec 1992, pp 325-332.

SOFIA MUNICIPALITY FEATURES IN GOES PROJECT SYSTEM IMPLEMENTATION

Nina Dobrinkova, Nikodim Lazarov, Valentin Marinov

Institute for Parallel Processing, BAS
Acad. G. Bonchev str. bl.25A
1113 Sofia, Bulgaria

1 Intorduction

Sofia is one of the oldest cities in Europe and the largest city of the Republic of Bulgaria, with almost two million citizens. The boost of the city economy and population cause a lot of environmental, traffic and transport issues that the Municipal Administration has to solve in the next years. The overall objective of Sofia Master Plan is the direct development to a balanced and stable environment of good quality. The transportation system of Sofia is a major part of the national transport system. Three Trans-European Transport Corridors cross the city: 4, 8 and 10. Public transport is well developed, reliable and important to the city's economy; it is provided by means of underground trains, buses, trams and electric buses. More information can be found on <http://www.sofia.bg/en>. GOES project has been coordinated in Sofia municipality by two directorates, which are described in brief. The Directorate - Defense and Civil Mobilization and Crisis Management, is responsible for crisis management in disaster situations; organizes the protection of sites of critical infrastructure in time of war and crisis; develops Sofia Municipality Disaster Protection Plan and organizes its implementation; develops measures for risk prevention, adequate and effective management in case of event and the aftermath of crises of different nature; coordinates activities and tasks to overcome the consequences of crises and for the improvement of early warning system and crisis management by non-military character of the territory of Sofia Municipality; prepares an annual report on risk prevention and crisis actions; organizes the training of voluntary units

and population in case of crises. The Directorate of EU Programs, Projects and Representative Offices, is directly subordinated to the Mayor of Sofia Municipality and is responsible for the organization and coordination of the execution of EU-funded projects in the city. Both directorates are responsible for the project implementation and good results locally on the municipal territory and together with the rest of the GOES consortium partners has achieved incensement of preparedness, awareness and maximum cooperation in an inadequate response to emergency situations by avoiding and solving delays and deficiencies in communication between local actors involved in various capacities in prevention and emergency management. Organized collection on daily basis of all relevant information on road conditions related to any criticisms and suggestions on alternative routes. Developed a network that conveys this information to the regional civil protection structures and to the main network in order to promptly inform citizens based on standardized and automated procedures to exchange across the partner territories. Optimized Sofia municipal systems for collecting and transmitting information concerning the civil protection particularly on natural disasters. Achieved faster response times to the emergency protection system. Disseminate information among the relevant stakeholders and public bodies. Created a database of the natural disasters which impact on the feasibility of the road. Trained Sofia municipal staff for first reaction and response.

2 IICT-BAS and Helix LTD software development efforts

According to the collected data by every test case area in the framework of GOES project [1, 2] a common vision for the system design has been done and implemented in a way to share information on some issues, related to traffic management in Sofia municipality. The system allow the interaction between mobile groups on the roads and devices called "mobile" such as PDA or tablet, and Server based environment to exchange data via the web application and support the everyday work of the responsible authorities. This was developed with various services available as open source including those communication, management and publication of information in a geographic context. Helix LTD has developed the software basis and IICT-BAS has adapted and modified it according to the Sofia municipal needs. The system architecture includes OpenLayers as a free released JavaScript library, which is working with FreeBSD allowing the inclusion of a map in a web page. The platform is used so widely around the world and among the projects that we can cite the OpenStreetMap project <http://www.openstreetmap.org/> as famous reference or crowd mapping Ushahidi project <http://ushahidi.com/products/crowdmap> as relevant ones. The base layer is the active background graphics used in the map. It can set only the basic level and will always appear below the other layers. The base rate also sets the active system map coordinates and the zoom levels availability. The non Base Layers can be stacked to other levels that can come from different data sources and can be viewed independently from each other. The sources can be: raster layers such as Google,



Figure 1: Main page of GOES system.

Image, KaMap, KaMapCache, MapGuide, MapServer, MultiMap, VirtualWorld, Yahoo and others, and vector layers like GML, Boxes, PointTrack, GeoRSS, Markers, Vector, WFS. The software has main page through which the users can submit an emergency case shown on figure 1. After the user enters the main menu e-mail and password are asked by the system for authentication, shown on figure 2. The next step is done by the user can, who enter into the collector information page a claim for a problem on the road infrastructure, shown on figure 3. The operational room has main console where all declared cases are listed and operational teams are responsible to solve the problems according to the priorities given in advance by the operative group manager. Figure 4 represent the view of the operational room visual tool.

3 Changes on the GOES project base software done by IICT-BAS team

Changes on the GOES project can be basically summarized in the following change log:

DB changes - database create script:

- Changed PWD column in sa_utente table to varchar(32) since MD5 has length 32.
- Changed default password for admin to MD5 equivalent.



The image shows a user authentication interface for the GOES system. At the top, there is a logo with the word "GOES" in large, bold, white letters. The "G" is red, the "O" is yellow, and the "ES" is green. Above the "G" is a small red car icon, and above the "S" is a small green satellite dish icon. Below the logo, the text "GOOD ON EMERGENCY SITUATION" is written in a smaller, grey font. Below this, there are two input fields. The first is labeled "E-Mail:" and the second is labeled "Парола:" (Password:). Both labels are in a bold, black font. Below the password field is a button labeled "Влез" (Login) in a bold, black font. The entire interface is set against a light yellow background.

Figure 2: User authentication to the system.

Code changes:

- Added ForgottenPassword.aspx - user interface for sending a password reset to the specified email of the user.
- Added ChangePassword.aspx - user interface for changing the password once the user has logged in.
- Changed all password creation and verification to use MD5 encoding. This means that passwords are stored as MD5 in DB and are checked in the server code as MD5 strings.
- Successful logging through LogInA.asp creates a session cookie in ASP.NET as well.
- Web services in ASP.NET that manage signals are now Session enabled.
- Web services in ASP.NET that manage signals are authenticated against anonymous usage, so that it is impossible to delete anything unless a user has logged in.
- Prevent SQL Injection in LogInA.asp through the TxtMail input field.

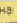
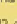

Подаване на сигнал	
* Задължително	** Адрес и/или местоположение
Подаване на сигнал:	
<input type="text"/>	
Описание:	
<input type="text"/>	
Намирате се на: **	
<input type="text"/>	
Адрес: * (пример: бул. Дондуков 2А)	
<input type="text"/>	
Карта:	
Open Street Map За да отбележите местоположението си на картата натиснете с мишката  (активирайте функцията на браузъра си за позициониране, за да отбележите географските си координати), след това натиснете с мишката  за да дефинирате местоположението, от където подавате сигнала. В противен случай напишете адреса в полетата по-горе. Географска ширина: (пример: 42.41) Географска дължина: (пример: 23.21)	
<input type="text"/> <input type="text"/>	
Позиционирай на картата по предоставените координати	
Позиционирай на картата по предоставените координати	
Запази	
	

Figure 3: Web-based report for sending information in operational room.

- Map control in the InserimentoB.asp and Inserimento.asp now updates the longitude/latitude controls accordingly straight on the client-side through JS

These changes address various kinds of issues, falling into different categories - security, privacy, better UX, etc. The changes in the database are direct result from the changes in the main part of the web application. They are necessary requirements for the correct functionality of storing and changing the passwords of users. We will try to go through every change by describing why it was necessary, what was intended by altering the behavior of the application, what issue was tackled and how it was accomplished. These changes do not intend to represent the best practices in the web nowadays, but rather prevent certain security and privacy issues and finally provide more fluent user-experience to those using the system. At the end of the day this is the ultimate goal.

3.1 Forgotten password and change password pages

The GOES system before the changes didn't provide a mechanism to the users so that they can change their own passwords. This is an unnecessary limitation to the users as once their profile has been created, they couldn't set their own password that they can feel comfortable with. They were provided with a computer generated

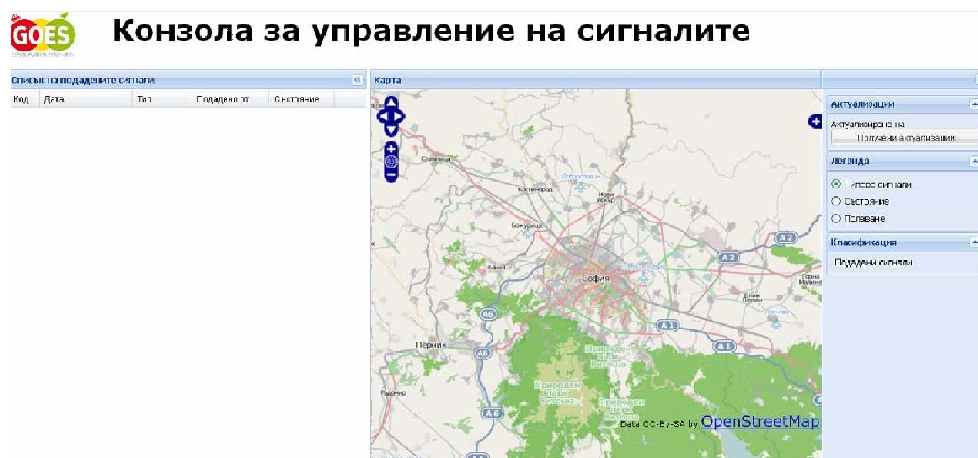


Figure 4: Operational room console.


random string that cannot be easily memorized and thus may very well result is a note next to the operator's monitor free to the other people in the room to copy. Furthermore there is another security implication - it is a good practice to frequently change one's password, thus limiting the options to brut-forcing guessing it. Due to the reasons stated above we decided that it would be best if the user has the option to change their own password to something they can feel comfortable with. For that the following interface (fig.5) was wrapped into a web page.

Once the user has authenticated, she/he can go to the respective page for changing the password. There the new password should be entered twice thus making sure the entered string is the one intended by the user. The other case - of the user forgetting her/his password is still covered since it is a very common scenario. The idea is that if the user cannot log in as they don't know their own password, they are given the option to get a new randomly-generated password that they can use to enter the system. This password is emailed to the address they have entered in the provided web page interface (fig.6).

That way they should log into their mail account, get their new password and use it to enter the system. At this stage it is highly advisable, but not necessary, for them to change the password they have received with a one that they feel more comfortable with.

3.2 Storing passwords in MD5 string format

Passwords are very sensitive information and therefore they should be treated as such. Keeping the password in plain text is very dangerous both from privacy and security standpoints. Having the password in readable form may result in unauthorized usage of other users' credentials. For more information on that matter, the reader is advised



Смяна на парола

Нова парола:

Повтори паролата:

Figure 5: Change of password page.



Паролата ще бъде изпратена на посочената електронна поща

Електронна поща:

Figure 6: Confirmation from the system for the new available password.

to visit the following web site <http://www.plaintextoffenders.com/>. Having in mind the security implications of storing the password in plain-text a decision to use MD5 to store them was taken. MD5 is a cryptographic function that produces a hash value with 128 bit length. Using this method every string can be crunched down to 32 hexadecimal integers. Thus the password field in the database was changed so that now it takes 32 characters, which is the length of a single MD5 encoding. In the system itself a helper method was developed that converted any input string into an MD5 string. Using this helper method the newly created password or the changed password was stored into the database for the respective user. Furthermore when a users is in the process of logging in the input password was converted to MD5 and was compared to the respective record from the database. This resulted in better security and improved managing of the user information. Currently only the user knows her/his password and there is no way for any individual with access to the

database, be it authorized or unauthorized, to read or reproduce the password from the DB records.

3.3 Login in both Classic ASP and ASP.NET - crossing the technological boundaries of the application

The GOES system is based on various technologies that tend to complement each other. On the server-side there are modules create using the mature framework of classic ASP and others based on the ASP.NET framework. Since they are very different in their nature sometimes it is difficult to manage them work together. Such an issue was the login process. As the user logs in once, she/he could do this providing either of the frameworks, but not both of them at the same time. The login page was create using the classic ASP framework. To tackle this obstacle, without forcing the user to login twice or change the user-experience in any way, the following routine was developed. Once the user enters the respective credentials, the data is first send to a specifically created ASP.NET page using AJAX technology to authenticate that user. If that login is successful, then the HTML form is submitted back to the classic ASP module for authenticating there. Otherwise the user is notified of the unsuccessful attempt and is asked to try again. As a result session cookies are created in both frameworks storing the respective user data and keeping the user authenticated flag raised.

3.4 Authenticated web services

The previously described change was a very vital step to the following important improvement to the security of the system - the execution of web services. The web services part of the GOES system was created to manage signals sent by citizens. The signals can be listed, changed and even deleted. However there was no limitation to who calls these services. This means that any anonymous user can do any of the mentioned above calls. In order to prevent that every web service method was limited to being used by authenticated users only. Thus once the user was authenticated, is authorized to use these methods. The limitation can go further by specifying which users manage signals, but that will require further changes to the implementation.

3.5 Preventing SQL Injection

SQL Injection is a very common security attack. It aims to compromise the integrity of the relational database backend, which is the case with the GOES system. The attack takes advantage of poorly implemented SQL queries and the most common symptom is concatenating user input without evaluating or validating it. If the user input starts with a semi-colon, which means end of SQL statement, then any SQL command can be used either to select sensible data, or to modify or delete content. In the case of the GOES system, the Login page was prone to such attacks, where the username was directly concatenated in the SQL query for checking if that user exists. A method was implemented that sanitized the input to be compliant with

SQL syntax in such a way that it does not interfere with the correct execution of the program. This resulted in special characters like new line, single and double quotes and other characters to be escaped. SQL injection is not possible with the ASP.NET web service methods since the content that is part of the SQL query is converted to integer and if that does not happen an exception is thrown that prevents further execution of the incorrect user input.

3.6 Client-side improvements in the UI

Along with the server-side improvements and security fixes, the client-side of the application needed attention as well. The form for reporting new events in the field to the system needed a UI boost by providing a way for the latitude/longitude fields to get populated by interacting with the map control. The map control, based on the OpenLayers framework exposes various event handling to happen. That way when the marker for setting the reported event's location was put on the map, an event was dispatched. Handling it we were able to extract the geographical location of the marker on the map and populate that data into the HTML input fields through JavaScript. Furthermore the whole UI had to be translated(localized) to Bulgarian. Although there were mechanisms that attempted to stream-line that process, there were quite a few places, where this was not possible. Tracking down these changes required extensive browsing through every layer of the application - from pure HTML, through JavaScript controls, to backend logic.

4 Conclusions

The software which is implemented in Sofia municipality has changed the way of reporting emergency cases on municipal level. Also the software has improved the way of communication between the mobile teams, who work on operative regime and collect data for problem zones. The GOES software has improved also the way of reporting of the problematic areas on the municipal territory. That improved also the man power use and limited the financial losses.

5 Acknowledgements

The paper has been supported by Good On Emergency Situation project with acronym GOES, grant agreement reference No 070401/2010/579105/SUB/C4.

References

- [1] Dobrinkova N., Marinov V., GOES Project – Good on Emergency Situations, BGSIAM11, 21-22 December 2011, Sofia, Bulgaria, 2012, pp 32-37.

- [2] Dobrinkova N., Marinov V., "GOES System Implemented in Sofia Municipality", 12th International Multidisciplinary Scientific Geoconference SGEM2012, 2012, ISSN 1314-2704, p.385- p. 392.

INFLUENCE OF THE NUMBER OF ANTS ON MONO-OBJECTIVE ANT COLONY OPTIMIZATION ALGORITHM FOR WIRELESS SENSOR NETWORK LAYOUT

Stefka Fidanova, Pencho Marinov

Institute for Parallel Processing, BAS
Acad. G. Bonchev str. bl.25A
1113 Sofia, Bulgaria
stefka@parallel.bas.bg, pencho@parallel.bas.bg

1 Introduction

A sensor is a device which can collect and transmit data. First the wireless sensor networks was used by militarist for reconnaissance and surveillance [2], but after that starts civil use. Examples for possible applications are forest fire prevention, volcano eruption study [15], health data monitoring [18], civil engineering [12]. Sensor networks depend on deployment of sensors over a physical location to fulfill a desired task. The sensors can sense temperature, voltage, or chemical substances. A Wireless Sensor Network (WSN) allows automatically monitoring of almost any phenomenon. A WSN node contains several components including the radio, battery, microcontroller, analog circuit, and sensor interface. In battery-powered systems, higher data rates and more frequent radio use consume more power. There are several open issues for sensor networks such as signal processing [13], deployment [17], operating cost, localization and location estimation.

One of the nodes of the WSN has special role. It is a High Energy Communication Node (HECN) which collects data from hall the network and transmits them to the main computer to be proceeded. The sensors transmit their data to HECN, either directly or via hops, using nearby sensors as communication relays. When deploying a WSN, the positioning of the sensor nodes becomes one of the major concerns. The

coverage obtained with the network and the economic cost of the network depends directly of it. WSN can have large numbers of nodes, and therefore the task of selecting the geographical positions of the nodes for an optimally designed network can be very complex. Thus it is unpractical to solve the problem with traditional numerical methods. In this case most appropriate is to apply some metaheuristic method.

The problem is multi-objective with two objective functions. They are minimizing the energy depletion of the nodes in the network and minimizing the number of the nodes. The full coverage of the network and connectivity are considered as constraints. It is a NP-hard multi-objective problem. We convert the problem to mono-objective multiplying the two objective functions. Thus we simplify the problem. But it continue to be NP problem. We propose mono-objective ant algorithm which solves the WSN layout problem. Our aim is to study the influence of the number of ants on algorithm performance and quality of the achieved solutions and to find the minimal number of ants which are enough to achieve good solutions.

Jourdan [8] solved an instance of WSN layout using a multi-objective genetic algorithm. In there formulation a fixed number of sensors had to be placed in order to maximize the coverage. In some applications most important is the network energy. In [7] is proposed ACO algorithm and in [16] is proposed evolutionary algorithm for this variant of the problem. In [4] is proposed ACO algorithm taking in to account only the number of the sensors. In [10] are proposed several evolutionary algorithms to solve the problem. In [9] is proposed genetic algorithm which achieves similar solutions as the algorithms in [10], but it is tested on small test problems.

The paper is organized as follows. In Section 2 the WSN is introduced and the layout problem is formulated. Section 3 presents the ACO algorithm. In Section 4 we show the experimental results. Conclusion is in the Section 5.

2 Problem Formulation

A wireless sensor network (WSN) consists of spatially distributed autonomous sensors to cooperatively monitor physical or environmental conditions, such as temperature, sound, vibration, pressure, motion or pollutants. The development of wireless sensor networks was motivated by military applications such as battlefield surveillance and are now used in many industrial and civilian application areas, including industrial process monitoring and control, machine health monitoring, environment and habitat monitoring, healthcare applications, home automation, and traffic control.

In addition to one or more sensors, each node in a sensor network is typically equipped with a radio transceiver or other wireless communications device, a small microcontroller, and an energy source, usually a battery. A sensor node might vary in size from that of a box to the size of a grain of dust, although functioning "motest" of genuine microscopic dimensions have yet to be created. The cost of sensor nodes is similarly variable, ranging from hundreds of dollars to a few pennies, depending on the size of the sensor network and the complexity required of individual sensor nodes. Size and cost constraints on sensor nodes result in corresponding constraints on resources such

as energy, memory, computational speed and bandwidth.

Each sensor node sens an area around itself. The sensing radius determines the sensitivity range of the sensor node. The nodes communicate among themselves using wireless communication links, determined by a communication radius. The HECN is responsible for external access to the network. Therefore, every sensor node in the network must have communication with the HECN. Since the communication radius is often much smaller than the network size, direct links are not possible for peripheral nodes. A multi-hop communication path is then established for those nodes that do not have the HECN within their communication range.

A non-fixed amount of sensor nodes has to be placed in a terrain providing full coverage. The objectives are to construct the network with minimal number of sensors, which is cheapest for construction and with minimal energy, which is cheapest for exploitation, while keeps the connectivity of the network. When the sensor transmits data it uses energy from battery. Every sensor transmits his data and the data coming from sensors which are fare from the HECN. Thus the quantity of the transmuted data defines the energy. The node with highest energy defines the energy of the network.

3 Mono-Objective ACO for WSN Layout

We apply ant colony optimization to solve the problem. The idea for ant algorithm comes from real ant behaviors. When walk they put on the ground chemical substance called pheromone. The ants smell the pheromone and follow the path with a stronger pheromone concentration. Thus they find shorter path between the nest and the food. The ACO algorithm uses a colony of artificial ants that behave as cooperative agents. With the help of the pheromone they try to construct better solutions and to find the optimal ones. The problem is represented by graph and the solution is represented by a path in the graph or by tree in the graph. First we initialize the pheromone. Ants start from random nodes and construct feasible solutions. When all ants construct their solution we update the pheromone. Ants compute a set of feasible moves and select the best one, according transition probability. The transition probability p_{ij} , to chose the node j when the current node is i , is based on the heuristic information η_{ij} and on the pheromone level τ_{ij} of the move, where $i, j = 1, \dots, n$.

$$p_{ij} = \frac{\tau_{ij}^{\alpha} \eta_{ij}^{\beta}}{\sum_{k \in \{allowed\}} \tau_{ik}^{\alpha} \eta_{ik}^{\beta}} \quad (1)$$

The ant selects the move with highest probability. The initial pheromone is set to a small positive value τ_0 and then ants update this value after completing the construction stage [1, 5]. The pheromone corresponds to the global memory of the ants, their experience to solve the problem. The heuristic information is a priori knowledge for the problem. In our implementation we use MAX-MIN Ant System (MMAS) [3], which is one of the most successful ant approach. The main feature of MMAS is using a fixed upper bound τ_{max} and a lower bound τ_{min} of the pheromone. Thus

the accumulation of big amounts of pheromone by part of the possible movements and repetition of same solutions is partially prevented. In our case the graph of the problem is represented by square grid. The ants will deposit their pheromone on the nodes of the grid. We will deposit the sensors on the nodes of the grid. The solution is represented by tree starting by the high energy communication node. An ant starts to create the rest of the solution from a random node which communicates with HECN. Using transition probability (eqn. 1), the ant chooses the next node to go on. If there is more than one node with same probability, the ant chooses one of them randomly. Construction of the heuristic information is a crucial point in ant algorithms. Our heuristic information is a product of three values (eqn. 2).

$$\eta_{ij}(t) = s_{ij}l_{ij}(1 - b_{ij}), \quad (2)$$

where s_{ij} is the number of the new points which the sensor will cover, and

$$l_{ij} = \begin{cases} 1 & \text{if communication exists;} \\ 0 & \text{if there is not communication,} \end{cases} \quad (3)$$

b is the solution matrix and the matrix element $b_{ij} = 1$ when there is sensor on this position otherwise $b_{ij} = 0$. With s_{ij} we try to increase the points covered by one sensor and thus to decrease the number of sensors we need. With l_{ij} we guarantee that all sensors will be connected. The search stops when $p_{ij} = 0$ for all values of i and j .

The pheromone trail update rule is given by:

$$\tau_{ij} \leftarrow \rho\tau_{ij} + \Delta\tau_{ij}, \quad (4)$$

$$\Delta\tau_{ij} = \begin{cases} 1/F(k) & \text{if } (i, j) \in \text{iteration best solution,} \\ 0 & \text{otherwise.} \end{cases}$$

We decrease the pheromone with a parameter $\rho \in [0, 1]$. This parameter models evaporation in the nature and decreases the influence of old information in a search process. After that we add the new pheromone which is proportional to the value of the objective function. If the pheromone of some node becomes less than the lower bound of the pheromone we put it to be equal to the lower bound and thus we prevent the pheromone of some nodes to become very low close to 0 and to be undesirable. It is a kind of diversification of the search. F is the objective function. The aim is to add more pheromone on good solutions and thus to force the ants to search around them for better solutions. The objective function is:

$$F(k) = f_1(k) \times f_2(k), \quad (5)$$

where $f_1(k)$ is the number of the sensors achieved by the k -th ant and $f_2(k)$ is the energy of the solution of the k -th ant.

4 Experimental Results

Every ant start to create their solution from random point. In our case it is a random point which communicates with the HECN. Thus the ant algorithm uses small number of agents (ants). Less number of ants means less memory, which is important when we solve large problems. The aim of this work is to learn the influence of the number of the ants on quality of the solution.

We have created a software which realizes our ant algorithm. Our software can solve any rectangular area, the communication and the coverage radius can be different and can have any positive value. The HECN can be fixed in any point in the area. The program is written in C language and the tests are run in computer with Intel Pentium processor with 2.8 GHz. In our tests we use an example where the area is square and consists of 500 points in every side. The coverage and communication radii are cover 30 points. The HECN is fixed in the center of the area.

In our previous work [6] we show that our ant algorithm outperforms existing algorithms for this problem. There, after several runs of the algorithm we specify the most appropriate values of its parameters. We apply MAX-MIN ant algorithm with the following parameters: $\alpha = \beta = 1$, $\rho = 0.5$.

We convert the problem from multi-objective to mono-objective. Multi-objective optimization (MOP) is the process of simultaneously optimizing two or more conflicting objectives subject to certain constraints. If a multi-objective problem is well formed, there should not be a single solution that simultaneously minimizes each objective to its fullest.

Multi-Objective Optimization (MOP) has his roots in the nineteenth century in the work of Edgeworth and Pareto in economics [11]. The optimal solution for MOP is not a single solution as for mono-objective optimization problems, but a set of solutions defined as Pareto optimal solutions. A solution is Pareto optimal if it is not possible to improve a given objective without deteriorating at least another objective. The main goal of the resolution of a multi-objective problem is to obtain the Pareto optimal set and consequently the Pareto front. One solution dominates another if minimum one of its components is better than the same component of other solutions and other components are not worse. The Pareto front is the set of non dominated solutions.

In ACO if we fix the number of iterations and double the number of ants the execution time will be doubled. We study the influence of the number of ants on the quality of the solutions. We fixed the number of the iterations to be 60 and the number of ants to have following values $\{1, 2, 3, 4, 5, 6, 7, 8, 9, 10\}$.

We run our ACO algorithm 30 times with every one of the ants number. We extract the Pareto front from the optimal solutions of this 30 runs. On the Table 1 we show the achieved nondominated solutions (Pareto fronts). Analyzing the table we observe that the Pareto front achieved by 6 ants dominates the Pareto fronts achieved by 1, 2, 3 and 4 ants. The Pareto fronts achieved by 8, 9 and 10 ants are identical. The Pareto Front achieved by 7 ants dominates this achieved by 8 ants and respectively by 9 and 10 ants. The Pareto front achieved by 4 ants is a part of the Pareto front

Table 1: Experimental results

ants	Pareto front (Energy)																			
1	53										58					63				
2	53					54					55					57				
3	53					54					55					57				
4	52					53					55					57				
5	52					53					54	55				57				
6	51					53	54					55				57				
7	51					53					54					57				
8	51					53	54					57								
9	51					53	54					57								
10	51					53	54					57								
Sensor	239	238	237	236	235	234	233	232	231	230	229	228	227	226	225					

achieved by 5 ants, but consists one solution less.

We prepare the Pareto front achieved by all runs of the algorithm with any number of ants (from 1 to 10) and we call it common Pareto front. Let we have a set of number of sensors from 225 to 239. If for some number of sensors there are not corresponding energy in the common Pareto front, we put the energy to be equal to the point of the front with less number of sensors. We can do this because if we take some solution and if we include a sensor close to the HECN it will not increase the value of the energy and will increase with 1 only the number of the sensors. Thus there is corresponding energy to any number of nodes. This front we will call Extended front. In our case the Extended front is $\{(239, 51), (238, 51), (237, 51), (236, 53), (235, 53), (234, 53), (233, 54), (232, 55), (231, 57), (230, 57), (229, 57), (228, 57), (227, 57), (226, 57), (225, 57)\}$.

We include additional criteria to can decide which Pareto front is better. We will calculate the distance between a Pareto front and the Extended front. To calculate the distance we extend every of the Pareto fronts in a similar way as the common Pareto front. The distance between a Pareto front and the Extended front is the sum of the distances between the points with a same number of sensors, or it is the difference between their energy. These distances are always positive because the Extended front dominates the Pareto fronts. Thus by this criteria the best Pareto front will be the closest to the Extended front.

Table 2: Distances from Extended front

ants	5	6	7
Distance	11	2	2

In Table 2 we show the distances between the Extended front and the Pareto fronts

achieved by 5, 6 and 7 ants. Analyzing the Table 2 we conclude that the distance between the Extended front and the Pareto front achieved by 6 and 7 ants is shortest. When the ACO algorithm uses more ants, then the execution time increase and the used memory by the algorithm increases, which is very important when we solve large problems. Thus we decide that the best number of ants to solve wireless sensor layout problem is equal to 6.

5 Conclusion

In this paper we study the influence of the number of the ants in the algorithm performances when we solve the wireless sensor network. Less number of ants leads to the less running time and less memory, which is important for real applications. We vary the number of used ants when we fix the number of iterations. We include the concept of Extended front as additional tool to compare two Pareto fronts which do not dominate each other. The best Pareto front we achieve when the number of ants is equal to 6.

Acknowledgments: This work has been partially supported by the Bulgarian National Scientific Fund under the grants DID 02/29-”Modeling Processes with fixed development rules” and DTK 02/44-”Effective Monte Carlo Methods for large-scale scientific problems”.

References

- [1] E. BONABEAU, M. DORIGO, G. THERAULAZ, *Swarm Intelligence: From Natural to Artificial Systems*, Oxford University Press, 1999.
- [2] K. DEB, A. PRATAP, S. AGRAWAL, T. MEYARIVAN, *A Fast and Elitist Multi-objective Genetic Algorithm: Nsga-ii*, IEEE Transactions on Evolutionary Computation, **6**(2), 2002, 182–197.
- [3] M. DORIGO, T. STUTZLE. *Ant Colony Optimization*, MIT Press, 2004.
- [4] S. FIDANOVA, P. MARINOV, E. ALBA, *Ant Algorithm for Optimal Sensor Deployment*, Computational Intelligence, K. Madani, A.D. Correia, A. Rosa, J. Filipe (eds.), Studies of Computational Intelligence, **399**, Springer, 2012, 21 - 29.
- [5] S. FIDANOVA, K. ATANASOV *Generalized Net Model for the Process of Hibrde Ant Colony Optimization* Comptes Rendus de l’Academie Bulgare des Sciences, **62**(3), 2009, 315 - 322.
- [6] S. Fidanova, M. Shindarov, P. Marinov *Multi-Objective Ant Algorithm for Wireless Sensor Network Positioning* Comptes Rendus de l’Academie Bulgare des Sciences, (in press).

- [7] H. HERNANDEZ, C. BLUM, *Minimum Energy Broadcasting in Wireless Sensor Networks: An ant Colony Optimization Approach for a Realistic Antenna Model*, J. of Applied Soft Computing, **11**(8), 2011, 5684–5694.
- [8] D.B. JOURDAN, *Wireless Sensor Network Planning with Application to UWB Localization in GPS-denied Environments*, Massachusetts Institute of Technology, PhD thesis, 2000.
- [9] A. KONSTANTINIDIS, K. YANG, Q. ZHANG, D. ZAINALIPOUR-YAZTI, *A multi-objective Evolutionary Algorithm for the deployment and Power Assignment Problem in Wireless sensor Networks*, J. of Computer networks, **54**(6), 2010, 960–976.
- [10] G. MOLINA, E. ALBA, EL-G. TALBI, *Optimal Sensor Network Layout Using Multi-Objective Metaheuristics*, Universal Computer Science **14**(15), 2008, 2549–2565.
- [11] V. K. MATHUR, *How Well do we Know Pareto Optimality?* J. of Economic Education **22**(2), 1991, 172 - 178.
- [12] J. PAEK, N. KOTHARI, K. CHINTALAPUDI, S. RANGWALA, R. GOVINDAN, *The Performance of a Wireless Sensor Network for Structural Health Monitoring*, In Proc. of 2nd European Workshop on Wireless Sensor Networks, Istanbul, Turkey, Jan 31 – Feb 2, 2005.
- [13] G. J. POTTIE, W. J. KAISER, *Embedding the Internet: Wireless Integrated Network Sensors*, Communications of the ACM, **43**(5), 2000, 51–58.
- [14] T. STUTZLE, H.H. HOOS, *MAX-MIN Ant System*, Future Generation Computer Systems **16**, 2000, 889–914.
- [15] G. WERNER-ALLEN, K. LORINEZ, M. WELSH, O. MARCILLO, J. JONSON, M. RUIZ, J. LEES, *Deploying a Wireless Sensor Network on an Active Volcano*, IEEE Internet Computing **10**(2), 2006, 18–25.
- [16] S. WOLF, P. MEZZ, *Evolutionary Local Search for the Minimum Energy Broadcast Problem*, in C. Cotta, J. van Hemezel (eds.), VOCOP 2008, Lecture Notes in Computer Sciences No. 4972, Springer, Germany, 2008, 61–72.
- [17] Y. XU, J. HEIDEMANN, D. ESTRIN, *Geography Informed Energy Conservation for Ad Hoc Routing*, Proceedings of the 7th ACM/IEEE Annual International Conference on Mobile Computing and Networking, Italy, 16-21 July 2001, 70–84.
- [18] M. R. YUCE, S .W. NG, N. L. MYO, J. Y. KHAN, W. LIU, *Wireless Body Sensor Network Using Medical Implant Band*, Medical Systems **31**(6), 2007, 467–474.
- [19] E. ZITZLER, L. THIELE, *Multiobjective Evolutionary Algorithms: A Comparative Case Study and the Strength Pareto Approach*, IEEE Transactions on Evolutionary Computation, **3**(4), 1999, 257–271.

NEW SPINOR MODELS IN TWO DIMENSIONS WITH \mathbb{Z}_2 -REDUCTIONS

V. S. Gerdjikov

Institute for Nuclear Research and
Nuclear Energy,
Bulgarian Academy of Sciences,
72 Tzarigradsko chaussee,
1784 Sofia, Bulgaria

1 Introduction

In contemporary theoretical physics spinor models play important role Nambu–Jona-Lasinio–Vaks–Larkin models [8, 10] and Gross–Neveu models [6, 9] have been proposed initially as models for describing the strong interactions. Later [13] it was proven that the two-dimensional versions of these models are integrable by the inverse scattering method (ISM) [11, 2]. In the same paper [13] Zakharov and Mikhailov proposed a third class of spinor models related to the orthogonal groups.

The aim of the present report is to outline the main results of [3] and to derive new types of integrable spinor models by applying additional \mathbb{Z}_2 -reductions to their Lax representations. In doing this we will be using the reduction group [7]. Next we describe the spectral properties of the Lax operators.

We start in Section 2 by some preliminaries concerning the spinor models and the reduction group of Mikhailov [7]. In Section 3 we derive the \mathbb{Z}_2 -reduced spinor models. Section 4 is devoted to the spectral properties of the \mathbb{Z}_2 -reduced Lax operators and the symmetries of their discrete eigenvalues.

2 Preliminaries

The integrability of the 2-dimensional versions of the Nambu–Jona-Lasinio–Vaks–Larkin (NJLVL) and the Gross–Neveu model (GN) was discovered by Zakharov and Mikhailov in [12]. They showed that NJLVL models are related to $su(N)$ algebras, while the Gross–Neveu models are related to the $sp(N)$. In the same paper an additional type of spinor models related to the algebras $so(N)$ was discovered; we will call them Zakharov–Mikhailov (ZM) models.

Let us first recall the Lax representations of these models [13].

$$\begin{aligned} \Psi_\xi &= U(\xi, \eta, \lambda) \Psi(\xi, \eta, \lambda), & \Psi_\eta &= U(\xi, \eta, \lambda) \Psi(\xi, \eta, \lambda), \\ U(\xi, \eta, \lambda) &= \frac{U_1(\xi, \eta)}{\lambda - a}, & V(\xi, \eta, \lambda) &= \frac{V_1(\xi, \eta)}{\lambda - a}, \end{aligned} \quad (1)$$

where $\eta = t + x$, $\xi = t - x$ and a is a real number. We also impose the \mathbb{Z}_2 -reduction:

$$U^\dagger(x, t, \lambda) = -U(x, t, \lambda^*), \quad V^\dagger(x, t, \lambda) = -V(x, t, \lambda^*). \quad (2)$$

The compatibility condition of the above linear problems reads:

$$U_\eta - V_\xi + [U, V] = 0, \quad (3)$$

which is equivalent to

$$U_{1,\eta} + \frac{1}{2a}[U_1, V_1(\xi, \eta)] = 0, \quad V_{1,\xi} - \frac{1}{2a}[V_1, U_1(\xi, \eta)] = 0. \quad (4)$$

From these equations, fixing up properly the gauge, (see [12]) there follows that

$$U_1(\xi, \eta) = -i\phi J_1^0 \phi^{-1}, \quad V_1(\xi, \eta) = i\psi I_1^0 \psi^{-1}, \quad (5)$$

where J_1^0 and I_1^0 are properly chosen constant elements (choice of the gauge) of the corresponding simple Lie algebra \mathfrak{g} . In what follows we fix up $J_1^0 = -I_1^0 = J$ and choose J for each of the above mentioned models accordingly. The matrix valued functions $\phi(\xi, \eta)$ and $\psi(\xi, \eta)$ take values in the corresponding simple Lie group and are fundamental solutions of the following ODE's:

$$\begin{aligned} \psi_\xi &\equiv -\frac{U_1(\xi, \eta)}{2a} \psi(\xi, \eta) = \frac{i}{2a} \phi J \hat{\phi} \psi(\xi, \eta), \\ \phi_\eta &\equiv \frac{V_1(\xi, \eta)}{2a} \phi(\xi, \eta) = \frac{i}{2a} \psi J \hat{\psi} \phi(\xi, \eta). \end{aligned} \quad (6)$$

Here and below by ‘hat’ we will denote the inverse matrix, i.e. $\hat{\psi} \equiv (\psi)^{-1}$.

In this way we get three classes of spinor models. Below, following [13] we briefly outline their derivation.

i) Nambu-Jona-Lasinio-Vaks-Larkin models. Here we choose $\mathfrak{g} \simeq su(N)$. Then $\psi(\xi, \eta)$ and $\phi(\xi, \eta)$ are elements of the group $SU(N)$ and by definition $\hat{\psi}(\xi, \eta) = \psi^\dagger(\xi, \eta)$, $\hat{\phi}(\xi, \eta) = \phi^\dagger(\xi, \eta)$. We choose $J = \text{diag}(1, 0, \dots, 0)$ and as a result only the first columns $\phi^{(1)}$, $\psi^{(1)}$ and the first rows $\hat{\phi}^{(1)}$, $\hat{\psi}^{(1)}$ enter into the systems (6). If we introduce the notations:

$$\phi_\alpha(\xi, \eta) = \phi_{\alpha,1}^{(1)}, \quad \psi_\alpha(\xi, \eta) = \psi_{\alpha,1}^{(1)}, \quad (7)$$

then the explicit form of the system is:

$$\frac{\partial \phi_\alpha}{\partial \eta} = \frac{i}{2a} \psi_\alpha \sum_{\beta=1}^N \psi_\beta^* \phi_\beta, \quad \frac{\partial \psi_\alpha}{\partial \xi} = \frac{i}{2a} \phi_\alpha \sum_{\beta=1}^N \phi_\beta^* \psi_\beta. \quad (8)$$

The corresponding action functional is:

$$A_{\text{NJLVL}} = \int_{-\infty}^{\infty} dx dt \left(i \sum_{\alpha=1}^N \left(\phi_\alpha^* \frac{\partial \phi_\alpha}{\partial \eta} + \psi_\alpha^* \frac{\partial \psi_\alpha}{\partial \xi} \right) - \frac{1}{2a} \left| \sum_{\alpha=1}^N (\psi_\alpha^* \phi_\alpha) \right|^2 \right). \quad (9)$$

ii) Gross-Neveu models. Here we choose $\mathfrak{g} \simeq sp(2N, \mathbb{R})$; then $\psi(\xi, \eta)$ and $\phi(\xi, \eta)$ are elements of the group $\mathfrak{G} \simeq SP(2N, \mathbb{R})$. Following [13] we use the standard definition of symplectic group elements:

$$\hat{\psi}(\xi, \eta) = \mathfrak{I} \psi^T(\xi, \eta) \hat{\mathfrak{I}}, \quad \hat{\phi}(\xi, \eta) = \mathfrak{I} \phi^T(\xi, \eta) \hat{\mathfrak{I}}, \quad \mathfrak{I} = \begin{pmatrix} 0 & -\mathbb{1} \\ \mathbb{1} & 0 \end{pmatrix}. \quad (10)$$

Then the corresponding Lie algebraic elements acquire the following block-matrix structure:

$$U_1(\xi, \eta) = \begin{pmatrix} A & B \\ C & -A^T \end{pmatrix}, \quad (11)$$

where A, B, C are arbitrary real $N \times N$ matrices. Next we choose

$$J = \begin{pmatrix} 0 & B_0 \\ 0 & 0 \end{pmatrix}, \quad B_0 = \text{diag}(1, 0, \dots, 0, 0). \quad (12)$$

As a consequence again only the first columns $\phi^{(1)}$, $\psi^{(1)}$ and the first rows $\hat{\phi}^{(1)}$, $\hat{\psi}^{(1)}$ enter into the systems (6). If we introduce the N -component complex vectors:

$$\phi_\alpha(\xi, \eta) = \frac{1}{2}(\phi_{\alpha,1}^{(1)} + i\phi_{N+\alpha,1}^{(1)}), \quad \psi_\alpha(\xi, \eta) = \frac{1}{2}(\psi_{\alpha,1}^{(1)} + i\psi_{N+\alpha,1}^{(1)}) \quad (13)$$

then the explicit form of the system is:

$$\frac{\partial \phi_\alpha}{\partial \eta} = \frac{i}{a} \psi_\alpha \sum_{\beta=1}^N (\psi_\beta \phi_\beta^* - \psi_\beta^* \phi_\beta), \quad \frac{\partial \psi_\alpha}{\partial \xi} = -\frac{i}{a} \phi_\alpha \sum_{\beta=1}^N (\phi_\beta \psi_\beta^* - \phi_\beta^* \psi_\beta). \quad (14)$$

The functional of the action is:

$$A_{\text{GN}} = \int_{-\infty}^{\infty} dx dt \left(i \sum_{\alpha=1}^N \left(\phi_{\alpha}^* \frac{\partial \phi_{\alpha}}{\partial \eta} + \psi_{\alpha}^* \frac{\partial \psi_{\alpha}}{\partial \xi} \right) - \frac{1}{2a} \left(\sum_{\alpha=1}^N (\psi_{\alpha}^* \phi_{\alpha} - \phi_{\alpha}^* \psi_{\alpha}) \right)^2 \right). \quad (15)$$

iii) **Zakharov–Mikhailov models.** Now we choose $\mathfrak{g} \simeq so(N, \mathbb{R})$; then $\psi(\xi, \eta)$ and $\phi(\xi, \eta)$ take values in the group $\mathfrak{G} \simeq SO(N, \mathbb{R})$. Following [13] we use the standard definition of orthogonal group elements:

$$\hat{\psi}(\xi, \eta) = \psi^T(\xi, \eta), \quad \hat{\phi}(\xi, \eta) = \phi^T(\xi, \eta). \quad (16)$$

Now we choose

$$J = E_{1,N} - E_{N,1}, \quad (17)$$

where the $N \times N$ matrices E_{kp} are defined by $(E_{kp})_{nm} = \delta_{kn} \delta_{pm}$. As a consequence now the first and the last columns $\phi^{(1)}, \phi^{(N)}, \psi^{(1)}, \psi^{(N)}$ and the first and the last rows $\hat{\phi}^{(1)}, \hat{\phi}^{(N)}, \hat{\psi}^{(1)}, \hat{\psi}^{(N)}$ enter into the systems (6). If we introduce the N -component complex vectors:

$$\phi_{\alpha}(\xi, \eta) = \frac{1}{2}(\phi_{\alpha,1}^{(1)} + i\phi_{\alpha,N}^{(N)}), \quad \psi_{\alpha}(\xi, \eta) = \frac{1}{2}(\psi_{\alpha,1}^{(1)} + i\psi_{\alpha,N}^{(N)}) \quad (18)$$

then the explicit form of the system becomes:

$$\begin{aligned} i \frac{\partial \psi_{\alpha}}{\partial \xi} &= \frac{i}{a} \sum_{\beta=1}^N (\phi_{\alpha}^* \phi_{\beta} \psi_{\beta} - \phi_{\alpha} \phi_{\beta}^* \psi_{\beta}), \\ i \frac{\partial \phi_{\alpha}}{\partial \eta} &= \frac{i}{a} \sum_{\beta=1}^N (\psi_{\alpha}^* \psi_{\beta} \phi_{\beta} - \psi_{\alpha} \psi_{\beta}^* \phi_{\beta}), \end{aligned} \quad (19)$$

This system has as action functional

$$\begin{aligned} A_{\text{ZM}} &= \int_{-\infty}^{\infty} dx dt \left(i \sum_{\alpha=1}^N \left(\phi_{\alpha}^* \frac{\partial \phi_{\alpha}}{\partial \eta} + \psi_{\alpha}^* \frac{\partial \psi_{\alpha}}{\partial \xi} \right) - \frac{1}{2a} \left(\sum_{\alpha,\beta=1}^N (\phi_{\alpha}^* \phi_{\beta} - \phi_{\beta}^* \phi_{\alpha})(\psi_{\alpha}^* \psi_{\beta} - \psi_{\beta}^* \psi_{\alpha}) \right) \right). \end{aligned} \quad (20)$$

For more details of deriving the models see [13].

3 \mathbb{Z}_2 -Reductions of the spinor models

Using the ideas of the reduction group [7] below we construct new spinor models in two dimensions generalizing the ones in [12]. We start with the Lax representation:

$$\begin{aligned}\Psi_\xi &= U_R(\xi, \eta, \lambda)\Psi(\xi, \eta, \lambda), & U_R(\xi, \eta, \lambda) &= \frac{U_1(\xi, \eta)}{\lambda - a} + \frac{CU_1(\xi, \eta)C^{-1}}{\epsilon\lambda^{-1} - a}, \\ \Psi_\eta &= V_R(\xi, \eta, \lambda)\Psi(\xi, \eta, \lambda), & V_R(\xi, \eta, \lambda) &= \frac{V_1(\xi, \eta)}{\lambda + a} + \frac{CV_1(\xi, \eta)C^{-1}}{\epsilon\lambda^{-1} + a},\end{aligned}\quad (21)$$

where $\epsilon = \pm 1$, $a \neq 1$ is a real number and C is an involutive automorphism of \mathfrak{g} . Obviously this Lax representation along with the typical reduction (2) satisfies also:

$$U_R(\xi, \eta, \lambda) = CU_R(\xi, \eta, \epsilon\lambda^{-1})C^{-1}, \quad V_R(\xi, \eta, \lambda) = CV_R(\xi, \eta, \epsilon\lambda^{-1})C^{-1}, \quad (22)$$

which is automatically compatible with the Lax representation [7].

The new Lax representation is:

$$\frac{\partial U_R}{\partial \eta} - \frac{\partial V_R}{\partial \xi} + [U_R, V_R] = 0, \quad (23)$$

which is equivalent to

$$U_{1,\eta} + [U_1, V_R(\xi, \eta, a)] = 0, \quad V_{1,\xi} + [V_1, U_R(\xi, \eta, -a)] = 0. \quad (24)$$

Next we apply the same way of deriving the models as in Section II; obviously, due to the additional terms in U_R and V_R we get additional terms in the models. In what follows we also list some typical choices for the automorphism C . Skipping the details we get:

i) \mathbb{Z}_2 -NJLVL models. Here $\mathfrak{G} \simeq SU(N)$ and the system takes the form:

$$\begin{aligned}i\frac{\partial \vec{\phi}}{\partial \eta} + \frac{1}{2a}\vec{\psi}(\vec{\psi}^\dagger \vec{\phi}) + \frac{1}{\epsilon a^{-1} + a}C\vec{\psi}(\vec{\psi}^\dagger \hat{C}\vec{\phi})(\xi, \eta) &= 0, \\ i\frac{\partial \vec{\psi}}{\partial \xi} + \frac{1}{2a}\vec{\phi}(\vec{\phi}^\dagger \vec{\psi}) + \frac{1}{\epsilon a^{-1} + a}C\vec{\phi}(\vec{\phi}^\dagger \hat{C}\vec{\psi})(\xi, \eta) &= 0.\end{aligned}\quad (25)$$

where $\vec{\psi} = (\psi_{\alpha,1}, \dots, \psi_{\alpha,N})^T$ and $\vec{\phi} = (\phi_{\alpha,1}, \dots, \phi_{\alpha,N})^T$.

For the automorphism C of the $SU(N)$ group we may have

$$\text{a) } C_N = \text{diag}(\epsilon_1, \epsilon_2, \dots, \epsilon_N), \quad \text{b) } C'_N = \begin{pmatrix} 1 & 0 \\ 0 & C_{N-1} \end{pmatrix}. \quad (26)$$

where $\epsilon_j = \pm 1$ and C_{N-1} belongs to the Weyl group of $SU(N-1)$ and is such that $C_{N-1}^2 = \mathbb{1}$. These two special choices of C are such that $\lim_{\xi \rightarrow \pm\infty} U_R(\xi, \eta) = \lim_{\xi \rightarrow \pm\infty} CU_R(\xi, \eta)\hat{C}$.

ii) **\mathbb{Z}_2 -GN models.** Here $\mathfrak{G} \simeq SP(2N, \mathbb{R})$ and we consider two typical choices for the automorphism C :

$$\text{a) } C = \begin{pmatrix} C_1 & 0 \\ 0 & C_1 \end{pmatrix}, \quad \text{b) } C' = \begin{pmatrix} 0 & C_2 \\ C_2 & 0 \end{pmatrix}, \quad (27)$$

where $C_1^2 = C_2^2 = \mathbf{1}$. This leads to two different systems of GN-type. Using the N -component vectors $\vec{\psi}$ and $\vec{\phi}$ we can write them down in compact form:

$$\begin{aligned} \frac{\partial \vec{\phi}}{\partial \eta} &= -\frac{i}{a} \vec{\psi} \left((\vec{\psi}^\dagger, \vec{\phi}) - (\vec{\phi}^\dagger, \vec{\psi}) \right) - \frac{2i}{a + \epsilon a^{-1}} C_1 \vec{\psi} \left((\vec{\psi}^\dagger C_1 \vec{\phi}) - (\vec{\phi}^\dagger C_1 \vec{\psi}) \right), \\ \frac{\partial \vec{\psi}}{\partial \xi} &= \frac{i}{a} \vec{\phi} \left((\vec{\psi}^\dagger, \vec{\phi}) - (\vec{\phi}^\dagger, \vec{\psi}) \right) + \frac{2i}{a + \epsilon a^{-1}} C_1 \vec{\phi} \left((\vec{\psi}^\dagger C_1 \vec{\phi}) - (\vec{\phi}^\dagger C_1 \vec{\psi}) \right). \end{aligned} \quad (28)$$

The corresponding action can be written as follows:

$$\begin{aligned} A_{\mathbb{Z}_2, \text{GNa}} &= \int_{-\infty}^{\infty} dx dt \left(i \left(\vec{\phi}^\dagger \frac{\partial \vec{\phi}}{\partial \eta} + \vec{\psi}^\dagger \frac{\partial \vec{\psi}}{\partial \xi} \right) - \frac{1}{2a} \left((\vec{\psi}^\dagger, \vec{\phi}) - (\vec{\phi}^\dagger, \vec{\psi}) \right)^2 \right. \\ &\quad \left. - \frac{1}{\epsilon a^{-1} + a} \left((\vec{\psi}^\dagger C_1 \vec{\phi}) - (\vec{\phi}^\dagger C_1 \vec{\psi}) \right)^2 \right). \end{aligned} \quad (29)$$

The second \mathbb{Z}_2 -reduced GN-system is:

$$\begin{aligned} \frac{\partial \vec{\phi}}{\partial \eta} &= -\frac{i}{a} \vec{\psi} \left((\vec{\psi}^\dagger, \vec{\phi}) - (\vec{\phi}^\dagger, \vec{\psi}) \right) + \frac{2i}{a + \epsilon a^{-1}} C_2 \vec{\psi}^* \left((\vec{\psi}^T C_2 \vec{\phi}) + (\vec{\psi}^\dagger C_2 \vec{\phi}^*) \right), \\ \frac{\partial \vec{\psi}}{\partial \xi} &= \frac{i}{a} \vec{\phi} \left((\vec{\psi}^\dagger, \vec{\phi}) - (\vec{\phi}^\dagger, \vec{\psi}) \right) + \frac{2i}{a + \epsilon a^{-1}} C_2 \vec{\phi}^* \left((\vec{\phi}^T C_2 \vec{\psi}) + (\vec{\phi}^\dagger C_2 \vec{\psi}^*) \right). \end{aligned} \quad (30)$$

These equations can be obtained from the action:

$$\begin{aligned} A_{\mathbb{Z}_2, \text{GNb}} &= \int_{-\infty}^{\infty} dx dt \left(i \left(\vec{\phi}^\dagger \frac{\partial \vec{\phi}}{\partial \eta} + \vec{\psi}^\dagger \frac{\partial \vec{\psi}}{\partial \xi} \right) - \frac{1}{2a} \left((\vec{\psi}^\dagger, \vec{\phi}) - (\vec{\phi}^\dagger, \vec{\psi}) \right)^2 \right. \\ &\quad \left. - \frac{1}{\epsilon a^{-1} + a} \left((\vec{\phi}^\dagger C_2 \vec{\psi}^*) + (\vec{\phi}^T C_2 \vec{\psi}) \right)^2 \right). \end{aligned} \quad (31)$$

iii) **\mathbb{Z}_2 -ZM models.** Here $\mathfrak{G} \simeq SO(N, \mathbb{R})$. Again we used N -component vectors to cast the \mathbb{Z}_2 -reduced ZM systems in the form:

$$\begin{aligned} \frac{\partial \vec{\psi}}{\partial \xi} &= \frac{i}{a} \left(\vec{\phi}^* (\vec{\phi}^T, \vec{\psi}) - \vec{\phi} (\vec{\phi}^\dagger, \vec{\psi}) \right) + \frac{2i}{a + \epsilon a^{-1}} C \left(\vec{\phi}^* (\vec{\phi}^T C \vec{\psi}) - \vec{\phi} (\vec{\phi}^\dagger C \vec{\psi}) \right), \\ \frac{\partial \vec{\phi}}{\partial \eta} &= \frac{i}{a} \left(\vec{\psi}^* (\vec{\psi}^T, \vec{\phi}) - \vec{\psi} (\vec{\psi}^\dagger, \vec{\phi}) \right) + \frac{2i}{a + \epsilon a^{-1}} C \left(\vec{\psi}^* (\vec{\psi}^T \hat{C} \vec{\phi}) - \vec{\psi} (\vec{\psi}^\dagger \hat{C} \vec{\phi}) \right), \end{aligned} \quad (32)$$

where the involutive automorphism C can be chosen as one of the type:

$$\text{a) } C = \text{diag}(\epsilon_1, \epsilon_2, \dots, \epsilon_2, \epsilon_1), \quad \text{b) } C' = \begin{pmatrix} 1 & 0 \\ 0 & C_3 \end{pmatrix}, \quad (33)$$

with $\epsilon_j = \pm 1$ and $C_3^2 = \mathbb{1}$. For this choices of C we have $\lim_{\xi \rightarrow \pm\infty} U_R(\xi, \eta) = \lim_{\xi \rightarrow \pm\infty} C U_R(\xi, \eta) \hat{C}$. The action for the reduced ZM models is provided by:

$$\begin{aligned} A_{\mathbb{Z}_2, \text{ZM}} = & \int_{-\infty}^{\infty} dx dt \left(i \left(\vec{\phi}^\dagger \frac{\partial \vec{\phi}}{\partial \eta} + \vec{\psi}^\dagger \frac{\partial \vec{\psi}}{\partial \xi} \right) + \frac{1}{a} (\vec{\psi}^\dagger, \vec{\phi}^*) (\vec{\phi}^T, \vec{\psi}) \right. \\ & \left. - \frac{1}{a} (\vec{\phi}^\dagger, \vec{\psi}) (\vec{\psi}^\dagger, \vec{\phi}) + \frac{2}{a + \epsilon/a} \left((\vec{\psi}^\dagger C \vec{\phi}^*) (\vec{\phi}^T C \vec{\psi}) - (\vec{\phi}^\dagger C \vec{\psi}) (\vec{\psi}^\dagger C \vec{\phi}) \right) \right). \end{aligned} \quad (34)$$

4 Spectral properties of the reduced Lax operators

Here we briefly outline the construction of the fundamental analytic solutions of the Lax operator L_R . First we introduce the Jost solutions:

$$\begin{aligned} \lim_{\xi \rightarrow \infty} \Psi_{R,+}(x, t, \lambda) \mathcal{E}_R^{-1}(x, t, \lambda) &= \mathbb{1}, \quad \lim_{\xi \rightarrow -\infty} \Psi_{R,-}(x, t, \lambda) \mathcal{E}_R^{-1}(x, t, \lambda) = \mathbb{1}, \\ \mathcal{E}_R(x, t, \lambda) &= \exp \left(-i \frac{J\xi}{\lambda - a} - i \frac{CJC^{-1}\xi}{\epsilon\lambda^{-1} - a} \right), \end{aligned} \quad (35)$$

The scattering matrix is defined by:

$$T_R(\lambda, \eta) = \hat{\Psi}_{R,+}(x, t, \lambda) \Psi_{R,-}(x, t, \lambda) \quad (36)$$

The continuous spectrum of L_R (21) fills up the curves on the complex λ -plane on which the exponential $\mathcal{E}_R(x, t, \lambda)$ is oscillating

$$\text{Re} \left(-i \frac{J\xi}{\lambda - a} - i \frac{CJC^{-1}\xi}{\epsilon\lambda^{-1} - a} \right) = \text{Im} \left(\frac{J\xi}{\lambda - a} + \frac{CJC^{-1}\xi}{\epsilon\lambda^{-1} - a} \right) = 0. \quad (37)$$

Below we consider four different cases depending on the choice of ϵ and C . For convenience we denote $\lambda = \lambda_0 + i\lambda_1$ where λ_0 and λ_1 are real.

Case a): $CJ\hat{C} = J$ and $\epsilon = 1$. Condition (37) becomes: $\lambda_1(\lambda_0^2 + \lambda_1^2 - 1) = 0$.

Thus the continuous spectrum of L_{i} consists of $\mathbb{R} \cup \mathbb{S}^1$, where \mathbb{S}^1 is the unit circle with center at the origin. The discrete spectrum of L_R contains quadruplets $\lambda_k, \lambda_k^*, 1/\lambda_k$ and $1/\lambda_k^*$ of discrete eigenvalues, see fig. 1a).

Case b): $CJ\hat{C} = J$ and $\epsilon = -1$. The analog of eq. (37) is:

$$\text{Im} \left(\frac{J\xi}{\lambda - a} + \frac{CJC^{-1}\xi}{-\lambda^{-1} - a} \right) = 0. \quad (38)$$

The continuous spectrum of L_{ii} consists of the real axis \mathbb{R} only. The discrete spectrum of L_{R} consists of quadruplets $\lambda_k, \lambda_k^*, -1/\lambda_k$ and $-1/\lambda_k^*$ and of the doublet i and $-i$, see fig. 1b).

Case c): $CJ\hat{C} = -J$ and $\epsilon = 1$. The continuous spectrum of L_{R} fills up the real axis \mathbb{R} . The discrete spectrum consists of quadruplets $\lambda_k, \lambda_k^*, 1/\lambda_k$ and $1/\lambda_k^*$ and doublets (if $|\lambda_k| = 1$) of discrete eigenvalues, see fig. 1c).

Case d): $CJ\hat{C} = -J$ and $\epsilon = -1$. From eq. (38) we find:

$$\lambda_1 \left(\left(\lambda_0 - \frac{2a}{1-a^2} \right)^2 + \lambda_1^2 - c_1^2 \right) = 0, \quad c_1 = \frac{a^2 + 1}{|a^2 - 1|}. \quad (39)$$

Thus the continuous spectrum of L_{iv} consists of $\mathbb{R} \cup \mathbb{S}^1$, where \mathbb{S}^1 is a circle centered at $2a/(1-a^2)$ and radius c_1 . The discrete spectrum of L_{R} consists of quadruplets $\lambda_k, \lambda_k^*, -1/\lambda_k$ and $-1/\lambda_k^*$, see fig. 1d).

Remark 1 For the NJLVL models with $\mathfrak{g} \simeq su(N)$ and $J = \text{diag}(1, 0, \dots, 0)$ only cases a) and b) are relevant; there are no automorphisms of $su(N)$ transforming J into $-J$.

In all the cases described above one should avoid discrete eigenvalues lying on the continuous spectrum of L_{R} .

Next we can construct the FAS using the Gauss factors of the scattering matrix $T(\lambda, t)$, see [13, 3]. This allows one to apply the Zakharov-Shabat dressing method for constructing the soliton solutions of the \mathbb{Z}_2 -reduced spinor models, very much along the ideas of [13]. Unfortunately now there is no natural point in \mathbb{C} at which the RHP can be normalized, which presents an additional difficulty in applying the dressing method.

5 Conclusion

We have proposed a new class of \mathbb{Z}_2 -reduced spinor models. The spectral properties and the construction of the FAS for their reduced Lax operators L_{R} are outlined.

New classes of generalized GN-type spinor models can be constructed choosing appropriate rank-2 matrices for J instead of eq. (12). Such models will have $4N$ independent components and the inverse scattering problem for their Lax operators will be regular. One can also consider reductions with automorphisms C such that $CJ\hat{C} \neq \pm J$, as well as to explore the supersymmetric generalizations of the above models.

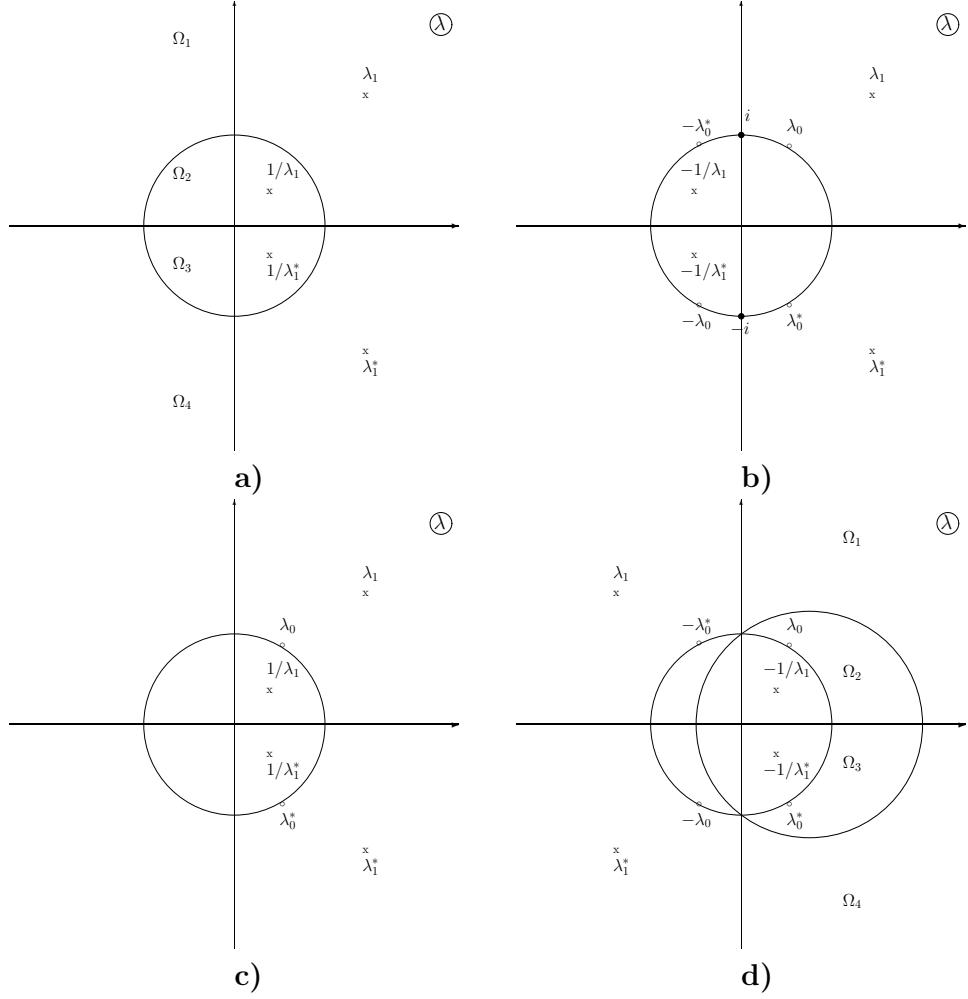


Figure 1: The continuous and the discrete spectrum of the operators L_R for the 4 different cases as described in the text. In the last case d) we have chosen $a = 1/3$.

Acknowledgements

I am grateful to Professor A. V. Mikhailov and Professor A. S. Sorin for useful suggestions and discussions. I also acknowledge a grant with the JINR, which allowed me to work on the topic 01-3-1073-2009/2013 of Dubna scientific plan and to participate in the XV SYMPHYS conference in Dubna.

References

- [1] M. J. Ablowitz, D. J. Kaup, A. C. Newell and H. Segur. *The inverse scattering transform – Fourier analysis for nonlinear problems*, Studies in Appl. Math. **53**, 249–315 (1974).
- [2] L. D. Faddeev and L. A. Takhtadjan. *Hamiltonian approach in the theory of solitons*, Springer Verlag, Berlin, (1987).
- [3] V. S. Gerdjikov. \mathbb{Z}_2 -reductions of spinor models in two dimensions. **arXiv:1210.3722v1 [nlin.SI]**. Submitted to "Physics of Atomic Nuclei", .
- [4] V. S. Gerdjikov, N. A. Kostov and T. I. Valchev. *Solutions of multi-component NLS models and Spinor Bose-Einstein condensates*. Physica D **238**, 1306–1310 (2009); **ArXiv:0802.4398 [nlin.SI]**.
- [5] V. S. Gerdjikov, G. Vilasi, A. B. Yanovski. *Integrable Hamiltonian Hierarchies. Spectral and Geometric Methods* Lecture Notes in Physics **748**, Springer Verlag, Berlin, Heidelberg, New York (2008). ISBN: 978-3-540-77054-1.
- [6] P. J. Gross and A. Neveu. *Dynamical symmetry breaking in asymptotically free field theories*. Phys. Rev. D **10**, 3235–3253 (1974).
- [7] A. V. Mikhailov. *The reduction problem and the inverse scattering method*. Physica D **3**, 73–117 (1981).
- [8] Y. Nambu and G. Jona-Lasinio. *Dynamical Model of Elementary Particles Based on an Analogy with Superconductivity. I*. Phys. Rev. **122**, 345–358 (1961).
- [9] A. Neveu and N. Papanicolaou. *Integrability of the classical $[\bar{\psi}_i\psi_i]_2^2$ and $[\bar{\psi}_i\psi_i]_2^2 - \bar{\psi}_i\gamma_5\psi_i]_2^2$ interactions*. Commun. Math. Phys. **58**, 31–64, (1978). DOI: 10.1007/BF01624787
- [10] V. G. Vaks and A. I. Larkin. *Application of Superconductivity theory methods to the problem of the masses of elementary particles*. ZhETF **40**, 282–285 (1961).
- [11] V. E. Zakharov, S. V. Manakov, S. P. Novikov, L. P. Pitaevskii. *Theory of solitons: the inverse scattering method*. (Plenum, N.Y.: Consultants Bureau, 1984).

- [12] V. E. Zakharov and A. V. Mikhailov. *Relativistic-invariant 2-dimensional field theory models integrable by the inverse scattering method.* *Zh. Exp. Teor. Fiz.* **74**, 1953–1973 (1978) (in Russian).
- [13] V. E. Zakharov and A. V. Mikhailov. *On the Integrability of Classical Spinor Models in Two-Dimensional Space-Time.* *Commun. Math. Phys.* **74**, 21–40 (1980).

ON THE PEAKON AND SOLITON SOLUTIONS OF AN INTEGRABLE PDE WITH CUBIC NONLINEARITIES

Rossen Ivanov, Tony Lyons

School of Mathematical Sciences,
Dublin Institute of Technology,
Kevin Street, Dublin 8, IRELAND
Rossen.Ivanov@dit.ie, Tony.Lyons@mydit.ie

1 Introduction

The interest inspired by the Camassa-Holm (CH) equation and its singular peakon solutions [1] prompted the search for other integrable equations with similar properties. An integrable peakon equation with cubic nonlinearities was first discovered by Qiao [12] and studied further in e.g. [13, 14]. Another equation with cubic nonlinearities was introduced by V. Novikov in [10]. The Lax pair for Novikov's equation is given in [7]. In fact the Qiao equation

$$m_t + (m(u^2 - u_x^2))_x = 0, \quad m = u - u_{xx} \quad (1)$$

together with the CH equation

$$m_t + 2u_x m + u m_x = 0, \quad m = u - u_{xx} \quad (2)$$

belong to the bi-Hamiltonian hierarchy of equations described by Fokas and Fuchssteiner [4]. It is known that the Qiao equation has a distinctive W/M -shape travelling wave solution [12, 13]. The peakons of Novikov's equation were studied in [8] while $2 + 1$ dimensional generalizations of Qiao's hierarchy are studied in [3]. Single and, multi-peakon dynamics, weak kink, kink-peakon, and stability analysis of the Qiao equation were studied in [15] and [5], while other types of solitons are studied in [9]. Results

for the CH and related equations are available in the monographs [6, 2, 11] and the references therein. Equation (1) may also be written as

$$m_t + (u^2 - u_x^2)m_x + 2u_x m^2 = 0. \quad (3)$$

Qiao introduced a 2×2 Lax pair for this equation given by the linear system $\Psi_x = \mathbf{U}\Psi$ and $\Psi_t = \mathbf{V}\Psi$ where

$$\begin{aligned} \mathbf{U} &= \begin{pmatrix} -\frac{1}{2} & \frac{1}{2}m\lambda \\ -\frac{1}{2}m\lambda & \frac{1}{2} \end{pmatrix}, \\ \mathbf{V} &= \begin{pmatrix} \lambda^{-2} + \frac{1}{2}(u^2 - u_x^2) & -\lambda^{-1}(u - u_x) - \frac{1}{2}m\lambda(u^2 - u_x^2) \\ \lambda^{-1}(u + u_x) + \frac{1}{2}m\lambda(u^2 - u_x^2) & -\lambda^{-2} - \frac{1}{2}(u^2 - u_x^2) \end{pmatrix}. \end{aligned} \quad (4)$$

Another equation from the same hierarchy is

$$m_t + \left(\frac{1}{m^2}\right)_x - \left(\frac{1}{m^2}\right)_{xxx} = 0. \quad (5)$$

The (white) soliton solutions of (1) and (5) were previously found in [16, 18]. These results rely on the fact that the spectral problem for (1) is gauge-equivalent to the one for the mKdV equation. In this communication we first discuss the peakon solutions of (1). Then we present soliton solutions which approaching a constant value as $|x| \rightarrow \infty$ (dark solitons). To this end we are going to reformulate the spectral problem in the form of a Schrödinger operator, which is also the spectral problem for the KdV equation.

2 Peakon solutions

In [7] there is a remark on the peakons of Qiao's equation, stating that their computation is problematic since one encounters a square of a delta-function. This difficulty can be avoided by the following transformation of (1). Assuming peakon solutions which vanish as $x \rightarrow \pm\infty$ and writing

$$m(x, t) = \sum_{k=1}^N p_k(t) \delta(x - x_k(t))$$

one can integrate (1) to find

$$\partial_t \int_{-\infty}^x m(y, t) dy + (u^2 - u_x^2)m(x, t) = 0,$$

giving

$$\partial_t \left(\sum_{k=1}^N p_k(t) \theta(x - x_k(t)) \right) + (u^2 - u_x^2)m(x, t) = 0,$$

It follows that

$$\sum_{k=1}^N \dot{p}_k(t) \theta(x - x_k(t)) - \sum_{k=1}^N p_k(t) \dot{x}_k(t) \delta(x - x_k(t)) + (u^2 - u_x^2) \sum_{k=1}^N p_k(t) \delta(x - x_k(t)) = 0,$$

which is only possible if

$$\dot{p}_k(t) = 0, \quad (6)$$

$$\dot{x}_k(t) = (u^2 - u_x^2)_{x=x_k(t)}. \quad (7)$$

The $N = 1$ peakon solution is easily obtained from the above system, $u(x, t) = \pm \sqrt{c} e^{-|x-ct|}$ where $p_1 = 2\sqrt{c} = \text{constant}$. This solution was reported in [7].

To compute the two-peakon solution we notice that

$$H = \frac{1}{2} \int m u \, dx = \frac{1}{2} p_1^2 + \frac{1}{2} p_2^2 + p_1 p_2 e^{-|x_1 - x_2|}$$

is a conserved quantity. Therefore $\Delta = x_1 - x_2$ is time independent, i.e. the distance between the two peakons is constant and they move together. This explains the M-shape travelling wave solution mentioned earlier, see for example Fig.1. The solution is

$$u(x, t) = \frac{1}{2} p_1 e^{-|x-ct|} + \frac{1}{2} p_2 e^{-|x-ct-\Delta|}, \quad c = \frac{1}{2} p_1 p_2 e^{-|\Delta|}.$$

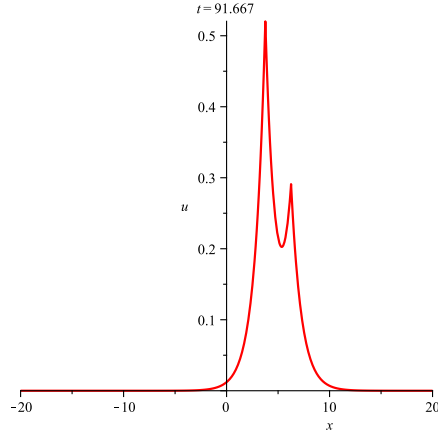


Figure 1: Two peakon profile, $p_1 = 1$, $p_2 = 0.5$, $\Delta = 2.5$.

3 Soliton solutions

3.1 Reformulation of the spectral problem

Let us consider solutions such that

$$m(x, t) > 0, \quad \lim_{x \rightarrow \pm\infty} m(x, t) = m_0, \quad (8)$$

where m_0 is a positive constant. Let us also assume that $m(x, \cdot) - m_0 \in \mathcal{S}(\mathbb{R})$ for any value of t . One can reformulate the spectral problem into a scalar one as follows. Introducing $\Psi = (\psi, \phi)^T$ the matrix Lax pair written in components becomes

$$\begin{aligned} 2\psi_x &= -\psi + m\lambda\phi \\ 2\phi_x &= -m\lambda\psi + \phi. \end{aligned}$$

With a change of coordinates

$$\partial_y = \frac{2}{m} \partial_x, \quad \psi = \frac{1}{\lambda} \left[\frac{\phi}{m} - \phi_y \right] \quad (9)$$

we obtain the following scalar spectral problem for $\phi(y, \lambda)$ (we omit the argument t which acts as an external parameter for the spectral problem being considered)

$$-\phi_{yy} + \left[\left(\frac{1}{m} \right)_y + \frac{1}{m^2} \right] \phi = \lambda^2 \phi. \quad (10)$$

Note that this is a Schrödinger's operator with a potential

$$U(y, t) = \left(\frac{1}{m} \right)_y + \frac{1}{m^2}. \quad (11)$$

It is well known how to recover $U(y, t)$ from the scattering data of (10), however the solution is $m(y, t)$ and its recovery from $U(y, t)$ necessitates solving a nonlinear (Riccati) equation. We can express $m(y, t)$ in terms of the eigenfunctions of the Schrödinger's operator. We introduce $\rho(y, \lambda) = \frac{\phi_y}{\phi}$ from which we immediately obtain

$$\rho_y + \rho^2 = \frac{\phi_{yy}}{\phi} = U(y) - \lambda^2.$$

If we define $\rho_0(y) = \rho(y, 0)$ then we have

$$U(y) = \rho_{0,y} + \rho_0^2.$$

However, comparing this with (11) we find a solution $\frac{1}{m} = \rho_0$ or

$$m(y, t) = \frac{1}{\rho_0(y, t)} = \frac{\phi(y, t, \lambda)}{\phi_y(y, t, \lambda)} \Big|_{\lambda=0} \quad (12)$$

So far we have worked with y as our variable instead of x . However we can treat y as a parameter, and then (12) represents the solution in parametric form, while the original variable x follows from (9), (12) by:

$$x(y, t) = 2 \ln \phi(y, t, 0) + \text{const.} \quad (13)$$

Assuming that $\phi(y, t, 0)$ is positive everywhere, we have a solution in parametric form (12), (13) given entirely in terms of the eigenfunctions $\phi(y, t, 0)$. We can formally write this solution as

$$m(x, t) = 2 \int_{-\infty}^{\infty} \delta(x - 2 \ln \phi(y, t, 0)) dy. \quad (14)$$

where we neglect the constant appearing in (13).

3.2 Inverse scattering and Soliton solutions

It follows from (8) and (11) that $U(y)$ does not decay to 0 as $y \rightarrow \pm\infty$. As such we need to introduce the modified potential

$$\tilde{U}(y) = U(y) - \frac{1}{m_0^2}, \quad (15)$$

which clearly satisfies $\lim_{|y| \rightarrow \infty} \tilde{U}(y) = 0$. So we have

$$-\phi_{yy} + \left[U(y) - \frac{1}{m_0^2} \right] \phi = \left(\lambda^2 - \frac{1}{m_0^2} \right) \phi,$$

or, introducing a new spectral parameter

$$k^2 = \lambda^2 - \frac{1}{m_0^2} \quad (16)$$

we have a standard spectral problem

$$-\phi_{yy}(k, y) + \tilde{U}(y)\phi(k, y) = k^2\phi(k, y), \quad \tilde{U}(y) \in \mathcal{S}(\mathbb{R}). \quad (17)$$

However when $\lambda = 0$ we find $k = \pm \frac{i}{m_0}$. This means that if we take an eigenfunction $\phi(k, y)$ of (17) which is analytic in the upper (lower) complex k -plane, we should evaluate it at $k = \frac{i}{m_0}$ ($k = -\frac{i}{m_0}$):

$$m(y, t) = \frac{\phi(y, t, k)}{\phi_y(y, t, k)} \Big|_{k=\pm \frac{i}{m_0}} \quad (18)$$

$$x(y, t) = 2 \ln \phi \left(y, t, \pm \frac{i}{m_0} \right). \quad (19)$$

The spectral theory for the problem (17) is well developed, e.g. [17]. We are going to use these results to construct the soliton solutions of (1), (5). One can introduce

scattering data as usual. For the time-dependence of the scattering data one needs the time-evolution of the eigenfunction $\phi(k, x)$. The Lax-pair in x and t variables for (1) has the form

$$\phi_{xx} = \frac{m_x}{m} \phi_x + \left(\frac{1}{4} - \frac{m_x}{2m} - \frac{m^2}{4} \lambda^2 \right) \phi, \quad (20)$$

$$\phi_t = \frac{1}{\lambda^2} \left[\frac{u_x + u_{xx}}{m} \right] \phi - \left[\frac{u + u_x}{\lambda^2 m} + \frac{u^2 - u_x^2}{2} \right] \phi_x + \gamma \phi, \quad (21)$$

where γ is an arbitrary constant. Asymptotically as $x \rightarrow \pm\infty$ equation (21) becomes

$$\phi_t \rightarrow - \left[\frac{1}{\lambda^2} + \frac{m_0^2}{2} \right] \phi_x + \gamma \phi.$$

In terms of the (y, k) -variables letting $y \rightarrow \pm\infty$ we find,

$$\phi_t \rightarrow - \frac{m_0^3}{2} \left[\frac{k^2 m_0^2 + 3}{k^2 m_0^2 + 1} \right] \phi_y + \gamma \phi, \quad (22)$$

since $\lim_{|y| \rightarrow \infty} m = \lim_{|y| \rightarrow \infty} u = m_0$. Defining Jost solutions by

$$\lim_{y \rightarrow \pm\infty} \varphi_{\pm}(y, k) e^{iky} = 1, \quad (23)$$

such that

$$\varphi_-(y, k) = a(k) \varphi_+(y, k) + b(k) \bar{\varphi}_+(y, k), \quad k \in \mathbb{R} \quad (24)$$

and noting that $\varphi_- \rightarrow a e^{-iky} + b e^{iky}$ when $y \rightarrow \infty$ it follows from (22)

$$a_t = \frac{m_0^3}{4} \left[\frac{k^2 m_0^2 + 3}{k^2 m_0^2 + 1} \right] (ika) + \gamma a, \quad b_t = - \frac{m_0^3}{4} \left[\frac{k^2 m_0^2 + 3}{k^2 m_0^2 + 1} \right] (ikb) + \gamma b.$$

Requiring $a_t = 0$, we find

$$b_t = -ik \frac{m_0^3}{2} \left(\frac{k^2 m_0^2 + 3}{k^2 m_0^2 + 1} \right) b(k, t)$$

and thus for the scattering coefficient $r \equiv b/a$ we have

$$r(k, t) = r(k, 0) \exp \left[-ik \frac{m_0^3}{2} \left(\frac{k^2 m_0^2 + 3}{k^2 m_0^2 + 1} \right) t \right], \quad (25)$$

while the analogue on the discrete spectrum $k = i\kappa_n$, is given by

$$R_n(t) \equiv \frac{b(i\kappa_n)}{ia'(i\kappa_n)} = R_n(0) \exp \left[\frac{\kappa_n m_0^3 (3 - \kappa_n^2 m_0^2)}{2(1 - \kappa_n^2 m_0^2)} t \right]. \quad (26)$$

It is convenient to introduce a dispersion law $f(\kappa) = \frac{\kappa m_0^3 (3 - \kappa^2 m_0^2)}{2(1 - \kappa^2 m_0^2)}$. Then we can write

$$R_n(t) = R_n(0) \exp(f(\kappa_n)t). \quad (27)$$

For further convenience we introduce

$$\xi_n \equiv y - \frac{f(\kappa_n)}{2\kappa_n}t - \frac{1}{2\kappa_n} \ln \frac{R_n(0)}{2\kappa_n}.$$

The eigenfunctions of the spectral problem (17) are well known, see e.g. [17]. In the purely N -soliton case the eigenfunction analytic in the lower complex k -plane is the Jost solution $\varphi_+(y, k)$ defined in (23) which has the form

$$\varphi_+(y, t, k) = e^{iky} \left(1 + \sum_{n=1}^N \frac{\Gamma_n(y, t)}{k - i\kappa_n} \right) \quad (28)$$

with the residues $\Gamma_n(y, t)$ satisfying a linear system

$$\Gamma_n(y, t) = iR_n(t)e^{-2\kappa_n y} \left(1 + i \sum_{m=1}^N \frac{\Gamma_m(y, t)}{\kappa_n + \kappa_m} \right).$$

The time-dependence of the scattering data is given by (27). The N -soliton solution then is given in parametric form by (18) and (19) for the eigenfunction (28). The condition $0 < \kappa_n < m_0^{-1}$ is sufficient to ensure smoothness of the solitons.

3.3 Example: One-Soliton Solution

The one-soliton solution corresponds to one discrete eigenvalue $k_1 = i\kappa_1$, where κ_1 is real, positive and $\kappa_1 < m_0^{-1}$. The eigenfunction in this case is (28)

$$\varphi_+(y, t, k) = e^{iky} \left(1 + \frac{1}{k - i\kappa_1} \cdot \frac{iR_1(t)e^{-2\kappa_1 y}}{1 + \frac{R_1(t)}{2\kappa_1}e^{-2\kappa_1 y}} \right). \quad (29)$$

Evaluated at $k = \frac{-i}{m_0}$ we find

$$\varphi_+(y, t, \frac{-i}{m_0}) = e^{\frac{-iy}{m_0}} \left(1 - \frac{1}{\frac{1}{m_0} + \kappa_1} \cdot \frac{R_1(t)e^{-2\kappa_1 y}}{1 + \frac{R_1(t)}{2\kappa_1}e^{-2\kappa_1 y}} \right).$$

From (18) and (19) we obtain the one-soliton solutions

$$x(y, t) = \frac{2y}{m_0} + 2 \ln \left(1 - \frac{\kappa_1 m_0 e^{-\kappa_1 \xi_1}}{(1 + \kappa_1 m_0) \cosh \kappa_1 \xi_1} \right), \quad (30)$$

$$m(y, t) = \frac{m_0}{1 + \frac{\kappa_1^2 m_0^2 \operatorname{sech}^2 \kappa_1 \xi_1}{1 - m_0 \kappa_1 \tanh \kappa_1 \xi_1}}. \quad (31)$$

The extremum (minimum) of m occurs when $\xi_1 = \frac{1}{4\kappa_1} \ln \left(\frac{1 - m_0 \kappa_1}{1 + m_0 \kappa_1} \right)$. This is a constant value, e.g. the soliton moves with a velocity $\frac{f(\kappa_1)}{2\kappa_1}$ that depends on the dispersion law (i.e. the chosen equation from the hierarchy). The profile of the dark soliton is given in Fig. 2.

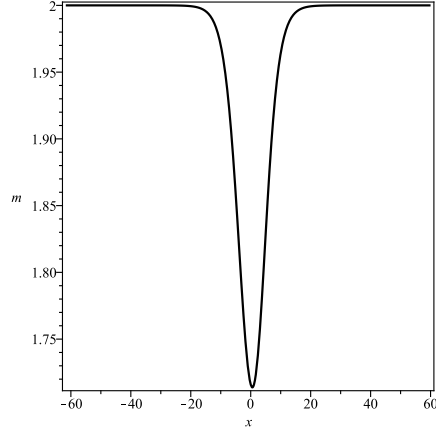


Figure 2: One soliton profile, $m_0 = 2$, $\kappa_1 = 0.2$.

3.4 Example: Two soliton solution

In the case of two discrete eigenvalues we compute

$$\varphi_+(y, t, \frac{-i}{m_0}) = e^{\frac{y}{m_0}} \frac{1 + \nu_1 e^{-2\kappa_1 \xi_1} + \nu_2 e^{-2\kappa_2 \xi_2} + \left(\frac{\kappa_1 - \kappa_2}{\kappa_1 + \kappa_2}\right)^2 \nu_1 \nu_2 e^{-2\kappa_1 \xi_1 - 2\kappa_2 \xi_2}}{1 + e^{-2\kappa_1 \xi_1} + e^{-2\kappa_2 \xi_2} + \left(\frac{\kappa_1 - \kappa_2}{\kappa_1 + \kappa_2}\right)^2 e^{-2\kappa_1 \xi_1 - 2\kappa_2 \xi_2}} \quad (32)$$

where the following notation is utilized:

$$\nu_j = \frac{\frac{1}{m_0} - \kappa_j}{\frac{1}{m_0} + \kappa_j}, \quad j = 1, 2.$$

From (18) and (19) we obtain the two-soliton solutions:

$$x(y, t) = \frac{2y}{m_0} + 2 \ln \frac{\Delta_1}{\Delta_2} \quad (33)$$

$$m(y, t) = \frac{m_0}{1 + \frac{m_0 \Delta_3}{\Delta_1 \Delta_2}}. \quad (34)$$

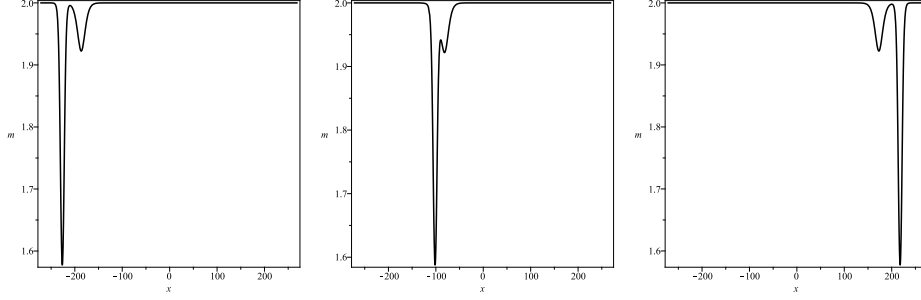


Figure 3: Snapshots of the two (dark) soliton solution of the Qiao equation (1), for three values of t : -30 , -12 and 30 . The other parameters are $m_0 = 2$, $\kappa_1 = 0.1$, $\kappa_2 = 0.25$.

where the following notations are used:

$$\begin{aligned}
\Delta_1(y, t) &= 1 + e^{-2\kappa_1\xi_1} + e^{-2\kappa_2\xi_2} + \left(\frac{\kappa_1 - \kappa_2}{\kappa_1 + \kappa_2}\right)^2 e^{-2\kappa_1\xi_1 - 2\kappa_2\xi_2} \\
\Delta_2(y, t) &= 1 + \nu_1 e^{-2\kappa_1\xi_1} + \nu_2 e^{-2\kappa_2\xi_2} + \left(\frac{\kappa_1 - \kappa_2}{\kappa_1 + \kappa_2}\right)^2 \nu_1 \nu_2 e^{-2\kappa_1\xi_1 - 2\kappa_2\xi_2} \\
\Delta_3(y, t) &= \frac{4\kappa_1^2}{m_0^{-1} + \kappa_1} e^{-2\kappa_1\xi_1} + \frac{4\kappa_2^2}{m_0^{-1} + \kappa_2} e^{-2\kappa_2\xi_2} \\
&\quad + \frac{8(\kappa_1 - \kappa_2)^2}{m_0(m_0^{-1} + \kappa_1)(m_0^{-1} + \kappa_2)} e^{-2\kappa_1\xi_1 - 2\kappa_2\xi_2} \\
&\quad + \frac{4\kappa_2^2\nu_1}{m_0^{-1} + \kappa_2} \left(\frac{\kappa_1 - \kappa_2}{\kappa_1 + \kappa_2}\right)^2 e^{-4\kappa_1\xi_1 - 2\kappa_2\xi_2} \\
&\quad + \frac{4\kappa_1^2\nu_2}{m_0^{-1} + \kappa_1} \left(\frac{\kappa_1 - \kappa_2}{\kappa_1 + \kappa_2}\right)^2 e^{-2\kappa_1\xi_1 - 4\kappa_2\xi_2}. \tag{35}
\end{aligned}$$

The interaction of two dark solitons is illustrated in Fig. 3.

4 Conclusions

In this paper we demonstrated firstly, how to obtain peakon solutions of the Qiao equation and secondly how the spectral problem for the Qiao equation can be reduced to the one for the standard Schrödinger operator. Hence the soliton solutions ('dark' solitons) can be obtained in a straightforward manner. This necessitates constant boundary conditions for the solution and also a restriction on the discrete eigenvalues $0 < \kappa_n < m_0^{-1}$. It is interesting what happens to the solutions if this condition is violated. Based on the similarity with Camassa-Holm equation it is likely that there

are breaking waves present in this case. Moreover, the equation (1) has a conservation law in the form $X_x(x, t)m(X, t) = m(x, 0)$ where X is the solution of

$$X_t(x, t) = u^2(X, t) - u_x^2(X, t), \quad X(x, 0) = x.$$

This last equation is analogous to (6) in the peakon case. It is likely that this conservation law will play an essential role in the study of the well-posedness, existence and breaking of solutions.

5 Acknowledgments

This material is based upon works supported by the Science Foundation Ireland (SFI), under Grant No. 09/RFP/MTH2144.

References

- [1] R. Camassa and D. Holm, An integrable shallow water equation with peaked solitons, *Phys. Rev. Lett.* **71** (1993) 1661–1664.
- [2] A. Constantin, *Nonlinear Water Waves with Applications to Wave-Current Interactions and Tsunamis* (SIAM, Philadelphia, 2011).
- [3] P.G. Estévez, Generalized Qiao hierarchy in $2 + 1$ dimensions: Reciprocal transformations, spectral problem and non-isospectrality, *Phys. Lett. A* **375** (2011) 537–540.
- [4] A. Fokas and B. Fuchssteiner, On the structure of symplectic operators and hereditary symmetries, *Lett. Nuovo Cimento* **28** (1980) 299–303.
- [5] G. Gui, Y. Liu, P.J. Olver and C. Qu, Wave-Breaking and Peakons for a Modified Camassa-Holm Equation, *Comm. Math. Phys.* (2012) DOI:10.1007/s00220-012-1566-0
- [6] D. D. Holm, T. Schmah and C. Stoica, *Geometric Mechanics and Symmetry* (Oxford University Press, Oxford, 2009).
- [7] A.N.W. Hone and Jing Ping Wang, Integrable peakon equations with cubic nonlinearity, *J. Phys. A: Math and Theor.* **41** (2008) 372002 (10pp).
- [8] A.N.W. Hone, H. Lundmark, and J. Szmigielski, Explicit multipeakon solutions of Novikov’s cubically nonlinear integrable Camassa-Holm type equation, *Dynamics of Partial Differential Equations* **6** (2009) 253–289.
- [9] R. Ivanov and T. Lyons, Dark solitons of the Qiao’s hierarchy, *J. Math. Phys.* **53** (2012) 123701.
- [10] V. Novikov, Generalizations of the Camassa-Holm equation, *J. Phys. A: Math. Theor.* **42** (2009) 342002 (14pp)
- [11] P. Popivanov, A. Slavova, *Nonlinear waves. An Introduction*, ISAAC series on Analysis, Applications and Computation **4** (World Scientific, NJ, 2011).
- [12] Z. Qiao, A new integrable equation with cuspons and W/M -shape-peaks solitons, *J. Math. Phys.* **47** (2006) 112701 (9 pp).
- [13] Z. Qiao, New integrable hierarchy, its parametric solutions, cuspons, one-peak solitons, and M/W -shape peak solitons, *J. Math. Phys.* **48** (2007) 112701 (19 pp).
- [14] Z. Qiao and L. Liu, A new integrable equation with no smooth solitons, *Chaos, Solitons and Fractals* **41** (2009) 587–593.
- [15] Z. Qiao, B. Xia and J. Li, Integrable system with peakon, weak kink and kink-peakon interactional solutions, arXiv:1205.2028v2 [nlin.SI] (2012)

- [16] S. Sakovich, Smooth soliton solutions of a new integrable equation by Qiao, *J. Math. Phys.* **52** (2011) 023509 (9 pages).
- [17] V.E. Zakharov, S.V. Manakov, S.P. Novikov and L.P. Pitaevskii, *Theory of solitons: the inverse scattering method*, (Plenum, New York, 1984).
- [18] Zhaqilaoa, Zhijun Qiao, N-soliton solutions of an integrable equation studied by Qiao, arXiv:1101.5742v1 [nlin.SI].

MODELLING A SYSTEM WITH DISCRETE EVENTS

Stoyan Kapralov, Valentina Dyankova

Technical University Gabrovo
Gabrovo, Bulgaria

I. INTRODUCTION

Computer modeling is one of the most powerful tools of knowledge, analysis and design. It allows for experimenting with objects when the real actions are not possible or the objective is a research to track their behavior. Essentially, the methodology for computer modeling is to replace the real object with its model. Working with a model allows for a relatively quick exploration of the properties and behavior of objects in arbitrary situations. In this context, imitation experiments provide the opportunity to study objects in sufficient fullness. If conducted in an information-educational environment they could be used as a means of developing students' research. In this sense we can talk about creating a learning concept which utilizes the software technology to simulate the behavior of an object model.

The paper presents the general structure of modeling a system with discrete event simulation. Models with discrete events correspond to those systems in which changes of the states of the system are carried out in discrete moments of time. This paper studies the basic concepts [5] in discrete event modeling in an ICT educational environment.

II. PRELIMINARIES

The published results on the process of creating a model of a discrete event system fall into the following groups:

1. Creating a model that serves a particular area. This group contains most publications describing the concrete realization of the modeling process. Each implementation is oriented to the characteristics of the particular subject area and to the ultimate goal of using the model – planning of transport in the German food industry [14], accident management and methodical identification of the "bugs" system [12], plants production systems [3], extending the life of components in medical devices [7], modeling of distributed computing environments in web-based computing [1].

2. Usage of a specific tool for modeling a discrete event system. Publications in this group focus on the ability of specific simulation tools and the implementation specifics: the features of the object-oriented language and the use of visual design [6], using finite automata with variables [13], using Petri Nets in the power system [2], using the SystemVerilog simulation system [10], using the SimEvents Matlab set [15]

3. Detailed elaboration of a specific part of the entire modeling process. Publications in this group contain detailed solutions to a specific stage of the entire simulation process. For example, error detection [9].

The core of each of the groups above integrates the following restrictions:

- Inability to present a generalized model of the process of modeling a discrete event system. In this sense, each example in item 1 should be seen as a specification of the generic model for a specific subject area.

- Focus on tools for creating a discrete-event model at the expense of the nature of the modeling process. This is a prerequisite for conventional thinking in the terminology of the specific system for formalization of knowledge. The latter limits the possibility for refinement of the theory through the deductive method according to the objectives and to be interpreted in terms of the chosen technological approach.

- The refinement of individual parts of the modeling process outside the context of the overall process can lead to loss of information necessary to achieve different stages in the modeling process.

III. PRESENTATION

A. Choosing a methodology for designing a discrete-event model.

The aim is to create an adaptive learning model to study the process of modeling of systems with discrete events, which is closest to the scientific status of the student, while professional competence is formed in this process.

The lack of uniformity in the output platform for studying the process of discrete-event simulation is the basis for the selection of such a method in its structure, which interprets the systems with discrete events as knowledge systems, enabling:

- relative autonomy and independence of the system used for the formalization;
- sequential separation into component processes that are logically connected in hierarchical relationships. The latter allow for in-depth attention to detail of the design process, depending on the objectives.
- dynamism and mobility in the accumulation of new facts about the system. Each of these facts must be interpreted in relation to the others and to allow it to be explored in relation to others. Hierarchy can be expanded in depth, allowing knowledge to be extended based on different theoretical and practical platforms.

In this context, the modeling of systems with discrete events is considered the most general process, independent of the subject area and the used formalism. For such an organization of the process of discrete-event systems design we will employ methodology that uses the idea of the structured analysis and design technique (SADT) for structuring the process of discrete-event simulation.

SADT [4] is used successfully for a wide range of tasks such as long-term strategic design, automated manufacturing and design and others. The versatility of the method allows it to be applied in teaching modeling of discrete-event systems. In its basis lies studying of the system, starting with a general overview, further detailing its constituent parts and hierarchical organization of the system levels. Thus it is possible to decompose the design functions and to establish hierarchical relationships between the functional subsystems. This process can be defined as follows:

1. Determination of a Complex Objective (CO) – it is determined by the practical use of the model taking into account the specific subject area. Use of formalism is not required.
2. Establishing of the Integrated Objectives (IO). IC is the goal of the activity, a constituent of the overall activity of a system for the implementation of a complex goal. In this context during the implementation of this stage the stages to reach the CO are determined. At this point, the logical structure in the behavior of the real system is taken into account as well as the functional dependencies among the subsystems. The analysis of the behavior of each subsystem provides for a choice of formalism, in the terms of which it is modeled. In this sense different formalisms can be applied, allowing for the optimal modeling of the individual subsystems.
3. Defining the Particular Goals (PG) and the action parameters. Each activity consists of a set of actions which ensure reaching the purpose of the activity, which incorporates them. We will call the objectives of these actions PG. The definition of PG is limited to the hierarchical decomposition of the activities' exercise. Each action is directed to an object. Each object has properties. The properties of the object to which the action is directed are defined as parameters of the action. Each activity is interpreted in terms of the chosen formalism by creating a model of the activity.
4. Determination of Educational Elements (EE). Includes defining the operations constituting any action. Thus, the learning element can be defined as a simple teaching skill specific to the used modeling formalism. At this stage in-depth knowledge of the specific tools for the selected formalism.

In this way the considered process of decomposition of the goals in the design of a system with discrete events will be interpreted in terms of discrete-event simulation.

B. Discrete-event modeling

Discrete event modeling of any real process requires time and presence of random elements that change in a discrete fashion. [82] It requires a process to be considered as a system - a set of objects (people, equipment) that interact to achieve one or more common goals. Discrete-event simulation as a particular kind of technology can be divided into the following stages, consistent with the methodology given in A.

1. Structural analysis. At this stage a formalization of the structure of the real process is performed through its decomposition into the constituent parts of a system. In this context, discrete-event simulation requires the determination of the following structural features of this system:

- *System status* (CO) - it is a relationship between the objects in the system at any given time. It is represented by a set of variables that contain all the information necessary to describe the system at any point of time.
- *Event* (IO) - a demand for a particular kind of service. It changes the state of the system (e.g. arrival of a customer, airplane landing, etc.). The event is a dynamic unit of any model working as an imitation of the real process.
- *Current event* (IO) - marking the event, being executed or pending execution, depending on the availability of relevant data required for processing the event. This selection can be accomplished by saving or printing the information for the event. Minimum information required includes the type of event and time.
- *Action* (PG) – a basic step of the activity performed by an object when interacting with other objects in the system. It is set as a time of specified duration. For example, the time for serving an object. This period is characterized by the model developers and is determined by one of the following ways:
 - Deterministic (e.g. always 5 minutes)
 - Statistical (such as a random sample of the numbers 4, 7, 9 with equal probability)

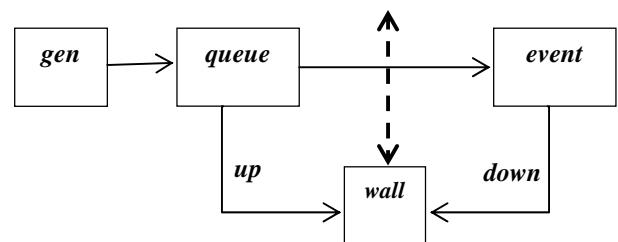


Figure 1.

- Using a function that depends on the variables of the system and / or the properties of the object (e.g. the time an aircraft clears the runway depends on the number of passengers on board)

The duration of the proposed action is calculated at its occurrence (its start) and is assigned to a variable. Each unit of elapsed time will alter the remaining duration of the action by decreasing it, in other words the value of the variable will be decremented. With such a formalization of the action it will end when the variable becomes 0.

- *Objects* (EE, parameters) - any object from the system, which has to be explicitly represented in the model (such as a person, a machine or a control unit). Language constructs, reflecting its nature can be used to for its representation. In C++ , most often it is a structure (struct)

- *Properties or attributes* (EE, parameters) - these are the properties of each object. For example, if the object is a plane such properties can be: destination, number of passengers, airline fuel, landing time, etc. It is particularly important to separate those properties that are relevant to the interaction of objects in the model. For example, the amount of fuel is such a property, if priority is given to an aircraft with little remaining fuel. These properties will be called *key properties*.

- *List* (EE, parameters) – a set (permanent or temporary) of related objects. These objects are connected in a data structure based on the logical relationship between them. This data structure can be for example a priority queue (the aircrafts are served according to their remaining fuel), FIFO queue (customers are served in order of arrival) and others.

- *Time* (EE, parameters) – the time during which the process is being modeled. It is represented by a variable reflecting the time interval during which the process is modeled. It is marked by *Clock* in the text below.

2. *Formalized description of the model*. This is a graphical representation of the Simulation Model. An oriented graph is used (Fig. 1) whose nodes can be defined as follows:

- *Event Generator (gen)* - creates new events and transmits them to other nodes in the model.

- *Queue (queue)* - can be given priority or no priority.

- *Wall (wall)* - if the wall affects an *up* signal from a node, the wall rises and events cannot be processed. A *down* signal from another node takes off the wall.

- *Current Event (event)* - an action that takes place in the current time

C. Examples of a discrete-event model

Example 1: AERIAL airport has only one runway for take-off and landing so that the runway can be used by

only one plane. This means that some planes have to circle over the airport until their turn to land comes and others have to wait on the ground to take off. The plane expecting permission to land has a priority over the ones waiting for a takeoff. Among the planes waiting to land the highest priority has the one with the least fuel.

Write a program that performs the runway control process of 500 units of time (prints whether the plane is taking off or landing; for the taking off planes prints the time of arrival of the aircraft, for the landing airplanes prints the remaining fuel and the time at which the aircraft has arrived above the airport). A take-off airplane frees the runway in 90 units of time, and a landing plane – in $2 * R$, where R is the number of passengers on the plane. Request for landing or a take-off is done by a random number generator – a random number is generated between 0 and 799. The distribution of intervals is given in Table 1, and the remaining fuel for airplanes is given by the formula $n / 10$.

The model with discrete events has the following components:

- *System status*

$C_i(t)$ - The number of departing planes awaiting serving at a time t

$C_k(t)$ - The number of landing planes awaiting serving at a time t

$C_p(t)$ - A value of 0 or 1 depending on whether the runway is occupied or free at any time t

$C_o(t)$ - The remaining time for the runway to be occupied.

- *Event*

Arrival of a plane (modeled by the random number generator)

Serving a taking off airplane (when it occupies the runway)

Serving a landing airplane (when it occupies the runway)

- *Current Eventt*

Serving a plane (landing or taking off). This includes printing of a field from the information part (time of

TABLE I.

<i>Distribution of the random</i>	<i>Aircraft action</i>	<i>Number of passengers</i>
-----------------------------------	------------------------	-----------------------------

<i>numbers</i>		
0 – 99	landing	35
99 – 200	taking off	
301 – 399	landing	49
500 – 599	taking off	
700 – 799	landing	28

arrival) and the key field (fuel remaining) for the landing aircraft and the information part for the take-off airplane (time of arrival).

- *Action*

Serving a taking off plane. Identified with the time remaining to serve a taking off plane. It is kept as the value of the *ti* variable which is initialized deterministically (90 units).

Serving a landing airplane. Identified with the time remaining to serve a landing plane. It is kept as the variable of the *tk* variable which is initialized as a function (equal to twice the number of passengers on the plane)

Objects – taking off and landing airplane.

Attributes

The departing plane has no specific attributes, but is identified with the time in which it has arrived. Therefore, the informational part for this object is of type *int*

The hovering airplane has a key attribute of remaining fuel ($n/10$), where *n* is the generated number, the number of passengers, which determines the time the runway is freed and the plane's arrival time. Therefore the types of the key field and the informational part are *int* and *plane*, where

```
struct plane {int count; int time};
```

List

All take-off planes are arranged in a queue *q*: *Queue* < int >

All landing airplanes are connected into a priority queue *qp*: *PriorityQueue* < int, *plane* >

Time

It is presented using the *Clock* variable, taking values from 1 to 500. The current value of this variable is the current point of time.

The software model can be defined as follows:

```
Queue<int> q;
PriorityQueue<int, plane> qp;

int clock, ti = 0, tk = 0;
int CiT = 0, CkT = 0, CoT = 0;

bool CpT = true;

for (clock = 1; clock <= 500; clock++)
{ gen (clock, q, qp, CiT, CkT);
  if (CpT == (CoT == 0))
    event (q, qp, ti, tk, CoT);
  else CoT = ti>0 ? ti-- : tk--;
}
```

where:

void gen (int t, Queue<int>&q, PriorityQueue<int,plane>&qp, int&CiT, int&CkT)– this function models the "arrival of a plane" event. In the body of the function an integer is generated in the range [0, 799], and depending on its value changes are made in the values of the parameters.

void event (Queue<int>&q, PriorityQueue<int,plane>&qp, int&ti, int&tk, int&CoT - this function models the "serving a taking off plane" and "serving a landing plane" events printing the relevant information and changes the values of the relevant parameters.

This process of traffic control does not contain a "wall" (wall). One such condition-wall might be: "If five airplanes are served consecutively, serve the one taking off (if any) irrespective of planes waiting to land." Integrating the model of the air traffic control restrictions arising from the condition-wall allows for the accumulation of facts about new properties using the experiment, induction, analogy. At the same time it provides the students with skills for operating in unusual surroundings and detecting conditions, enabling the use of the concept of discrete-event simulation.

Example 2: Bank MONPAY has two cashiers A and B. In order to study the need to create a new cash window, the bank managers gather information about the employment of staff and the number of customers who refuse to wait. The work-load of employees is measured by the percentage of working time during which they serve customers.

Write a program that models the activity of the two cashiers when serving customers for 2000 units of time, if you know that:

- At the beginning of the simulation there are no waiting customers, both cashiers are free and there are no served clients.
- For each client keep the time of arrival
- The customer selects the shorter queue. If the queues are equal choose one at random.
- The last customer can change queues
- The maximum queue is 10. This means that if a customer arrives when the two lines have 10 customers, he gives up.
- Service time per customer is calculated by the formula $5 \cdot (\text{SUM} - 36) + 44$, where SUM is the sum of 6 random numbers within the interval [6, 26]

After these 2000 units of time, the program should print:

- Total number of customers served
- Total number of customers who have given up
- Percentage of clients served by cashier A and cashier B
- Maximum length of both lines
- Average length of both lines
- Average waiting time
- Maximum waiting time

IV. ASSESSMENT METHODOLOGY

The thus determined goal of creating a generic model of the process of discrete-event simulation requires an in-depth analysis of the course of the students' thinking process. In particular how to manage in the different levels adequate to support the hierarchy of objectives. Here the interest is in the logical process of reaching certain knowledge, its qualitative origin. This determines the choice of research method - the method "field study" according to the characteristics described in [11].

The field research is based on naturalism. Flexibility is its main advantage. It allows for changing of direction. This means that the stages are not determined in advance - they evolve according to the process. In the beginning an overall picture of the "field" and then focus of attention is on the problems and the ways to resolve them.

Criteria and indicators in the study:

Criterion 1 (C1) - perception of each system with discrete events as an entity – a quality defined by its characteristic properties.

Indicators:

C1₁ - opportunity to interpret the behavior of the discrete-event system by the values of certain parameters.

C1₂ - opportunity to detect a new behavior of the system when changing the parameter values.

Criterion 2 (C2) - defining the component activities in the operation of a system with discrete events.

Indicators:

C2₁ - allows the application of deduction in the overall system behavior.

C2₂ – opportunity to define sufficient conditions for the occurrence of an event in the overall system behavior.

Criterion 3 (C3) - choice of formalism for modeling the component activities

Indicators:

C3₁ – opportunity to parameterize the component activities and to determine sufficient conditions to identify the activity.

C3₂ - determine the specific component activity.

Criterion 4 (C4) - formalization of actions in terms of the chosen formalism.

Indicators:

C4₁ - opportunity of using the concrete technology tools for system behavior modeling.

C4₂ – opportunity to detect critical parameters of the activity enabling its optimization within the chosen formalism.

V. EVALUATION OF RESULTS

The evaluation is performed on a five-point scale of students' achievements at the relevant criterion: low (1), satisfactory (2), good (3) Good (4), excellent (5). The score for each criterion is integrated from the individual performance indicators.

The general course of study can be divided into two phases. The first phase does not use the considered methodology. The results are evaluated separately for each of the stages (Table II) and summarized.

Phase 1

Each academic task for modeling a discrete-event system is considered in isolation and in the context of the subject area and studied formalism.

The results of this stage are as follows:

- Students cannot interpret the behavior of the system as a real-life object. They accept the latter as a training template for testing the selected tools for its formal representation.
- Students cannot disregard the details and to parameterize a random process.
- Students can transfer knowledge of template type – they attempt to repeat mechanically the modeling process in previous tasks without skills to report subject area specifics.

Inference: At this phase students misinterpret the task. They believe that their goal is testing the basic structures in the selected formalism.

TABLE II.

	Stage 1	Stage 2
C1	3	5
C2	2	5
C3	4	4
C4	4	4

Phase 2

Discrete-event systems are regarded as real-world objects, whose behavior can be studied using the deductive approach. The modeling of such an object is made using the method described in the hierarchical subordination of the goals.

The results of this stage demonstrate:

- The characteristic properties of a discrete-event system in a particular subject area are derived from the overall concept for the behavior of such a system.
- Opportunity to detect sufficient conditions for the occurrence of an event and adequately defining its parameters. This leads to the generation of ideas for a possible new occurrence of system behavior.

- Distancing from the details and considering the system as a whole concept allows for focusing the students' attention to the major events and the invariant manifestation of the process under consideration. They in turn are the basis for determining the logical relationships between the activities. This is used as a basis for detailing the activities and an appropriate formalism is selected according to this specification.

- The students find evidence for utilization of the system and relate it to specific events through appropriate parameter values.

- The students can transfer knowledge by analogy of sample model behaviors.

Inference: Students understand the nature of the process of modeling of a discrete-event system. They model any particular system by specification of the unified model. The process of modeling is not associated with a particular formalism and in this sense it is not regarded as generic for the discrete-event system. What's more, it provides freedom of choice, providing optimal presentation of the logical relationships between the different subsystems. Conditions are created for an adequate parameterization of the model to the subject area and exploration of its behavior by changing the parameter values.

VI. CONCLUSIONS

The considered concept of discrete event programming and its adaptation to the creation of a model of traffic control may be used in information and education environment as a tool for:

- Accumulation of facts about objects and their properties and organizing them into causality relations.
- Discovering in different situations the characteristic properties of a process in the system, not in isolation.
- Discovering the behavior of an object set of properties sufficient to enable the modeling of the object.
- Generating ideas for modeling relationships between objects.
- Discovering of border cases for the considered model and exploration of the behavior of objects in them.

REFERENCES

- [1] F.M. Alam, S. Mohan, S. Fowler and J.W., Gopalakrishnan, "A discrete event simulation tool for performance management of web-based applicationsystems", *Journal of Simulation*, vol. 6, Issue 1, February 2012, pp. 21-32
- [2] T. Biswas, A. Davari, and A. Feliachi., "Modeling and analysis of discrete event behaviors in power system using Petri nets", *System Theory*, 2004. *Proc. of the Thirty-Sixth Southeastern Symposium*
- [3] D. Côté, and R. St-Denis, "Component-Based Method for the Modeling and Control of Modular Production Systems", *IEEE Transactions on Control Systems Technology*, 2012
- [4] D. Marca and C. McGowan, *Structured Analysis and Design Technique*, McGraw-Hill, 1987
- [5] G.S. Fishman, *Principles of discrete event simulation*, John Wiley and Sons, New York, 1978.
- [6] P. Fritzson and P. Bunus, "Modelica – a general object-oriented language for continuous and discrete-event system modeling and simulation", *Proc.. 35th Annual Simulation Symposium*, 2002.
- [7] O.Heuermann, A. Fleischer and W. Fengler, "Discrete event simulation for complex high-power medical systems", *IEEE Transactions on Plasma Science*, vol. 40, Issue 7 PART 2, 2012, Article number A4
- [8] R. Kumar and V. Garg, *Modeling and control of logical discrete event systems*, Boston, MA: Kluwer Academic Publishers, 1995.
- [9] R.H.Kwong and D.L.Yonge-Mallo, "Fault Diagnosis in Discrete-Event Systems: Incomplete Models and Learning", *Systems, Man, and Cybernetics, Part B: Cybernetics*, *IEEE Transactions on* Volume: 41, Issue: 1, 2011
- [10] M. Paret, J. George and A Mohamed, "Modeling discrete event system with distributions using SystemVerilog", *Circuits and Systems (ISCAS)*, 2012 *IEEE International Symposium*
- [11] L.W.Neuman, *Social research methods: qualitative and quantitative approaches*, 2nd ed. Boston etc.: Allyn and Bacon, 1991
- [12] N. Shlayan and P. Kachroo, "Formal Language Modeling and Simulations of Incident Management", *IEEE Transactions on Intelligent Transportation Systems*, 19 June 2012
- [13] M. Skoldstam, K.Akesson, and M. Fabian, "Modeling of discrete event systems using finite automata with variables", *Decision and Control*, 2007 46th *IEEE Conference*
- [14] R.Sprenger, and L. Mönch, "A methodology to solve large-scale cooperative transportation planning problems", *European Journal of Operational Research*, vol. 223, Issue 3, pp.626–636, 16 December 2012
- [15] J. Zelenka, *Discrete event dynamic systems framework for analysis and modeling of real manufacturing system*, *Intelligent Engineering Systems (INES)*, 2010 14th *International Conference*

THE SPECIAL FUNCTIONS - CLASSICAL AND NEW, AND RELATIONS TO FRACTIONAL CALCULUS

Virginia Kiryakova

Institute of Mathematics and Informatics
Bulgarian Academy of Sciences,
Sofia -1113, Bulgaria
virginia@diogenes.bg

1 Introduction and definitions of the basic SF of FC

Special Functions (SF) are very old branch of mathematics. The search for a complete and unified theory of SFs has continued since the nineteenth century. Their importance as a tool of mathematical analysis is well known to the applied scientists and engineers dealing with the practical application of differential equations, and the variety of the problems leading to special functions stimulated the development of their theory. Most often, the SFs appear as solutions of some basic ODEs, and in solving PDEs by means of separation of variables method. For their definitions and well known examples, one can see in the manual books of the "*Classical Calculus*" era, as the Bateman Project [1]; the books of Luke; Abramowitz and Stegun, etc. From the contemporary point of view, almost all of the *Special Functions of Mathematical Physics* (we shall call them also "*Classical Special Functions*"), can be represented as *generalized hypergeometric* ${}_pF_q$ -functions, or more generally - as *Meijer's G-functions*, see such extended lists of representations in the "*after 80's*" books, like: [2]–[10]. Equipped with only these tables of *G*-functions and their few basic properties, even a beginner could be able to determine the relation between two special "named" functions, evaluate integrals of them, invert integral transforms, determine series expansions, etc. Also, nowadays they can be easily recognized and worked with efficiently by software packages for analytical calculus such as *Mathematica*,

Maple, Matlab, etc. See for example the extensive information at Wolfram's site, <http://functions.wolfram.com/>.

Even the SFs of the *Classical Calculus* are closely related to the *Fractional Calculus* (FC) (see [11], [7]–[10], [12]), as well as to the *Generalized Fractional Calculus* (GFC) (see for example [7], [13]), and shown to be representable as fractional order integration or differentiation operators of some basic elementary or other special functions. Relations of this kind provide also some alternative definitions for the special functions by means of Poisson- and Euler-type integral representations and Rodrigues type differential formulas. Example of such an unified approach on the SFs, based on a GFC, can be seen in Kiryakova [7, Ch.4] and [13].

Let us emphasize that the (classical) SFs (among them the Bessel and all cylindrical functions; the Gauss, Kummer, confluent and generalized hypergeometric functions; the classical orthogonal polynomials, the incomplete Gamma- and Beta-functions and Error functions, the Airy, Whittaker etc. named functions) are related to *integer order* (!) differential equations and systems. However, recently there is an increasing interest to use classes of special functions, referred to as “*Special Functions of Fractional Calculus*” (SF of FC) that play most important role in the theory of differentiation and integration of arbitrary order (i.e. FC) and appear as solutions of *fractional order* (!) differential equations and systems. A typical feature is that, in case of true non-integer order, *the SFs of FC do not fall in the G- and ${}_pF_q$ -functions scheme!* *Examples:* the Mittag-Leffler function, the Wright-Bessel (Bessel-Maitland) functions, the Wright generalized hypergeometric functions ${}_p\Psi_q$, the Fox H -function, and an increasing number of their specifications, involving sets of “fractional” (multi-)indices and closely related to operators and equations of fractional (multi-)order.

Definition 1. By a *Fox's H-function* we mean a generalized hypergeometric function, defined by means of the Mellin-Barnes type contour integral

$$H_{p,q}^{m,n} \left[z \left| \begin{matrix} (a_j, A_j)_1^p \\ (b_k, B_k)_1^q \end{matrix} \right. \right] = \frac{1}{2\pi i} \int_{\mathcal{L}} \mathcal{H}_{p,q}^{m,n}(s) z^{-s} ds, \quad z \neq 0, \quad (1)$$

where \mathcal{L} is a suitable contour (3 possible types) in \mathbb{C} , the orders (m, n, p, q) are non negative integers so that $0 \leq m \leq q$, $0 \leq n \leq p$, the parameters $A_j > 0, B_k > 0$ are positive, and $a_j, b_k, j = 1, \dots, p; k = 1, \dots, q$ can be arbitrary complex such that $A_j(b_k + l) \neq B_k(a_j - l' - 1)$, $l, l' = 0, 1, 2, \dots; j = 1, \dots, n; k = 1, \dots, m$, and the integrand in (1) (i.e. Mellin transform of (1)) has the form

$$\mathcal{H}_{p,q}^{m,n}(s) = \frac{\prod_{k=1}^m \Gamma(b_k + B_k s) \prod_{j=1}^n \Gamma(1 - a_j - A_j s)}{\prod_{k=m+1}^q \Gamma(1 - b_k - B_k s) \prod_{j=n+1}^p \Gamma(a_j + A_j s)}. \quad (1')$$

This is an analytic function of z in circle domains $|z| < \rho$ (or sectors of them, or in the whole \mathbb{C}), for the details see the above mentioned books, [2]–[10].

The most typical example of a special function which is a Fox H -function (practically all of them *do!*) but is *not* reducible to a Meijer G -function in the general case (of *irrational* A_j, B_k), is as follows.

Definition 2. The *Wright generalized hypergeometric function* ${}_p\Psi_q(z)$, called also *Fox-Wright function* (F-W ghf) is defined as:

$${}_p\Psi_q \left[\begin{matrix} (a_1, A_1), \dots, (a_p, A_p) \\ (b_1, B_1), \dots, (b_q, B_q) \end{matrix} \middle| z \right] = \sum_{k=0}^{\infty} \frac{\Gamma(a_1 + kA_1) \dots \Gamma(a_p + kA_p)}{\Gamma(b_1 + kB_1) \dots \Gamma(b_q + kB_q)} \frac{z^k}{k!} \quad (2)$$

$$= H_{p,q+1}^{1,p} \left[-z \middle| \begin{matrix} (1-a_1, A_1), \dots, (1-a_p, A_p) \\ (0, 1), (1-b_1, B_1), \dots, (1-b_q, B_q) \end{matrix} \right]. \quad (3)$$

When $A_1 = \dots = A_p = 1$, $B_1 = \dots = B_q = 1$, in (1') and (2), the Fox H -functions (1) and (3) reduce to simpler (but yet very wide ranged) *Meijer's G -functions*, denoted

as $G_{p,q}^{m,n} \left[\sigma \middle| \begin{matrix} (a_j)_1^p \\ (b_k)_1^q \end{matrix} \right]$. Respectively, the F-W ghf (2) becomes a ${}_pF_q$ -function:

$${}_p\Psi_q \left[\begin{matrix} (a_1, 1), \dots, (a_p, 1) \\ (b_1, 1), \dots, (b_q, 1) \end{matrix} \middle| z \right] = {}_pF_q(a_1, \dots, a_p; b_1, \dots, b_q; z).$$

Information on the "integer"-indices *generalized hypergeometric functions* (ghf-s) ${}_pF_q$ and Meijer's G -function existed even in the Bateman-Erdélyi book [1], Vol.1; see also [2]–[10].

Among the most popular SFs of FC, is the simplest ${}_p\Psi_q(z)$ -function with $p = 0, q = 1$, called Wright function when denoted $\varphi(\alpha, \beta; z)$, or Bessel-Maitland (Wright-Bessel) function when denoted by J_ν^μ as fractional index analogue of the Bessel function J_ν . The Mittag-Leffler function, titled as the "*Queen*"-function of FC (see [14]), is discussed in the next section.

2 Classical Mittag-Leffler functions

The Mittag-Leffler (M-L) functions seemed to be unknown, till recently, to the majority of applied scientists and mathematicians, simply because *they have been ignored in the common handbooks on (classical) special functions and in the tables of Laplace transforms*. However, a description of their basic properties appeared yet in the Bateman Project [1], Vol.3, in a chapter devoted to "miscellaneous functions". Yet in 1931, Hille and Tamarkin provided a solution, in terms of the M-L function, of the Abel integral equation of 2nd kind. Special attention and detailed study with some applications of M-L functions are given in the book of Dzrbashjan [15]. Recently, the recognition and importance of the M-L functions increased for describing fractional-order control systems (Podlubny [8]), fractional viscoelastic models (Mainardi [16]), for solving various fractional order differential and integral equations, etc. and this stimulated fractional analysts to develop new analytical and numerical results for them. Definitions and basic properties of the M-L functions can be found now in many contemporary books and surveys on FC, integral and differential equations, mechanics, etc., like: Podlubny [8], Kiryakova [7, Appendix], Gorenflo and Mainardi [14], Kilbas, Srivastava and Trujillo [10], etc.

Definition 3. The *Mittag-Leffler functions* E_α (Mittag-Leffler, 1902-1905) and $E_{\alpha,\beta}$ (Wiman 1905, Agarwal, 1953), defined by the power series

$$E_\alpha(z) = \sum_{k=0}^{\infty} \frac{z^k}{\Gamma(\alpha k + 1)}, \quad E_{\alpha,\beta}(z) = \sum_{k=0}^{\infty} \frac{z^k}{\Gamma(\alpha k + \beta)}, \quad \alpha > 0, \beta > 0, \quad (4)$$

are "fractional index" ($\alpha > 0$) extensions of the exponential and trigonometric functions like

$$\exp(z) = \sum_{k=0}^{\infty} \frac{z^k}{\Gamma(k+1)}, \quad \cos z = \sum_{k=0}^{\infty} \frac{(-1)^k z^{2k}}{\Gamma(2k+1)},$$

satisfying ODEs $D^n y(\lambda z) = \lambda^n y(\lambda z)$ of 1st and 2nd order ($n = 1, 2$).

Indeed, in the case of (4), we have *fractional order (FO) differential equations*, for example - the simple one: $D^\alpha y_\alpha(z) = \lambda y_\alpha(z)$ satisfied by the so-called α -*exponential function*, or *Rabotnov function*: $y_\alpha(z) = z^{\alpha-1} E_{\alpha,\alpha}(\lambda z^\alpha)$. More complicated FO differential and integral equations solved by M-L functions can be seen in the book [11], in our paper [17], others - in [8],[10], etc.

Each M-L function $E_\alpha(z), E_{\alpha,\beta}(z)$ is an entire function of order $\rho = 1/\alpha$ and of type 1; in a sense, *the simplest entire function of this order*. The fundamental role of (4) in FC and in solving problems by means of Laplace transform method, is due to the general form of their *Laplace transforms*:

$$\mathcal{L}\{z^{\beta-1} E_{\alpha,\beta}(-\lambda z^\alpha)\} = \frac{s^{\alpha-\beta}}{s^\alpha + \lambda}, \quad \Re(s) > |\lambda|^{1/\alpha}.$$

The *special functions of M-L type* $\mathcal{E}_k(z, \lambda; \alpha, \beta) := z^{\alpha k + \beta - 1} E_{\alpha,\beta}^{(k)}(\lambda z^\alpha)$, $k = 0, 1, 2, \dots$, introduced by Podlubny [8], satisfy more general fractional differential relations. Their Laplace images $(k! s^{\alpha-\beta}) / (s^\alpha \mp \lambda)^{k+1}$, $\Re(s) > |\lambda|^{1/\alpha}$, $k = 0, 1, 2, \dots$ have general form allowing to interpret after decompositions, almost all rational functions of s .

Let us stress on the place of the M-L functions among the other special functions. Most of them, the "classical" special functions of mathematical physics, are representable in terms of the Meijer G -functions. However, the M-L functions of *irrational index* $\alpha \neq p/q$ are *examples of Fox's H-functions* (1) *not reducible to G-functions*, i.e. they are typical *SF of FC*:

$$E_{\alpha,\beta}(z) = {}_1\Psi_1 \left[\begin{matrix} (1, 1) \\ (\beta, \alpha) \end{matrix} \middle| z \right] = H_{1,2}^{1,1} \left[-z \middle| \begin{matrix} (0, 1) \\ (0, 1), (1-\beta, \alpha) \end{matrix} \right]. \quad (5)$$

Examples of the M-L functions:

- $\alpha > 0, \beta = 1$: $E_{0,1}(z) = \frac{1}{1-z}$; $E_{1,1}(z) = \exp(z)$; $E_{2,1}(z^2) = \cosh z$, $E_{2,1}(-z^2) = \cos z$; $E_{1/2,1}(z^{1/2}) = \exp(z) [1 + \operatorname{erf}(z^{1/2})] = \exp(z) \operatorname{erfc}(-z^{1/2}) = \exp(z) \left[1 + \frac{1}{\sqrt{\pi}} \gamma\left(\frac{1}{2}, z\right) \right]$ (the error functions, or incomplete gamma functions);
- $\beta \neq 1$: $E_{1,2}(z) = \frac{e^z - 1}{z}$; $E_{1/2,2}(z) = \frac{\operatorname{sh}\sqrt{z}}{z}$; $E_{2,2}(z) = \frac{\operatorname{sh}\sqrt{z}}{\sqrt{z}}$, etc.
- $\beta = \alpha$: the α -exponential (Rabotnov) function $y_\alpha(z) = z^{\alpha-1} E_{\alpha,\alpha}(\lambda z^\alpha)$,

Several generalizations of M-L function (4) have been considered recently by taking parameters, additional to α, β , as $\rho > 0, l \in \mathbb{C}, m \in \mathbb{R}$. Such one, with 3 indices, is the *Prabhakar function*:

$$E_{\alpha,\beta}^\rho(z) = \sum_{k=0}^{\infty} \frac{(\rho)_k}{\Gamma(\alpha k + \beta)} \frac{z^k}{k!}. \quad (6)$$

3 Multi-index Mittag-Leffler functions

We consider a class of *special functions of Mittag-Leffler type* that are *multi-index analogues* of $E_{\alpha,\beta}(z)$. We replace the indices $\alpha:=1/\rho$, and $\beta:=\mu$, by 2 sets of multi-indices $\alpha \rightarrow \boldsymbol{\alpha} = (\alpha_1, \alpha_2, \dots, \alpha_m)$ and $\beta \rightarrow \boldsymbol{\beta} = (\beta_1, \beta_2, \dots, \beta_m)$, or in order to follow Dzrbashjan's denotations: $1/\rho \rightarrow (1/\rho_1, 1/\rho_2, \dots, 1/\rho_m)$ and $\mu \rightarrow (\mu_1, \mu_2, \dots, \mu_m)$.

Definition 4. Let $m > 1$ be an integer, $\rho_1, \dots, \rho_m > 0$ and μ_1, \dots, μ_m be arbitrary real (complex) numbers. By means of these “multi-indices”, the *multi-index Mittag-Leffler functions* (*multi-M-L f-s*) are defined as:

$$E_{\boldsymbol{\alpha}, \boldsymbol{\beta}}^m(z) := E_{(\frac{1}{\rho_i}), (\mu_i)}(z) = \sum_{k=0}^{\infty} \frac{z^k}{\Gamma(\mu_1 + k/\rho_1) \dots \Gamma(\mu_m + k/\rho_m)}. \quad (7)$$

Similar definition was used by Luchko [21], where he called (7) as *vector-index M-L functions*.

Theorem 1. The multi-index M-L functions (7) are entire functions of order ρ with $\frac{1}{\rho} = \frac{1}{\rho_1} + \dots + \frac{1}{\rho_m}$, and type $\sigma = \left(\frac{\rho_1}{\rho}\right)^{\frac{\rho}{\rho_1}} \dots \left(\frac{\rho_m}{\rho}\right)^{\frac{\rho}{\rho_m}} > 1$ (for $m > 1$). Setting $\mu = \mu_1 + \dots + \mu_m$, we have an asymptotic estimate, as:

$$|E_{(\frac{1}{\rho_i}), (\mu_i)}(z)| \leq C|z|^{\rho((1/2)+\mu-(m/2))} \exp(\sigma|z|^\rho), \quad |z| \rightarrow \infty.$$

Similarly to representation (5), we have the following

Lemma 2. The multi-index M-L functions (7) are typical representatives of the Wright generalized hypergeometric functions ${}_p\Psi_q$ and of the Fox H-functions, but of more general nature:

$$E_{(\frac{1}{\rho_i}), (\mu_i)}(z) = {}_1\Psi_m \left[\begin{matrix} (1, 1) \\ (\mu_i, \frac{1}{\rho_i})_1^m \end{matrix} \middle| z \right] = H_{1, m+1}^{1, 1} \left[-z \middle| \begin{matrix} (0, 1) \\ (0, 1), (1 - \mu_i, \frac{1}{\rho_i})_1^m \end{matrix} \right]. \quad (8)$$

Thus, the following Mellin-Barnes type integral representation holds:

$$E_{(\frac{1}{\rho_i}), (\mu_i)}(z) = \frac{1}{2\pi i} \int_{\mathcal{L}} \frac{\Gamma(s)\Gamma(1-s)}{\prod_{i=1}^m \Gamma(\mu_i - \frac{s}{\rho_i})} (-z)^{-s} ds, \quad z \neq 0,$$

based on the Mellin transform:

$$\mathcal{M} \left\{ E_{(\frac{1}{\rho_i}), (\mu_i)}(-z) \right\} (s) = \frac{\Gamma(s)\Gamma(1-s)}{\prod_{i=1}^m \Gamma(\mu_i - \frac{s}{\rho_i})}, \quad 0 < \Re(s) < 1. \quad (9)$$

As an analogue of the Laplace transform (\mathcal{L}) relationship between the classical M-L function (4) and the Wright function: $\mathcal{L} \left\{ \phi(\alpha, \beta; z) \right\} (s) = \frac{1}{s} E_{\alpha, \beta}(\frac{1}{s})$ (see in the books [8], [10]), we derive the following *new relation*.

Lemma 3.

$$\mathcal{L}\left\{{}_0\Psi_m\left[\begin{array}{c} - \\ (\mu_1, \frac{1}{\rho_1}), \dots, (\mu_m, \frac{1}{\rho_m}) \end{array} \middle| z\right]\right\}(s) = \frac{1}{s} E_{(\frac{1}{\rho_i}), (\mu_i)}\left(\frac{1}{s}\right), \quad \Re(s) > 0. \quad (10)$$

Here, the ${}_0\Psi_m$ -functions on the left-hand side are “fractional indices” analogues of the hyper-Bessel functions $J_{\nu_1, \dots, \nu_m}^{(m)}$ of Delerue [22], that is, of the ${}_0F_m$ -functions, to be discussed below as special cases of (7).

More details on the properties of the multi-M-L functions, relations to FC and GFC operators, and applications to fractional order differential equations, can be found in our works as [20],[23],[24], etc.

4 Examples of multi-index M-L functions

- For $m=1$, this is the classical M-L function $E_{1/\rho, \mu}(z)$ with all its special cases (Sect. 2), including also the so-called *Rabotnov function* (see [8]), or α -exponential function (see [10]): $y_\alpha(z) = z^{\alpha-1} E_{\alpha, \alpha}(\lambda z)$.

- For $m=2$, the function (7) denoted as $\Phi_{\rho_1, \rho_2}(z; \mu_1, \mu_2) = E_{(\frac{1}{\rho_1}, \frac{1}{\rho_2}), (\mu_1, \mu_2)}^{(2)}(z)$, is *Dzrbashjan's M-L type function* from [25]. Some of its particular cases are: the M-L function $E_{\alpha, \beta}(z)$; the Bessel function $J_\nu(z) = (z/2)^\nu E_{(1,1), (\nu+1,1)}(-z^2/4)$; *Struve and Lommel functions* $s_{\mu, \nu}(z)$, $H_\nu(z) = \text{const.} s_{\nu, \nu}(z)$.

The so-called *Wright function* has arisen in the studies of Fox (1928), Wright (1933), Humbert and Agarwal (1953), it is also referred to in [1], Vol.3. Initially, Wright defined it only for $\alpha > 0$, then prolonged its definition for $\alpha > -1$. Now, we see it as a case of multi-M-L function with $m=2$:

$$\phi(\alpha, \beta; z) = \sum_{k=0}^{\infty} \frac{1}{\Gamma(\alpha k + \beta)} \frac{z^k}{k!} = {}_0\Psi_1 \left[\begin{array}{c} - \\ (\beta, \alpha) \end{array} \middle| z \right] = E_{(\alpha, 1), (\beta, 1)}^{(2)}(z). \quad (11)$$

It plays important role in the solution of linear partial fractional differential equations as the *fractional diffusion-wave equation* studied by Nigmatullin (1984-1986, to describe the diffusion process in media with fractal geometry, $0 < \alpha < 1$) and by Mainardi et al. (1994-, see e.g. [26], for propagation of mechanical diffusive waves in viscoelastic media, $1 < \alpha < 2$). In the form $M(z; \beta) = \phi(-\beta, 1-\beta; -z)$, $\beta := \alpha/2$, it is recently called also as the *Mainardi function*, see [8, Ch.1]. In our denotations, it is $M(z; \beta) = E_{(-\beta, 1), (1-\beta)}^{(2)}(-z)$ and has examples like: $M(z; 1/2) = 1/\sqrt{\pi} \exp(-z^2/4)$ and the *Airy function*: $M(z; 1/3) = 3^{2/3} Ai(z/3^{1/3})$.

In other form and denotation, the Wright function is known as *Wright-Bessel*, or misnamed as *Bessel-Maitland function*:

$$\begin{aligned} J_\nu^\mu(z) &= \phi(\mu, \nu+1; -z) = {}_0\Psi_1 \left[\begin{array}{c} - \\ (\nu+1, \mu) \end{array} \middle| -z \right] \\ &= \sum_{k=0}^{\infty} \frac{(-z)^k}{\Gamma(\nu + k\mu + 1) k!} = E_{(1/\mu, 1), (\nu+1, 1)}^{(2)}(-z), \end{aligned} \quad (12)$$

again an example of the Dzrbashjan function. It is an obvious "fractional index" analogue of the classical Bessel function $J_\nu(z) = c(z/2) {}_0F_1(z^2/4)$, more exactly, of the Bessel-Clifford function $C_\nu(z)$.

Nowadays, several further "fractional-indices" generalizations of $J_\nu(z)$ are exploited, and we can present them as multi-M-L functions! Such one is the so-called *generalized Wright-Bessel (-Lommel) functions*, due to Pathak (1966-1967, see e.g. in [5]-[7]),

$$\begin{aligned} J_{\nu,\lambda}^\mu(z) &= (z/2)^{\nu+2\lambda} \sum_{k=0}^{\infty} \frac{(-1)^k (z/2)^{2k}}{\Gamma(\nu+k\mu+\lambda+1)\Gamma(\lambda+k+1)} \\ &= (z/2)^{\nu+2\lambda} E_{(1/\mu,1),(\nu+\lambda+1,\lambda+1)}^{(2)} \left(-(z/2)^2 \right), \quad \mu > 0, \end{aligned} \quad (13)$$

including, for $\mu = 1$, the *Lommel* (and thus, also the *Struve*) functions $J_{\nu,\lambda}^1(z) = \text{const } S_{2\lambda+\nu-1,\nu}(z)$, see e.g. in [1], Vol.2. Next one, is the *generalized Lommel-Wright function with 4 indices*, introduced by de Oteiza, Kalla and Conde (1986), $r > 0, n \in \mathbb{N}, \nu, \lambda \in \mathbb{C}$, see in [23]:

$$\begin{aligned} J_{\nu,\lambda}^{r,n}(z) &= (z/2)^{\nu+2\lambda} \sum_{k=0}^{\infty} \frac{(-1)^k (z/2)^k}{\Gamma(\nu+kr+\lambda+1)\Gamma(\lambda+k+1)^n} \\ &= (z/2)^{\nu+2\lambda} E_{(1/r,1,\dots,1),(\nu+\lambda+1,\lambda+1,\dots,\lambda+1)}^{(n+1)} \left(-(z/2)^2 \right). \end{aligned} \quad (14)$$

This is an interesting example of a multi-M-L function (7) with $m = n + 1$.

Series in systems of the fractional-indices analogues (12),(13),(14) of the Bessel functions in complex domain have been studied recently by Paneva-Konovska, as Cauchy-Hadamard, Abel and Tauber type theorems, and asymptotic formulas w.r.t. index $\nu \rightarrow \infty$, see e.g. [27], [28].

- For arbitrary $m \geq 2$: let $\forall \rho_i = \infty$ ($1/\rho_i = 0$) and $\forall \mu_i = 1, i = 1, \dots, m$. Then, from definition (7),

$$E_{(0,0,\dots,0),(1,1,\dots,1)}(z) = \sum_{k=0}^{\infty} z^k = \frac{1}{1-z}.$$

- Consider the case $m \geq 2, \forall \rho_i = 1, i = 1, \dots, m$, when:

$$E_{(1,1,\dots,1),(\mu_i+1)}^{(m)}(z) = {}_1\Psi_m \left[\begin{matrix} (1,1) \\ (\mu_i,1)_1^m \end{matrix} \middle| z \right] = \text{const } {}_1F_m(1; \mu_1, \mu_2, \dots, \mu_m; z)$$

reduces to ${}_1F_m$ - and to a *Meijer's* $G_{1,m+1}^{1,1}$ -function. Denote $\mu_i = \gamma_i + 1, i = 1, \dots, m$, and let additionally one of the μ_i to be 1, e.g.: $\mu_m = 1$, i.e. $\gamma_m = 0$. Then the multi-M-L function becomes a *hyper-Bessel function*, in the sense of Delerue [22]; see also Kiryakova [7] (App., and Ch. 3):

$$\begin{aligned} J_{\gamma_i, \dots, \gamma_{m-1}}^{(m-1)}(z) &= \left(\frac{z}{m} \right)^{\sum_{i=1}^{m-1} \gamma_i} E_{(1,1,\dots,1),(\gamma_1+1,\gamma_2+1,\dots,\gamma_{m-1}+1,1)}^{(m)} \left(-\left(\frac{z}{m} \right)^m \right) \\ &= \left[\prod_{i=1}^{m-1} \Gamma(\gamma_i+1) \right]^{-1} \left(\frac{z}{m} \right)^{\sum_{i=1}^{m-1} \gamma_i} {}_0F_{m-1} \left(\gamma_1+1, \gamma_2+1, \dots, \gamma_{m-1}+1; -\left(\frac{z}{m} \right)^m \right). \end{aligned} \quad (15)$$

In view of the above relation, functions (7), (8) with arbitrary $(\rho_1, \dots, \rho_m) \neq (1, \dots, 1)$ can be seen as *fractional-indices analogues of the hyper-Bessel functions* (15), which themselves are *multi-index* (but integer) *analogues* of the Bessel function. Functions (15) are closely related to the *hyper-Bessel operators*, introduced by Dimovski (1966), see details in Kiryakova et al. [7], Ch.3 and [29], and to the *normalized hyper-Bessel functions*, known also as *Bessel-Clifford functions of m -th order*:

$$C_{\nu_1, \dots, \nu_m}(z) = \sum_{k=0}^{\infty} \frac{(-1)^k z^k}{\Gamma(\nu_1 + k + 1) \dots \Gamma(\nu_m + k + 1) k!} = E_{(1, \dots, 1), (\nu_1 + 1, \dots, \nu_m + 1, 1)}^{(m+1)}(-z).$$

- One may consider *multi-index analogues of the Rabotnov (α -exponential function)*, with all $\mu_i = 1/\rho_i = \alpha > 0, i = 1, \dots, m$:

$$y_{\alpha}^{(m)}(z) = z^{\alpha-1} E_{(\alpha, \dots, \alpha), (\alpha, \dots, \alpha)}^{(m)}(z^{\alpha}) = z^{\alpha-1} \sum_{k=0}^{\infty} \frac{z^{\alpha k}}{[\Gamma(\alpha + \alpha k)]_m}; \quad \alpha = 1: \sum_{k=0}^{\infty} \frac{z^k}{[k!]_m}. \quad (16)$$

- In general, for rational values of $\forall \rho_i, i = 1, \dots, m$, the functions (7) are reducible to *Meijer's G -functions* (that is, to classical special functions).

As further *extensions of the multi-M-L functions* (7), we like to attract the attention to:

- The *multivariate M-L type functions* (Luchko [21])

$$E_{(a_1, \dots, a_n), b}(z_1, \dots, z_n) := \sum_{k=0}^{\infty} \sum_{\substack{l_1 + \dots + l_n = k \\ l_1 \geq 0, \dots, l_n \geq 0}} (k; l_1, \dots, l_n) \frac{\prod_{i=1}^n z_i^{l_i}}{\Gamma(b + \sum_{i=1}^n a_i l_i)},$$

where $(k; l_1, \dots, l_n)$ are the so-called multinomial coefficients).

- The *Mittag-Leffler type generalization* of both functions (6) and (7), in Kilbas-Srivastava-Trujillo [10], p.47:

$$E_{\rho}((\alpha_j, \beta_j)_{1,m}; z) = \sum_{k=0}^{\infty} \frac{(\rho)_k}{\prod_{j=1}^m \Gamma(\alpha_j k + \beta_j)} \frac{z^k}{k!}.$$

5 Relation of the multi-index M-L functions to a generalized fractional calculus

As an important class of SFs of FC, the multi-index M-L functions are closely related to the operators of *generalized fractional calculus* (GFC), developed by Kiryakova [7]. This is a theory, where we introduce *generalized operators of integration and differentiation of fractional (multi-) order*, based on compositions of finite number ($m > 1$) of classical fractional integration and differentiation operators, but written by means of *single* integral operators involving special functions in their kernels. The basic *operators of the classical FC* we are using as components, are the *Erdélyi-Kober* (E-K) *fractional integrals*

$$I_{\beta}^{\gamma, \delta} f(z) = \frac{1}{\Gamma(\delta)} \int_0^1 (1 - \sigma)^{\delta-1} \sigma^{\gamma} f(z \sigma^{\frac{1}{\beta}}) d\sigma, \quad (17)$$

and their respective *E-K fractional derivatives*. For $\gamma=0$, $\beta=1$ they reduce to the best known *Riemann-Liouville* (R-L) operator of integration of order $\delta>0$: $R^\delta f(z)$ and the *R-L fractional derivative*, $D^\delta f(z) := (d/dz)^n R^{n-\delta} f(z)$, $n := [\delta] + 1$ the smallest integer $\geq \delta$. In the *GFC*, instead of repeated integral representation for the commutative product $I_{(\beta_i),m}^{(\gamma_i),(\delta_i)} := \prod_{i=1}^m I_{\beta_i}^{\gamma_i,\delta_i}$ of operators (17), we consider the following new notion.

Definition 5. A *generalized fractional integral of multi-order* $\delta = (\delta_1 \geq 0, \dots, \delta_m \geq 0)$, or *multiple E-K integral* (of multiplicity $m > 1$), is defined by means of additional real parameters' sets $\gamma = (\gamma_1, \dots, \gamma_m)$ (multi-weight) and $\beta = (\beta_1 > 0, \dots, \beta_m > 0)$, as:

$$\begin{aligned} \tilde{I}f(z) &= I_{\beta,m}^{\gamma,\delta} f(z) = I_{(\beta_i),m}^{(\gamma_i),(\delta_i)} f(z) \\ &:= \int_0^1 H_{m,m}^{m,0} \left[\sigma \left| \begin{matrix} (\gamma_i + \delta_i + 1 - \frac{1}{\beta_i}, \frac{1}{\beta_i})_1^m \\ (\gamma_i + 1 - \frac{1}{\beta_i}, \frac{1}{\beta_i})_1^m \end{matrix} \right. \right] f(z\sigma) d\sigma, \end{aligned} \quad (18)$$

if $\sum_{i=1}^m \delta_i > 0$; and as the identity operator: $\tilde{I}f(z) = f(z)$, if $\delta_1 = \delta_2 = \dots = \delta_m = 0$.

The kernel-function $H_{m,m}^{m,0}$ is a special type of Fox's H -function (1).

The corresponding *generalized fractional derivatives* are defined analogously to the idea of the R-L fractional derivative D^δ (see e.g. in [11]), as $\tilde{D}f(z) = D_{(\beta_i),m}^{(\gamma_i),(\delta_i)} = D_\eta I_{(\beta_i),m}^{(\gamma_i),(\eta_i-\delta_i)}$ with integers $\eta_i \geq \delta_i$ and auxiliary differential operator D_η , a polynomial of $z(d/dz)$ of degree $\eta_1 + \dots + \eta_m$, see in [7], Ch. 5. They can be represented also symbolically as compositions of classical E-K fractional derivatives:

$$\tilde{D}f(z) = D_{(\rho_i),(\mu_i)} f(z) = z^{-1} \prod_{i=1}^m \left(z^{1+(1-\mu_i)\rho_i} D_{z^{\rho_i}}^{1/\rho_i} z^{(\mu_i-1)\rho_i} \right) f(z). \quad (19)$$

Various relations between the operators of classical FC (R-L and E-K fractional integrals and derivatives, both left- and right-hand sided) and the multi-M-L functions have been derived in our previous works like [20]. The most interesting and characteristic integro-differential relations for (7) however are given in terms of the GFC operators. For example, we have the following

Lemma 4. For $\lambda \neq 0$,

$$(\lambda z) I_{(\rho_i),m}^{(\mu_i-1),(1/\rho_i)} E_{(\frac{1}{\rho_i}),(\mu_i)}(\lambda z) = E_{(\frac{1}{\rho_i}),(\mu_i)}(\lambda z) - (1/\prod_{i=1}^m \Gamma(\mu_i)), \quad (20)$$

$$D_{(\rho_i),m}^{(\mu_i-1-1/\rho_i),(1/\rho_i)} E_{(\frac{1}{\rho_i}),(\mu_i)}(\lambda z) = (\lambda z) E_{(\frac{1}{\rho_i}),(\mu_i)}(\lambda z) + (1/\prod_{i=1}^m \Gamma(\mu_i - 1/\rho_i)). \quad (21)$$

From here one can easily derive that

Lemma 5. The multi-index M-L function satisfies a fractional order (exactly said, "multi-order" $(1/\rho_1, \dots, 1/\rho_m)$) differential equation

$$\tilde{D}E_{(\frac{1}{\rho_i}),(\mu_i)}(\lambda z) = D_{(\rho_i),(\mu_i)} E_{(\frac{1}{\rho_i}),(\mu_i)}(\lambda z) = \lambda E_{(\frac{1}{\rho_i}),(\mu_i)}(\lambda z), \quad \lambda \neq 0. \quad (22)$$

More detailed study on the result in Lemma 5 can be found in our paper [24], where we found the solution of a cauchy problem for equation (22) in terms of (7) by means of the so-called transmutation method.

6 Special functions as fractional differ-integrals of elementary functions

Usually, the SF of mathematical physics are defined *by means of power series representations*. However, some alternative representations can be also used as their definitions. Let us mention the well known *Poisson integrals* for the Bessel functions and the analytical continuation of the Gauss hypergeometric function by means of the *Euler integral formula*. The *Rodrigues differential formulas*, involving repeated (integer order) differentiation are used as definitions for the classical orthogonal polynomials; or - when involving differentiations of fractional order - for the respective special functions with not-integer indices. As for the other classical SF (most of them being generalized hypergeometric ${}_pF_q$ -functions), such type representations were till recently less popular and even unknown. Indeed, there existed various integral and differential formulas for them, but unfortunately – quite peculiar for each of the special functions, and scattered in the literature *without any common idea to relate them!* One of the *new general sights on the classical SF* is to look to all of them as special cases of the *G*- and *H*-functions. Another unifying approach is to consider the SF as fractional integrals or derivatives of some basic elementary or special functions. This idea comes from older papers like Lavoie, Osler and Tremblay [12], and has been recently successfully developed due to the tools of the generalized FC, see the books and surveys of Kiryakova [7, Ch. 4], [13]; Prudnikov, Brychkov, Marichev [6]; Podlubny [8], Kilbas, Srivastava and Trujillo [10], etc. In our paper [13], and partly in Ch. 4 of the book [7], we have proven the following general proposition.

Theorem 6. ([13]) *All the generalized hypergeometric functions ${}_pF_q$ can be considered as generalized (q -multiple) fractional integrals (18), or/and their respective generalized fractional derivatives $D_{(\beta_k),m}^{(\gamma_k),(\delta_k)}$, of one of the following 3 basic elementary functions, depending on whether $p < q$, $p = q$ or $p = q + 1$:*

$$\cos_{q-p+1}(z) \text{ (if } p < q \text{) , } z^\alpha \exp z \text{ (if } p = q \text{) , } z^\alpha (1 - z)^\beta \text{ (if } p = q + 1 \text{).} \quad (23)$$

Here the \cos_m -function is the *generalized cosine function of m -th order*:

$$y(z) = \cos_m(z) = {}_0F_{m-1} \left((k/m)_1^{m-1}; -(z/m)^m \right) = \sum_{k=0}^{\infty} \frac{(-1)^k z^{km}}{(km)!}, \quad (24)$$

which is the solution of the m -th order IVP

$$y^{(m)}(z) = -y(z); \quad y(0) = 1, y'(0) = \dots = y^{(m-1)}(0) = 0.$$

When $m = 2$, naturally we have the classical $\cos(z) = \cos_2(z)$.

Representations of the type of Th. 6 by means of (23) hold for all the (classical) special functions, being cases of the ${}_pF_q$ -functions and G -functions. Practically, behind the above theorem, there stay hidden 3 separate theorems, several lemmas and corollaries with proofs going in their own way, but ruled by the common idea: each ${}_pF_q$ -function is an E-K operator (of integration or differentiation) of a simpler ${}_{p-1}F_{q-1}$ -function, see [12]. These particular statements provide, besides *new classification of the classical SF (as SF of so-called "Bessel", "confluent", and "Gauss" type)*, also a long list of *new integral and differential formulas for them*, and in some cases, algorithms for numerical evaluation, see partly in [13] and [7, Ch.4]. Now, we continue the parallels between the "Classical SFs", and the "SFs of FC", showing that the latter also can be presented as fractional order (or multi-order) generalized integrals or derivatives of 3 basic kinds of elementary or simpler functions! To this end, a further extension of the GFC operators is used which is based, instead on compositions of E-K fractional integrals, on compositions of the so-called *Wright-Erdélyi-Kober* (W-E-K) *operators of fractional integration*:

$$W_{\beta,\lambda}^{\gamma,\delta} f(z) := I_{\beta,\lambda,1}^{\gamma,\delta} f(z) = \lambda \int_0^1 \sigma^{\lambda(\gamma+1)-1} J_{\gamma+\delta-\lambda(\gamma+1)/\beta}^{-\lambda/\beta} (\sigma^\lambda f(z\sigma) d\sigma, \quad (25)$$

where $\beta > 0, \lambda > 0, \delta \geq 0, \gamma$ are real parameters and J_ν^μ stands for the Wright-Bessel (Bessel-Maitland) function (12). When $\lambda = \beta$, (25) reduces to the classical E-K fractional integral (17).

Using compositions of W-E-K operators (25) introduces a further extension of the notion of generalized operators of fractional integration: with the same H -kernel-function and structure as (18), but with different parameters β_k and λ_k (Kalla and Galue, 1993; for the details, proper definitions and theory, see Kiryakova [31]). Further, for simplicity, we use the same denotations \tilde{I}, \tilde{D} for these generalized fractional integrals and derivatives.

Theorem 7. ([31]) *All the Wright generalized hypergeometric functions ${}_p\Psi_q$ can be represented as multiple (q -tuple) fractional integrals \tilde{I} , or respective fractional derivatives \tilde{D} , of one of the following 3 basic functions:*

$$\cos_{q-p+1}(z) \text{ (if } p < q), z^\alpha \exp z \text{ (if } p = q), {}_1\Psi_0(z; (\beta, B)) \text{ (if } p = q + 1). \quad (26)$$

The proof uses the fact that \tilde{I} is a commutative composition of $m = q$ W-E-K operators (25), and a lemma, representing each ${}_{p+1}\Psi_{q+1}$ -function as an W-E-K operator (25) of a ${}_p\Psi_q$ -function. Thus, by q subsequent steps, we come to one of the simpler functions ${}_0\Psi_{q-p}, {}_1\Psi_1$ or ${}_1\Psi_0 = H_{1,1}^{1,1}$. Theorem 7 suggests a *classification of the SF of FC in 3 classes*: "Bessel", "confluent" and "Gauss" type, depending on whether $p < q$, $p = q$ or $p = q + 1$, and several new integral and differential formulas, with possible hints for computational procedures. For example, the case $p < q$ of Th. 7 leads us to introduce the so-called *Wright hyper-Bessel functions* ${}_0\Psi_m$ with denotations $J_{\beta_1, \dots, \beta_m}^{B_1, \dots, B_m}(z)$ similar to these in (15), as *fractional analogues of the hyper-Bessel functions*, or as *multi-index analogues of the Bessel-Maitland function* $J_\nu^\mu(z)$, (12). The details and comments will be a purpose of a separate paper.

Here we concentrate *only on the case related to the multi-M-L functions*. We derive a Poisson type integral representation for them, as a corollary of Th.7 and representation (8) of $E_{(\frac{1}{\rho_i}),(\mu_i)}(z)$ as ${}_1\Psi_m$ -function, with $1 < m$.

Theorem 8. For $\mu_k \geq \frac{k}{m}, 0 < \rho_k < 1, k = 1, \dots, m$, the following Poisson-type integral representation of the multi-index M-L functions $E_{(\frac{1}{\rho_i}),(\mu_i)}(z)$ holds in terms of the multiple W-E-K operators, $c^* := \sqrt{m/(2\pi)^{m-1}}$:

$$E_{(\frac{1}{\rho_i}),(\mu_i)}(-z) = c^* I_{(\rho_k)_1^m, (1)_1^m, m}^{(\frac{k}{m}-1)_1^m, (\mu_k-\frac{k}{m})_1^m} \left\{ \cos_m(mz^{1/m}) \right\} \quad (27)$$

$$= c^* \int_0^1 H_{m,m}^{m,0} \left[\sigma \left| \begin{matrix} (\mu_k - 1/\rho_k, 1/\rho_k)_1^m \\ (k/m - 1, 1)_1^m \end{matrix} \right. \right] \cos_m(m(z\sigma)^{1/m}) d\sigma. \quad (28)$$

In the case of arbitrary μ_k and $\rho_k > 0$, $E_{(\frac{1}{\rho_i}),(\mu_i)}(z)$ can be seen as either generalized W-E-K fractional integrals, or generalized W-E-K derivatives (that is differ-integrals, in particular differentiations) of the generalized cosine function of order m .

This is a generalization of the Poisson integral for the Bessel functions. A proof of (28), independent of Th.7, follows by presenting all involved functions as H -functions, and evaluation the r.h.s. as an integral of product of two H -functions, according to a known formula ([2]-[7],[9]-[10]).

7 Open problems

As a *challenging open problem*, related to the Special Functions of Fractional Calculus (as are the multi-index M-L functions), we mention the possibilities for their numerical and graphical interpretations, plots and tables, and implementing in software packages as *Mathematica*, *Maple*, *Matlab*, etc. As mentioned earlier, the Classical Special Functions are already implemented there. For their Fractional Calculus analogues, numerical algorithms and software packages have been developed *only for the classical M-L function* $E_{\alpha,\beta}(z)$ and the Wright function $\phi(\alpha, \beta; z)$! Numerical results and plots for the M-L functions for basic values of indices can be found in Caputo-Mainardi [32] (one of the first attempts!) and Gorenflo-Mainardi [14]. Among the very recent achievements, we can mention: Podlubny [33] (a *Matlab* routine that calculates the M-L function with desired accuracy), Luchko et al., Diethelm et al. [34], [35] (algorithms for the numerical evaluation of the M-L function and package for computation with *Mathematica*), Luchko [36] (algorithms for computation of the Wright function with prescribed accuracy), etc.

Acknowledgement: This paper is supported by the Project ID 02/25/2009 of the NSF - Ministry of Education, Youth and Science of Bulgaria. It is performed also in the frames of the Bilateral Res. Project "Mathematical Modeling by Means of ..." between BAS and SANU (2012-2014).

References

- [1] A. Erdélyi et al. (Ed-s), Higher Transcendental Functions, Vol-s. 1-3, McGraw Hill, N. York, 1953.
- [2] A.M. Mathai, R.K. Saxena, The H -function with Applications in Statistics and Other Disciplines, Wiley East. Ltd., New Delhi, 1978.
- [3] H.M. Srivastava, B.R.K. Kashyap, Special Functions in Queuing Theory and Related Stochastic Processes, Acad. Press, N. York etc, 1981.
- [4] H.M. Srivastava, K.C. Gupta, S.P. Goyal, The H -Functions of One and Two Variables with Applications, South Asian Publs, New Delhi, 1982.
- [5] O.I. Marichev, Handbook of Integral Transforms of Higher Transcendental Functions: Theory and Algorithmic Tables, Ellis Horwood & Halsted Press, N. York etc., 1983.
- [6] A. Prudnikov, Yu. Brychkov, O. Marichev, Integrals and Series, Vol.3: Some More Special Functions, Gordon & Breach, N. York, 1992.
- [7] V. Kiryakova, Generalized Fractional Calculus and Applications, Longman & J. Wiley, Harlow - N. York, 1994.
- [8] I. Podlubny, Fractional Differential Equations, Acad. Press, San Diego etc., 1999.
- [9] A.A. Kilbas, M. Saigo, H-Transforms. Theory and Applications, Chapman & Hall, Boca Raton FL, 2004.
- [10] A. Kilbas, H.M. Srivastava, J.J. Trujillo, Theory and Applications of Fractional Differential Equations, Elsevier, Amsterdam etc., 2006.
- [11] S. Samko, A. Kilbas, O. Marichev, Fractional Integrals and Derivatives: Theory and Applications, Gordon and Breach, 1993.
- [12] J.L. Lavoie, T.J. Osler, R. Tremblay, Fractional derivatives and special functions, SIAM Review 18 (1976) 240-268.
- [13] V. Kiryakova, All the special functions are fractional differintegrals of elementary functions, J. Physics A: Math. & Gen. 30 (1997) 5085-5103.
- [14] R. Gorenflo, F. Mainardi, Fractional calculus: Integral and differential equations of fractional order, In: Fractals and Fractional Calculus in Continuum Mechanics (Eds: A. Carpinteri, F. Mainardi), 223-278, Springer, Wien-N. York, 1997.
- [15] M. Dzrbashjan, Integral Transforms and Representations of Functions in the Complex Domain, Nauka, Moscow, 1966 (In Russian).
- [16] F. Mainardi, Applications of fractional calculus in mechanics. In: Transform Methods and Special Functions, Varna'96 (Eds: P. Rusev, I. Dimovski, V. Kiryakova), 309-334, IMI-BAS, Sofia, 1996.
- [17] V. Kiryakova, Fractional order differential and integral equations with Erdélyi-Kober operators: Explicit solutions by means of the transmutation method, In: American Institute of Physics - Conf. Proc. # 1410 (2011) 247-258 (Proc. 37th Intern. Conf. AMEE' 2011), doi: 10.1063/1.3664376;
- [18] R. Gorenflo, A.A. Kilbas, S.V. Rogozin, On the generalized Mittag-Leffler type function, Integr. Transforms Spec. Funct. 7 (1998) 215-224.

- [19] A.A. Kilbas, M. Saigo, R.K. Saxena, Generalized Mittag-Leffler functions and generalized fractional calculus operators, *Integral Transf. Spec. Funct.* 15 (2004) 31-49.
- [20] V. Kiryakova, Multiple (multiindex) Mittag-Leffler functions and relations to generalized fractional calculus, *J. Comput. Appl. Math.* 118 (2000) 214-259.
- [21] Yu. Luchko, Operational method in fractional calculus, *Fract. Calc. Appl. Anal.* 2, No 4 (1999) 463-488.
- [22] P. Delerue, Sur le calcul symbolique à n variables et fonctions hyperbesseliennes (II), *Annales Soc. Sci. Bruxelles, Ser. 1*, 3 (1953) 229-274.
- [23] V. Kiryakova, The multi-index Mittag-Leffler functions as important class of special functions of fractional calculus, *Computers and Mathematics with Appl.* 59, No 5 (2010) 1885-1895, doi:10.1016/j.camwa.2009.08.025.
- [24] I. Ali, V. Kiryakova, S.L. Kalla, Solutions of fractional multi-order integral and differential equations using a Poisson-type transform, *J. Math. Anal. Appl.* 269 (2002) 172-199.
- [25] M. Dzrbashjan, On the integral transformations generated by the generalized Mittag-Leffler function, *Izv. Akad. Nauk Armen. SSR* 13 (1960) 21-63 (In Russian).
- [26] F. Mainardi, M. Tomirotti, On a special function arising in the fractional diffusion-wave equation. In: *Transform Methods and Special Functions, Sofia'94* (Eds: P. Rusev, I. Dimovski, V. Kiryakova), 171-183, SCT Publ., Singapore, 1994.
- [27] J. Paneva-Konovska, Cauchy-Hadamard, Abel and Tauber type theorems for series in generalized Bessel-Maitland functions, *C. R. Acad. Bulg. Sci.* 61 (2008) 9-14.
- [28] J. Paneva-Konovska, Theorems on the convergence of series in generalized Lommel-Wright functions, *Fract. Calc. Appl. Anal.* 10, No 1 (2007) 59-74.
- [29] I. Dimovski, V. Kiryakova, The Obrechhoff integral transform: Properties and relation to a generalized fractional calculus, *Numer. Funct. Anal. and Optimization* 21 (2000) 121-144.
- [30] F. Al-Musallam, V. Kiryakova, Vu Kim Tuan, A multi-index Borel-Dzrbashjan transform, *Rocky Mount. J. Math.* 32 (2002) 409-428.
- [31] V. Kiryakova, The special functions of fractional calculus as generalized fractional calculus operators of some basic functions, *Computers and Mathematics with Appl.* 59, No 3 (2010) 1128-1141, doi:10.1016/j.camwa.2009.05.014.
- [32] M. Caputo, F. Mainardi, A new dissipation model based on memory mechanism, *Pure and Appl. Geoph.* 91 (1971) 134-147 (Repr. in: *Fract. Calc. Appl. Anal.* 10 (2007) 309-324).
- [33] I. Podlubny and M. Kacenak, Mittag-Leffler function, Matlab Central File Exchange, File ID: #8738 (17 Oct. 2005), available at <http://www.mathworks.com/matlabcentral/fileexchange/8738>.
- [34] R. Gorenflo, J. Loutchko, Yu. Luchko, Computation of the Mittag-Leffler function $E_{\alpha,\beta}$ and its derivatives, *Fract. Calc. Appl. Anal.* 5, No 4 (2002) 491-518.

- [35] K. Diethelm, N. Ford, A. Freed, Yu. Luchko, Algorithms for the fractional calculus: A selection of numerical methods, *Computer Methods in Appl. Mechanics and Eng.* 194 (2005) 743-773.
- [36] Yu. Luchko, Algorithms for evaluation of the Wright function for the real arguments' values, *Fract. Calc. Appl. Anal.* 11, No 1 (2008) 57-75.

COMPARISON BETWEEN THE CONVERGENCE OF POWER AND MITTAG-LEFFLER SERIES

Jordanka Paneva-Konovska

Faculty of Applied Mathematics and Informatics,
Technical University of Sofia,
8, Kliment Ohridski bul.,
1000 Sofia, Bulgaria
yorry77@mail.bg

1 Introduction

In this paper we consider series in functions of Mittag-Leffler type, namely in $z^\alpha E_\alpha(z)$ and $z^\beta E_{\alpha,\beta}(z)$. We study their convergence, more precisely, we determine where these series converge and where do not, where the convergence is uniform and where is not. The radius of their disks of convergence is found and the behaviour on the boundaries of these domains is studied. Namely, we provide theorems of Cauchy-Hadamard, Abel and Fatou type and compare them with the classical results for the more popular power series. Such kind of results are provoked by the fact that the solutions of some fractional order differential and integral equations can be written in terms of series (or series of integrals) of Mittag-Leffler type functions and their generalizations (as for example in Kiryakova [2] and Sandev, Tomovski and Dubbeldam [10]).

For our purpose we need the definitions of the Mittag-Leffler (M-L) functions

$$E_\alpha(z) = \sum_{k=0}^{\infty} \frac{z^k}{\Gamma(\alpha k + 1)}, \quad E_{\alpha,\beta}(z) = \sum_{k=0}^{\infty} \frac{z^k}{\Gamma(\alpha k + \beta)}, \quad \alpha > 0, \beta > 0, \quad (1.1)$$

and introduce the following auxiliary Mittag-Leffler functions, related to (1.1):

$$\tilde{E}_0(z) = 1; \quad \tilde{E}_n(z) = z^n E_n(z), \quad n \in \mathbb{N},$$

$$\tilde{E}_{\alpha,0}(z) = 1; \quad \tilde{E}_{\alpha,n}(z) = \Gamma(n)z^n E_{\alpha,n}(z), \quad n \in \mathbb{N}; \quad \alpha > 0, \quad (1.2)$$

where $\tilde{E}_0(z)$, $\tilde{E}_{0,\beta}(z)$ and $\tilde{E}_{\alpha,0}(z)$ are added just for completeness.

Then we consider simultaneously the series in these functions (1.2), respectively:

$$\sum_{n=0}^{\infty} a_n \tilde{E}_n(z), \quad \sum_{n=0}^{\infty} a_n \tilde{E}_{\alpha,n}(z), \quad (1.3)$$

and the power series

$$\sum_{n=0}^{\infty} a_n z^n \quad (1.4)$$

with same complex coefficients a_n ($n = 0, 1, 2, \dots$).

We give some results for series of the kind (1.3) in the general case, proven in [7], and consider their behaviour on an arc of the unit circle $|z| = 1$, all the points of which (including the ends) are regular to the sum of the series. Such type of results have been also obtained for series in other special functions, for example, for series in Laguerre and Hermite polynomials (in Rusev [9]), and in previous author's papers, resp. for systems of Bessel functions ([4]) and of some other special functions of fractional calculus which are fractional indices analogues of the Bessel functions, as the Bessel-Maitland functions ([5], [6]) and the multi-index Mittag-Leffler functions (in the sense of Kiryakova [1]), see e.g. [8].

2 Theorems of Cauchy-Hadamard and Abel type

In the beginning we give a theorem of Cauchy-Hadamard type and a corollary for every one of the above mentioned series.

Theorem 2.1. (of Cauchy-Hadamard type). *The domain of convergence of each of the series (1.3) and (1.4) with complex coefficients a_n is the disk $|z| < R$ with a radius of convergence $R = 1/\Lambda$, where*

$$\Lambda = \limsup_{n \rightarrow \infty} (|a_n|)^{1/n}. \quad (2.1)$$

More precisely, the series (1.3) and (1.4) are absolutely convergent on the disk $|z| < R$ and divergent on the domain $|z| > R$. The cases $\Lambda = 0$ and $\Lambda = \infty$ can be included in the general case, provided $1/\Lambda$ means ∞ , respectively 0 .

Corollary 2.1.1. *Let each of the series (1.3) and (1.4) converge at the point $z_0 \neq 0$. Then it is absolutely convergent on the disk $D = \{z : |z| < |z_0|, z \in \mathbb{C}\}$. Inside of the disk $|z| < 1/\Lambda = R$, i.e. on each closed disk $|z| \leq r < R$ (Λ defined by (2.1)), the convergence is uniform.*

So, it turns out that each of the M-L series (1.3), as well as the power series (1.4), converges in a disk with one and the same radius R , and diverges on its outside. Moreover, on each closed disk $|z| \leq r < R$, the convergence is uniform. The very disk of convergence is not obligatory a domain of uniform convergence and on its boundary the series may even be divergent.

Let $z_0 \in \mathbb{C}$, $0 < R < \infty$, $|z_0| = R$, g_φ be an arbitrary angular domain with size $2\varphi < \pi$ and with vertex at the point $z = z_0$, which is symmetric with respect to the straight line defined by the points 0 and z_0 , and d_φ be the part of the angular domain g_φ , closed between the angle's arms and the arc of the circle with center at the point 0 and touching the arms of the angle.

The next theorem refers to the uniform convergence on the set d_φ and the convergence at the point z_0 , provided $|z| < R$ and $z \in g_\varphi$.

Theorem 2.2. (of Abel type). *Let $\{a_n\}_{n=0}^\infty$ be a sequence of complex numbers, Λ be the real number defined by (2.1), $0 < \Lambda < \infty$. Let $K = \{z : z \in \mathbb{C}, |z| < R, R = 1/\Lambda\}$. If $f(z)$, $g(z)$, $h(z; \alpha)$ are the sums respectively of the series (1.4) and (1.3) on the domain K , i.e.*

$$f(z) = \sum_{n=0}^{\infty} a_n z^n, \quad g(z) = \sum_{n=0}^{\infty} a_n \tilde{E}_n(z), \quad h(z; \alpha) = \sum_{n=0}^{\infty} a_n \tilde{E}_{\alpha, n}(z); \quad z \in K,$$

and these series converge at the point z_0 of the boundary of K , then the series (1.3) and (1.4) are uniformly convergent on the domain d_φ . and

$$\lim_{z \rightarrow z_0} f(z) = \sum_{n=0}^{\infty} a_n z_0^n, \quad \lim_{z \rightarrow z_0} g(z) = \sum_{n=0}^{\infty} a_n \tilde{E}_n(z_0),$$

$$\lim_{z \rightarrow z_0} h(z; \alpha) = \sum_{n=0}^{\infty} a_n \tilde{E}_{\alpha, n}(z_0),$$

provided $|z| < R$ and $z \in g_\varphi$.

The proofs of Theorems 2.1 and 2.2, except for the uniformity, are given in [7], while the proofs of Corollary 2.1.1 and the uniformity will be given elsewhere.

3 Fatou type theorems

Let $\{a_n\}_{n=0}^\infty$ be a sequence of complex numbers with $\limsup_{n \rightarrow \infty} (|a_n|)^{1/n} = 1/R$, and

$f(z)$ be the sum of the power series $\sum_{n=0}^{\infty} a_n z^n$ on the open disk $U(0; R) = \{z : z \in \mathbb{C}, |z| < R\}$, i.e.

$$f(z) = \sum_{n=0}^{\infty} a_n z^n, \quad z \in U(0; R).$$

Definition 3.1. *A point $z_0 \in \partial U(0; R)$ is called regular for the function f if there exist a neighbourhood $U(z_0; \rho)$ and a function $f_{z_0}^* \in \mathcal{H}(U(z_0; \rho))$ (the space of complex-valued functions, holomorphic in the set $U(z_0; \rho)$), such that $f_{z_0}^*(z) = f(z)$ for $z \in U(z_0; \rho) \cap U(0; R)$.*

By this definition it follows that the set of regular points of the power series is an open subset of the circle $C(0; R) = \partial U(0; R)$ with respect to the relative topology on $\partial U(0; R)$, i.e. the topology induced by that of \mathbb{C} .

In general, there is no relation between the convergence (divergence) of a power series at points on the boundary of its disk of convergence and the regularity (singularity) of its sum of such points. For example, the power series $\sum_{n=0}^{\infty} z^n$ is divergent at each point of the circle $C(0; 1)$ regardless of the fact that all the points of this circle, except $z = 1$, are regular for its sum. The series $\sum_{n=1}^{\infty} n^{-2} z^n$ is (absolutely) convergent at each point of the circle $C(0; 1)$, but nevertheless one of them, namely $z = 1$, is a singular (i.e. not regular) for its sum. But under additional conditions, imposed on the sequence $\{a_n\}_{n=0}^{\infty}$, such a relation do exists (see for details [3], vol.1, ch. 3, §7, 7.3, p.357).

Proposition referring to the above discussed properties holds also for series in the Laguerre and Hermite systems (see e.g. [9]). Here we give such type of theorem for series in Mittag-Leffler systems.

First, we remind the classical results in this direction.

Theorem 3.1. (of Fatou). *Let $\{a_n\}_{n=0}^{\infty}$ be a sequence of complex numbers satisfying the condition $\limsup_{n \rightarrow \infty} (|a_n|)^{1/n} = 1$ and $f(z)$ be the sum of the power series (1.4) on the disk $D = \{z : z \in \mathbb{C}, |z| < 1\}$, i.e.*

$$f(z) = \sum_{n=0}^{\infty} a_n z^n, \quad z \in D.$$

Let σ be an arbitrary arc of the unit circle $|z| = 1$ with all its points (including the ends) regular to the function f (resp. g or h). Let $\lim_{n \rightarrow \infty} a_n = 0$. Then the power series (1.4) converges, even uniformly, on the arc σ .

A statement analogous to this classical result, concerning the considered series of the type (1.3), is given below.

Theorem 3.2. (of Fatou type). *Let $\{a_n\}_{n=0}^{\infty}$ be a sequence of complex numbers satisfying the condition $\limsup_{n \rightarrow \infty} (|a_n|)^{1/n} = 1$ and $g(z)$, $h(z; \alpha)$ be the sums respectively of the first and second of the series (1.3) on the disk $D = \{z : z \in \mathbb{C}, |z| < 1\}$, i.e.*

$$g(z) = \sum_{n=0}^{\infty} a_n \tilde{E}_n(z), \quad h(z; \alpha) = \sum_{n=0}^{\infty} a_n \tilde{E}_{\alpha, n}(z); \quad z \in D.$$

Let σ be an arbitrary arc of the unit circle $|z| = 1$ with all its points (including the ends) regular to the function g (or resp. h). Let $\lim_{n \rightarrow \infty} a_n = 0$ and $\tilde{E}_n(z) \neq 0$ (respectively $\tilde{E}_{\alpha, n}(z) \neq 0$) for $z \in \sigma$. Then the first (resp. second) of the series (1.3) converges, even uniformly, on the arc σ .

The proof will be given elsewhere.

Acknowledgement: This paper is supported by the Project ID 02/25/2009 of the NSF - Ministry of Education, Youth and Science of Bulgaria. It is performed also in the frames of the Bilateral Res. Project "Mathematical Modeling by Means of ..." between BAS and SANU (2012-2014), and Research Project "Transform Methods, Special Functions, Operational Calculi and Applications" at IMI - BAS.

References

- [1] V. Kiryakova, The special functions of fractional calculus as generalized fractional calculus operators of some basic functions, *Computers and Mathematics with Appl.*, **59**, No 3 (2010), 1128–1141, doi:10.1016/j.camwa.2009.05.014.
- [2] V. Kiryakova, Fractional order differential and integral equations with Erdélyi-Kober operators: Explicit solutions by means of the transmutation method. *AIP Conf. Proc.*, **1410** (2011), 247–258 (AMEE' 2011), doi:10.1063/1.3664376.
- [3] A. Markushevich, *A Theory of Analytic Functions*, Vols **1, 2** (In Russian), Nauka, Moscow, 1967.
- [4] J. Paneva-Konovska, Tauberian theorem of Littlewood Type for series in Bessel functions of first kind. *Compt. rend. Acad. bulg. Sci.*, **62**, No 2 (2009), 161-166.
- [5] J. Paneva-Konovska, Cauchy-Hadamard, Abel and Tauber type theorems for series in generalized Bessel-Maitland functions, *Compt. Rend. Acad. Bulg. Sci.*, **61**, No 1 (2008), 09-14.
- [6] J. Paneva-Konovska, Theorems on the convergence of series in generalized Lommel-Wright functions. *Fract. Calc. Appl. Anal.*, **10**, No 1 (2007), 59–74.
- [7] J. Paneva-Konovska, Series in Mittag-Leffler functions: inequalities and convergent theorems. *Fract. Calc. Appl. Anal.*, **13**, No 4 (2010), 403–414.
- [8] J. Paneva-Konovska, The convergence of series in multi-index Mittag-Leffler functions. *Integr. Transf. Spec. Funct.* **23**, Issue No 3 (2012), 207–221 doi: 10.1080/10652469.2011.575567.
- [9] P. Rusev, *Classical Orthogonal Polynomials and Their Associated Functions in Complex Domain*, Publ. House Bulg. Acad. Sci., Sofia, 2005.
- [10] T. Sandev, Ž. Tomovski, J. Dubbeldam, Generalized Langevin equation with a three parameter Mittag-Leffler noise. *Physica A*, **390**, Issue 21–22 (15 October 2011), 3627–3636, doi: 10.1016/j.physa.2011.05.039.

CNN COMPUTING OF THE INTERACTION OF FLUXONS IN MODIFIED SINE-GORDON EQUATION

Maya Markova

Department of Informatics
University of Russe
Russe 7000
e-mail:maya.markova@gmail.com

1 Introduction

In this paper we shall study the interaction of the physical object - quantum of magnetic flow, called fluxon. Fluxons are stable in the sense that they can be conserved, their direction can be changed and they can contact electronic devices. Their advantage is that they process information with a very high speed and with a very low energy supply. For this reason, fluxons have applications in information processing of electronic devices. In fact fluxons arise in the well known Josephson Junction (JJ) which is used in many applications in superconductor electronics [6]. The equations which describe JJ are the following:

$$I = I_0 \sin \varphi, \quad (1)$$

$$\frac{d\varphi}{dt} = \frac{2\pi}{\Phi_0} v, \quad (2)$$

where I is the lossless supercurrent flowing through the JJ, I_0 - its maximum value called critical current of the JJ, $\varphi(t) = \Theta_1 - \Theta_2$ is the difference between the phases of the complex pair wave functions of the both superconductors, v - the voltage drop over the junction, $\Phi_0 = 2.07mV.ps$ is a fundamental constant called single flux quantum (SFQ).

In the investigation of fluxons, the famous sin-Gordon equation:

$$\frac{\partial^2 \varphi}{\partial x^2} - \frac{\partial^2 \varphi}{\partial t^2} = \sin \varphi, \quad (3)$$

In the analysis of JJ more generalized form of equation (1) can be proposed:

$$I = I_0 \sin \varphi + [G_0(v) + G_1(v) \cos \varphi]v, \quad (4)$$

where G_1 and G_0 are rather complex functions of voltage and temperature. If we consider G_1 and G_0 constant, then equation (3) can be written as follows:

$$\begin{aligned} \frac{\partial^2 \varphi}{\partial x^2} - \frac{\partial^2 \varphi}{\partial t^2} - \alpha(1 + \varepsilon \cos \varphi) \frac{\partial \varphi}{\partial t} = \\ = \sin \varphi - \gamma, \end{aligned} \quad (5)$$

$\gamma, \Gamma \equiv G_0(\Phi_0/2\pi I_0 C)^{1/2} = \text{const} > 0$, $0 < \varepsilon \equiv G_1/G_0 \ll 1$, $\alpha \in [10^{-2}, 10^{-4}]$. If α is very small equation (5) is equivalent to (3). Equation (5) actually describes dissipation in JJ. From the point of view of the analysis it will be easier to consider $G_0 = g_0(v)$ and $G_1 = g_1(v)$, $g_0, g_1 = \text{const}$ to be of quadratic form.

In this paper we shall consider the interaction of the solutions of equation (5) called fluxons. We shall present Cellular Neural Network (CNN) computing for the interactions of fluxon-antifluxon and a pair of two fluxons. First we shall present the results from the physical point of view. Then we shall construct CNN model of the modified sine-Gordon equation. Finally we shall provide the simulation results and discuss the obtained results.

2 Fluxon solutions of modified sine-Gordon equation and their interaction

R.Parmentier pointed out in [3] that equation (5) has two different from physical point of view solutions - plasma waves corresponding to the

swing (oscillation) of the pendulum and fluxon waves corresponding to the rotation of the pendulum. We shall look for travelling wave solutions of the constant speed $c^2 < 1$. This way from (5) with $\varepsilon = 0$ we get:

$$\frac{d^2\varphi}{d\xi^2} - \alpha \frac{c^2}{1-c^2} \left(\frac{d\varphi}{d\xi}\right)^2 = \frac{\sin \varphi - \gamma}{1-c^2}. \quad (6)$$

The standard change $\frac{d\varphi}{d\xi} = p(\varphi)$ in (6) leads to:

$$\frac{1}{2} \frac{d}{d\varphi}(p^2) - \alpha \frac{c^2}{1-c^2} p^2 = \frac{\sin \varphi - \gamma}{1-c^2},$$

i.e. we have obtained a linear first order ODE with respect to p^2 and with independent variable φ . Then we must solve the ODE with separate variables $(\frac{d\varphi}{d\xi})^2 = F(\varphi)$ etc. Then we obtain the solution of the modified sine-Gordon equation (5): $\varphi = \arcsin \gamma_0 + 2\arcsin(cn(\frac{1}{k}(\frac{\gamma_0}{2\Gamma c^2})^{\frac{1}{2}}(\xi - \xi_0), k))$, where $k = (\frac{2\gamma_0}{\gamma + \gamma_0})^{1/2}$, $\gamma_0 = \frac{2\Gamma c^2}{((1-c^2)^2 + 4\Gamma^2 c^2)^{1/2}}$.

Our next step is to discuss the interaction of the fluxons-antifluxons from physical point of view. We are interesting now in finding solutions of (5) written in the form [2]:

$$\psi = f(x)g(t) = tg\frac{\varphi}{4}, \quad (7)$$

i.e. $\varphi = 4\arctg(f(x)g(t))$. Then the solutions of our modified sine-Gordon equations are:

$$\begin{aligned} \psi_a &\approx \frac{1}{c} \begin{cases} -e^{\frac{x-ct}{\sqrt{1-c^2}}}, & x \rightarrow -\infty, & (IV) \\ e^{-\frac{x-ct}{\sqrt{1-c^2}}}, & x \rightarrow \infty, & (II). \end{cases} \\ \psi_f &\approx \frac{1}{c} \begin{cases} e^{\frac{x+ct}{\sqrt{1-c^2}}}, & x \rightarrow -\infty, & (I) \\ -e^{-\frac{x+ct}{\sqrt{1-c^2}}}, & x \rightarrow \infty, & (III) \end{cases}. \end{aligned}$$

Antifluxons are monotonically decreasing and they are denoted by II and IV. Respectively, fluxons I and III are monotonically increasing.

We shall discuss briefly the interaction of a pair of two fluxons satisfying (5)(see Fig.2). The corresponding solution $\varphi(t, x)$ is given by the formula: $\varphi = 4\arctg \frac{1-ABC}{B+C} = 4\arctg \frac{\frac{BC}{B} - A}{\frac{1}{B} + \frac{1}{C}}$, where $A = \frac{1-c_1c_2 - \sqrt{1-c_1^2}\sqrt{1-c_2^2}}{1+c_1c_2 + \sqrt{1-c_1^2}\sqrt{1-c_2^2}}$,

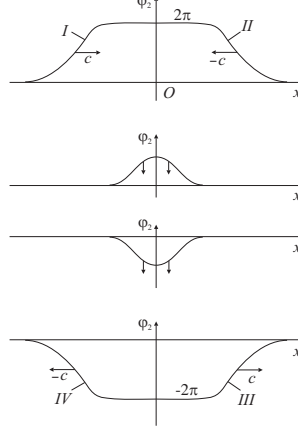


Fig.1. Interaction fluxon-antifluxon.

$0 < c_1, c_2 < 1$, $B = e^{-\frac{x-x_1-c_1 t}{\sqrt{1-c_1^2}}}$, $C = e^{-\frac{x-x_2-c_2 t}{\sqrt{1-c_2^2}}}$. After the collision with the second fluxon the first one gets the negative shift. Consequently, the slower fluxon moving to the right with velocity $c_1 > 0$ is shifting additionally backward. This way we conclude that after the collision the second fluxon gets the positive shift. Therefore, the faster fluxon moving to the right with velocity $c_2 > c_1 > 0$ is shifting additionally forward.

3 Cellular Neural Network computing of the interaction of fluxons

For solving modified sine-Gordon equation (5) spatial discretization will be applied. The equation is transformed into a system of ordinary differential equations which is identified as the state equations of a CNN with appropriate templates. We map $\varphi(x, t)$ into a CNN layer such that the state voltage of a CNN cell at a grid point is u_j . Let us consider one-dimensional CNN, where the CNN cells consist of a linear capacitor in parallel with a nonlinear inductor described by $i_j = f(\varphi_j) = \alpha(1 + \varepsilon \cos \varphi_j)u_j - \sin \varphi_j$ and where these cells are coupled to each other by linear inductors with inductance L . In terms of CNN circuit topology we can identify the following corresponding elements:

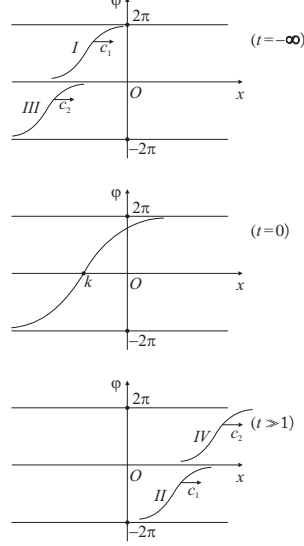


Fig.2. Interaction of a pair of fluxons.

1). CNN cell dynamics:

$$\frac{du_j}{dt} = \frac{1}{C}[I_j - f(\varphi_j)], \quad (8)$$

$$\frac{d\varphi_j}{dt} = u_j, 1 \leq j \leq N; \quad (9)$$

2). CNN synaptic law:

$$I_j = i_{L_j} - i_{L_{j+1}} = \frac{1}{L}(\varphi_{j-1} - 2\varphi_j + \varphi_{j+1}), \quad (10)$$

where $\varphi_j(t) = \int_{-\infty}^t u_j(\tau) d\tau$ is the flux-linkage at node j . Observe that the synaptic law (11) is a discrete Laplacian $A = [1, -2, 1]$ of the flux linkage φ_j .

Let us write the dynamics of our CNN model (8), (9), (10) in the following form:

$$\begin{aligned} \frac{du_j}{dt} = & (\varphi_{j-1} - 2\varphi_j + \varphi_{j+1}) - \\ & \alpha(1 + \varepsilon \cos \varphi_j)u_j - \sin \varphi_j \end{aligned} \quad (11)$$

$$\frac{d\varphi_j}{dt} = u_j, 1 \leq j \leq N.$$

We are looking for possible periodic state solutions of system (11) of the form [4]:

$$\varphi_{\Omega_0}(\omega_0) = \varphi_{m_0} \sin(\omega_0 t + j\Omega_0). \quad (12)$$

Because our CNN model (11) is a finite circular array of N cells we have finite set of spatial frequencies:

$$\Omega_0 = \frac{2\pi k}{N}, 0 \leq k \leq N - 1. \quad (13)$$

Remark 1. The relation between Cellular Neural Network (CNN) and the JTL array has been studied in many publications see for example [1],[6]. Two-dimensional array of Josephson Junctions is considered in [1]. Authors report the results of a Floquet analysis of such arrays of resistively and capacitively shunted JTLs in an external transverse magnetic field. The Floquet analysis indicates stable phase locking of the active junctions over a finite range of values of the bias current and junction capacitance, even in the absence of an external load.

4 Simulations and discussions

Simulating our CNN model (11) we obtain the following results. The solutions

$$\varphi_{\pm} = \pm 4 \arctg e^{\pm \frac{\xi - \xi_0}{\sqrt{1 - c^2}}} \quad (14)$$

are describing geometrically loops ξ varying from $\xi = -\infty$ to $\xi = +\infty$. If we take in both cases the sign " + " we obtain a positive loop, i.e. $\xi \in (-\infty, \infty) \Rightarrow \varphi \in (0, 2\pi)$, while if we take " - " in both cases we have again positive loop but $\xi \in (-\infty, +\infty) \Rightarrow \varphi \in (-2\pi, 0)$. The opposite signs give negative loops. Using a physical terminology: positive loops are fluxons and negative loops are antifluxons (Fig.3, Fig.4).

When the a pair of fluxons interact they can go through each other as a "double" solution (see Fig.5):

$$\varphi_D = 4 \arctg \left\{ \frac{sh[u(t - t_0)/\sqrt{1 - u^2}]}{uch[(x - x_0)/\sqrt{1 - u^2}]} \right\}, \quad (15)$$

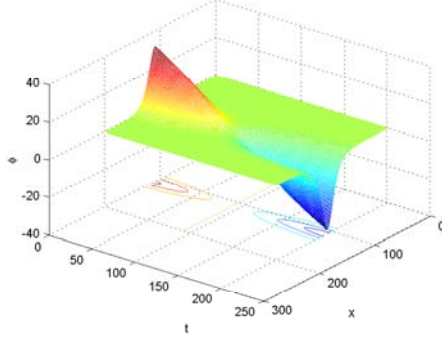


Fig.3.

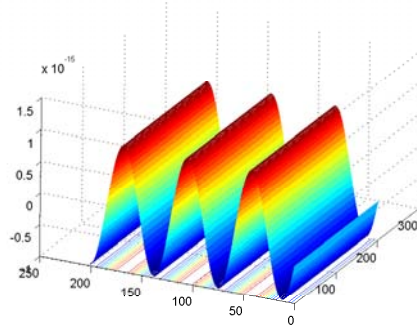


Fig.4.

or link in "breathon" having the form (see Fig.6):

$$\varphi_B = 4 \arctg \left\{ \frac{tg \nu \sin[(\cos \nu)(t - t_0)]}{ch[(\sin \nu)(x - x_0)]} \right\} \quad (16)$$

One can see that the slower fluxon moving to the right with velocity is shifting additionally backward. The faster fluxon moving to the right with velocity is shifting additionally forward.

Remark 2. We consider a CNN programmable realization allowing the calculation of all necessary processing steps in real time. The network parameter values of CNN model, described by the dynamical system (11), are determined in a supervised optimization process. During

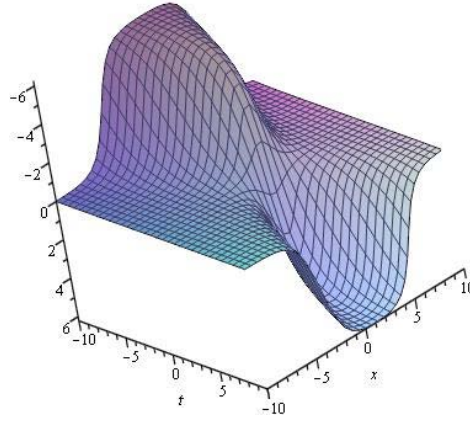


Fig.5.

the optimization process the mean square error is minimized using Powell method and Simulated Annealing [5]. The results are obtained by the CNN simulation system MATCNN applying 4th order Runge-Kutta integration.

5 Conclusions

In this paper we study the interaction of fluxons, which arise in Josephson Junction (JJ). We present theoretical results for the modified sine-Gordon equation from the physical point of view (Fig.1,2). Using the relation between Cellular Neural Network (CNN) and the JTL we obtain the corresponding CNN model. The obtain simulations (Fig.3,4,5,6) illustrate the proposed theoretical results.

REFERENCES

- [1] L. Fortuna, M.Frasca, A.Rizzo, "Self-organizing behavior of arrays of non identical Josephson junctions", 2002 IEEE International Symposium on circuits and systems, vol. 5, 2002, pp. 213-216.
- [2] G. Lamb, "Analytical descriptions of ultrashort optical pulse propagation in a resonant medium", Rev. Mod. Phys., vol. 43, 1971, pp. 99-124.

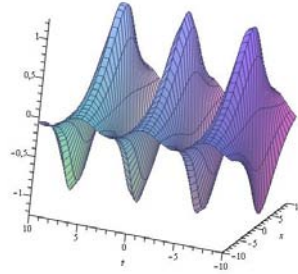


Fig.6.

[3] K. Lonngren, A. Scott, Eds., Solitons in action, Academic Press, 1978.

[4] A.Slavova, Cellular Neural Networks: Dynamics and Modelling, Kluwer Academic Publishers, 2003.

[5] R. Tetzlaff, F. Gollas, "Modeling complex systems by reaction-diffusion Cellular Nonlinear Networks with polynomial Weight-Functions", Proc. IEEE CNNA2005, 2005.

[6] B.Trees, D.Stround, "Two-dimensional arrays of Josephson junctions in a magnetic field: a stability analysis of synchronised states", Physical Review B, vol. 59, No. 10, March 1999, pp. 7108-7115

REVIEW ON ANALYTICAL APPROXIMATION FOR THE GENERALIZED LAPLACE'S EQUATION AND APPLICATIONS IN MULTISCALE MODELING

Rosangela F. Sviercoski

Institute for Information and
Communication Technologies, BAS
Acad. G. Bontchev str., bl. 25A
1113 Sofia, Bulgaria
rosviercoski@parallel.bas.bg

Many problems in science and engineering require the solution of the steady-state diffusion equation with a highly oscillatory diffusion coefficient. In this paper, we review an analytical approximation $\tilde{u}(x) \in L^p(\Omega)$, $1 \leq p \leq \infty$, for the generalized Laplace's equation $\nabla \cdot (K(x) \nabla u(x)) = 0$ in $\Omega \subset \mathbb{R}^n$, with some prescribed boundary conditions and where the diffusion coefficient function $K(x) \in L^p(\Omega)$ is defined as step function, not necessarily periodic.

By specifying the flow over the boundary of the given domain Ω , one way of quantifying the steady-state flow behavior in such a medium is by computing the solution $u(x) \in W^{1,p}(\Omega)$ of the generalized Laplace's Equation:

$$\nabla \cdot (K(x) \nabla u) = 0 \quad \text{in } \Omega \quad (1)$$

where the coefficient function $K(x)$ describes the heterogeneity of the medium over Ω , called the conductivity coefficient. In this paper, we study the case when the coefficient can be described generally as step function:

$$K(x) = \begin{cases} \xi_1 & \text{if } x \in \Omega_i \\ \xi_2 & \text{if } x \in \Omega \setminus \Omega_i \end{cases} \quad (2)$$

and (1) has some particular prescribed boundary conditions. We start by focusing on the case when $K(x)$ is periodic and the inclusions are symmetric, but general cases will also be considered. It is expected that a solution to (1) will depend on the type and smoothness of the coefficient function.

The first goal here is to review what has been done and further properties concerning an analytical approximation to a particular case of (1). The second is to try to motivate enthusiastic people to help by working on the problem.

The particular BVP that will be the center of the paper is the well known periodic cell-problem [9]. In the 2-dimensional case $i = 1, 2$ on a unit square:

$$\nabla \cdot (K(x) \nabla w_i(x)) = -\nabla \cdot (K(x) \nabla x_i) \quad \text{in} \quad \Omega = (0, 1)^1 \quad (3)$$

Note that there is $w_1(x)$ and the respective problem $w_2(x)$ in the x_2 direction. Note also that K(3) is a particular case of (1), by setting $u_1 = w_1 + x_1$, respectively $u_2 = w_2 + x_2$ and finally $u(x) = u_1(x) + u_2(x)$. The approximation $\tilde{w}_i(x) \in L^p(\Omega)$, for each $i = 1, 2$, from Sviercoski et al. [4] is given as:

$$\tilde{w}_i(x) = \int_0^{x_i} \frac{dx_i}{K(dx_i, x_j)} \left(\int_0^1 \frac{dx_i}{K(dx_i, x_j)} \right)^{-1} - x_i = u_i(x) - x_i \quad (4)$$

Consider, for a moment only $w_1(x_1, x_2)$ and the respective approximation $\tilde{w}_1(x)$. In this case, doing back substitution of (4) into (3), one has that:

$$\frac{\partial}{\partial x_1} \left(K(x) \frac{\partial \tilde{w}_1}{\partial x_1} \right) + \frac{\partial}{\partial x_2} \left(K(x) \frac{\partial \tilde{w}_1}{\partial x_2} \right) - \frac{\partial}{\partial x_1} (K(x) e_1) = -\frac{\partial}{\partial x_1} (K(x) e_1) \quad (5)$$

On the left hand side, the first term is zero and the second term may be extended continuously as zero, even though, it is not zero at the discontinuity points of $K(x)$ in the x_2 -direction.

Figure 1 illustrates the comparison between the approximation and the true solution.

One can also look at the comparison between the level curves from Figure 1, showing in Figure 2.

The challenge proposed here is that in order to obtain the respective solutions of the previous BVP's in $W^{1,p}(\Omega)$, one needs to identify a mollifier or a Green's function $\rho(x) = \rho(K(x)) \in C^\infty(\Omega)$ such that $\int_\Omega \rho(x) dx = 1$, to be able to apply the following result:

Lemma 1 *Let $w_1^h(x)$ be defined by the convolution:*

$$w_1^h(x) = h^{-n} \int_\Omega \rho_h(K(x - \zeta)) \tilde{w}_1(\zeta) d\zeta \quad (6)$$

with $h < \text{dist}(x, \partial\Omega)$. Then \tilde{w}_1 converges to $w_1^h \in W^{1,p}(\Omega)$ in the sense of $L^p(\Omega)$, $p < \infty$.

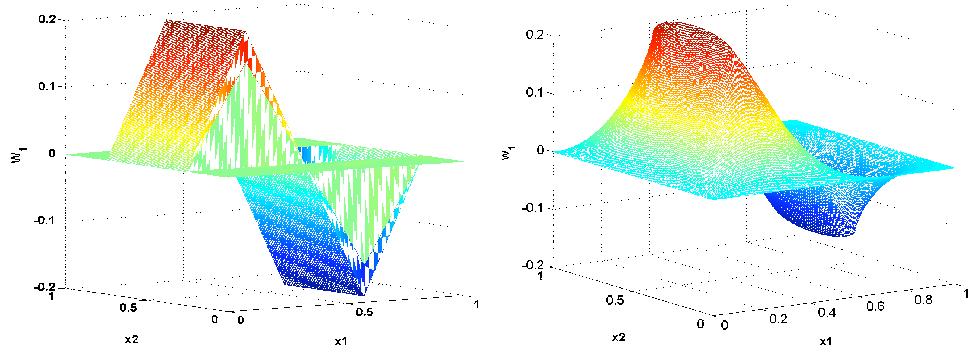


Figure 1: The approximation $\tilde{w}_1(x)$ **left** and the numerical $w_1(x)$ **right**, using $K(x)$ as in (2), with $\xi_1 = 10$ and $\xi_2 = 1$ with 1 square inclusion.

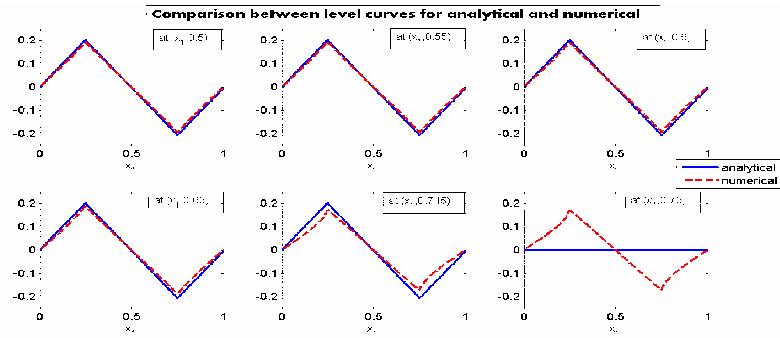


Figure 2: Comparison isolines between $\tilde{w}_i(x)$ and numerical $w_i(x)$, using $K(x)$ as in (2), with $\xi_1 = 10$ and $\xi_2 = 1$ with 1 square inclusion.

1 Homogenization and Multiscale Modeling

Among the many applications of the solution to equation (3) and of interest here is in the setting of homogenization and multiple scale analysis. For a throughout review on the subject, the reader is referred to [9].

In order to apply the results above, we set the macroscopic length scale, L , as the dimension of a reservoir, and l as the characteristic length of the medium. Then define the ratio $\varepsilon = \frac{l}{L}$, with x and $y = \frac{x}{\varepsilon}$ as the global and local variables. The coefficient and the solution have multiple scale and are assumed to be of the form $K^\varepsilon(x) = K(\frac{x}{\varepsilon}) = K(y)$ and $u(x, y) = u^\varepsilon(x)$. Hence, one looks for a solution given by the two-scale asymptotic expansion

$$u^\varepsilon(x) = u^0(x, y) + \varepsilon u^1(x, y) + h.o.t = u^0(x) + \sum_{i=1}^2 w_i(x) \frac{\partial u^0}{\partial x_i} + h.o.t \quad (7)$$

The Figure 3 illustrates a sequence of coefficients made out of periodic symmetrically centered square inclusions.

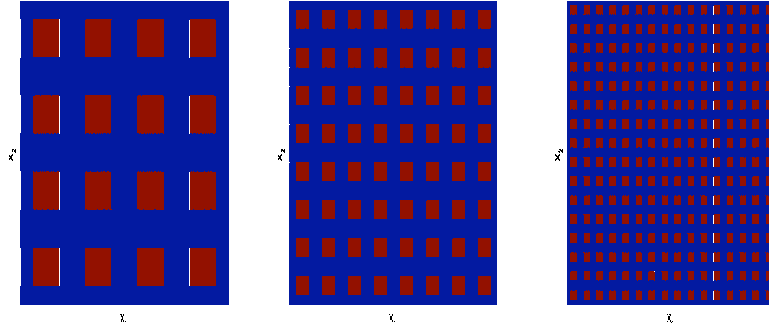


Figure 3: Sequence of $K^\varepsilon(x)$, with $\varepsilon = \frac{1}{4}, \frac{1}{8}, \frac{1}{16}$

The two-scale differentiation, $\nabla = \nabla_x + \varepsilon^{-1} \nabla_y$, is used in the substitution of $u^\varepsilon(x)$ into the BVP on the left of (8) to obtain, in the limit, the right one as:

$$\left\{ \begin{array}{ll} -\nabla \cdot (K^\varepsilon(x) \nabla u^\varepsilon(x)) = 1 & x \in \Omega \\ u^\varepsilon(x) = 0 & x \in \partial\Omega \end{array} \right. \quad \varepsilon \rightarrow 0 \quad \left\{ \begin{array}{ll} -\nabla \cdot (K^0 \nabla u^0(x)) = 1 & x \in \Omega \\ u^0(x) = 0 & x \in \partial\Omega \end{array} \right. \quad (8)$$

The upscaled or zeroth order solution $u^0(x)$ for the right hand side of (8) is obtained once the upscaled coefficient K^0 is found by:

$$K_{ij}^0 = \int_Y K(y) (\delta_{i,j} + \partial_{y_i} w_j(y)) dy \quad (9)$$

where each cell Y correspond to a subdomain of Ω , over which the solutions $w_1(y)$ and $w_2(y)$ for (3) are obtained and $\delta_{i,j}$ is the delta kronecker. The first medium from Fig. (3) can be seen as having 4 and the last 16 Y cells, for example. In this case, the cells are periodic and K^0 is computed only once, in contrast when the media is not periodic and K^0 needs to be computed for every different cell, as will be discussed on section 3.

The first result is that the direct substitution of (4) into (9) leads to the well known lower bound of K^0 , known here as \tilde{K} . Similarly, one can get the approximation to the dual cell problem, leading to the well known upper bound of the upscaled coefficient, \hat{K} . These bounds are the generalized Voigt-Reuss inequality (GVR) [9], and are summarized by:

$$\tilde{K} \leq K^0 \leq \hat{K}. \quad (10)$$

The lower bound is the arithmetic average of the harmonic average of $K(x)$ on each direction, whereas the upper bound is the harmonic of the arithmetic average of $K(x)$ on each direction. They are stricter and more accurate bounds than the classical Voigt-Reuss inequality given by the harmonic and arithmetic averages as lower and upper bounds of K^0 .

Other interesting results from [4] regards symmetrically centered inclusions, that turns out to be a key property in order to prove an additional properties of the approximation $\tilde{w}_i(x)$.

Theorem 1 *Let $\Omega = [0, 1]^2$ with $i, j = 1..2$. If $K(x)$ is periodic and, in addition to that it has its center of mass at $x = (\frac{1}{2}, \frac{1}{2})$, then the following can be proved:*

- (i) $\int_{\Omega} \tilde{w}_i(x) dx = 0$. *The zero mean property.*
- (ii) $\int_{\Omega} K(x) \frac{\partial \tilde{w}_i}{\partial x_j} dx = 0$ for $j \neq i$. *The off-diagonals of \tilde{K} , and respectively \hat{K} are zero.*
- (iii) $\int_{\Omega} \tilde{w}_i \tilde{w}_j dx = 0$ for $j \neq i$. *They are orthogonal.*

An Approximation to K^0 is proposed in Sviercoski [7]. The obvious motivation for seeking such an approximation comes from the high computational cost associated with computing K^0 numerically for real life applications. An illustration is shown in Figure 5, where in such a case, about 36 upscaled tensors are sought, which requires the numerical solution of about 72 problems such as described in 3. The approximation for the diagonal values are obtained by calculating the average between the arithmetic and geometric averages of bounds (10) above. The off-diagonals are derived using rotation of a diagonal matrix \mathbf{P} by an angle θ found by computing the center of mass of each cell. In 2-D, it is given as:

$$K^{\star} = \frac{1}{2} \begin{pmatrix} K_{11}^a + K_{11}^g & -b \sin(2\theta) \\ -b \sin(2\theta) & K_{22}^a + K_{22}^g \end{pmatrix} \quad (11)$$

There are two possible rotations, when the main diagonals of K^{\star} are equal or not. In each case, one can choose appropriately \mathbf{P} , and the coefficient b and also conditions on the angle θ to ensure that K^{\star} is a positive definite. An illustration of the

approximation, for the particular cases of square and circular inclusions with various heterogeneity ratio, is shown in Table 1.

square (ξ_1)	K^0	K^*	circular (ξ_1)	K^0	K^*
$1e-6$	$5.782e-1$	$5.8034e-1$	$1e-6$	$6.0789e-1$	$5.4600e-1$
$1e-5$	$5.782e-1$	$5.8035e-1$	$1e-5$	$6.0790e-1$	$5.4601e-1$
$1e-4$	$5.7827e-1$	$5.8042e-1$	$1e-4$	$6.0796e-1$	$5.4611e-1$
$1e-3$	$5.7896e-1$	$5.8109e-1$	$1e-3$	$6.0800e-1$	$5.4706e-1$
$1e-2$	$5.8575e-1$	$5.8770e-1$	$1e-2$	$6.1400e-1$	$5.5637e-1$
$1e-1$	$6.4799e-1$	$6.4890e-1$	$1e-1$	$6.6000e-1$	$6.6370e-1$
$1e+1$	$1.5452e+0$	$1.5475e+0$	$1e+1$	$1.5279e+0$	$1.5906e+0$
$1e+2$	$1.7117e+0$	$1.7176e+0$	$1e+2$	$1.6707e+0$	$1.8326e+0$
$1e+3$	$1.7323e+0$	$1.7386e+0$	$1e+3$	$1.6875e+0$	$1.8668e+0$
$1e+4$	$1.7343e+0$	$1.7408e+0$	$1e+4$	$1.6892e+0$	$1.8717e+0$
$1e+5$	$1.7345e+0$	$1.7410e+0$	$1e+5$	$1.6894e+0$	$1.8721e+0$
$1e+6$	$1.7346e+0$	$1.7410e+0$	$1e+6$	$1.6894e+0$	$1.8721e+0$

Table 1: A comparison between numerical K^0 and analytical K^* with varying ξ_1 and fixed $\xi_2 = 1$ from (2) with Ω_i as square and circular inclusions, occupying an area of $\frac{1}{4}$ of the cell, respectively. Note that error is below 10%, on average. Note also that the upscale coefficient approaches a limiting value as ξ_1 increases and decreases. The numerical values of K^0 for the circles were computed using triangular mesh, whereas for the analytical K^* , a rectangular mesh was used, with discretization size as 0.004. This might justify the larger errors between those values.

The first-order approximation of the solution to (8) on the left can also be estimated. While the zeroth order u^0 correspond to a smoothed out approximation of the true solution, the first-order representation from (7) adds heterogeneity to the solution through the cell solutions $w_i(x)$. In this case, the natural approximation is obtaining $u^*(x)$ by using K^* , instead of the true $u^0(x)$ and the $\tilde{w}_i(x)$. This has been done for linear and nonlinear cases in Sviercoski et. al [5, 6], where have been numerically demonstrated convergence properties. An illustration of those is shown in Figure 4.

1.1 Homogenization of Non-periodic Media

Even though theoretical results are generally in the context of periodic homogenization, the results follow for the case of non-periodic media. The reader interested in the mathematical formalism on this case, can consult Jikov et. al [9]. The Figure 5 illustrates the set up on a 2-D computational grid for a general non-periodic media. Observe also the potential high computational cost if one is interested in computing the numerical upscaled coefficient for the non-periodic case.

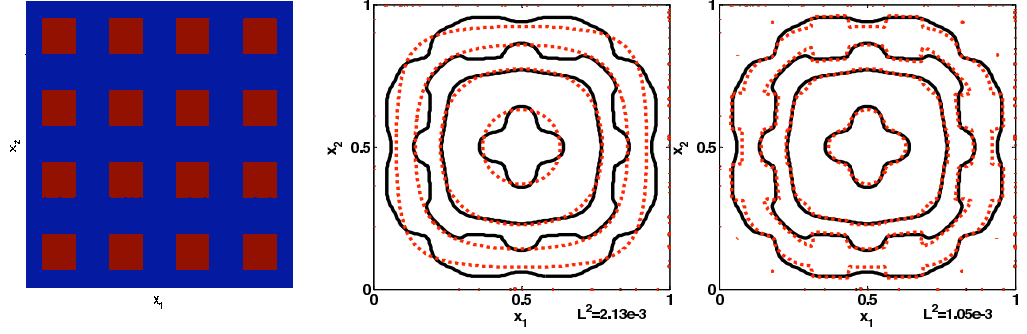


Figure 4: (Left): $K(x)$ from (2) with $\xi_1 = 10$ and $\xi_2 = 1$. (Center): Solid isolines are from the solution $u(x)$ and dashed ones come from the approximation $u^*(x)$ to (8). (Right): Dashed isolines are from $\tilde{u}^1(x)$, by using the first two terms of eq. (7). Note how $\tilde{u}^1(x)$ captures the heterogeneous features of $u(x)$, and also how the L^2 -error, shown at the bottom of the figures, drops by half when using $\tilde{u}^1(x)$ instead $u^*(x)$.

Example 1 was taken from [7] and illustrates the upscaled approximations to the following BVP on $\Omega = [0, 1]^2$, as:

$$\begin{cases} \nabla \cdot (K(x) \nabla u(x)) = 0 & x \in \Omega \\ u(0, x_2) = 10, \quad u(1, x_2) = 1 & x \in \partial\Omega \\ K(x) \frac{\partial u}{\partial \eta}(x_1, 0) = K(x) \frac{\partial u}{\partial \eta}(x_1, 1) = 0 & x \in \partial\Omega \end{cases} \approx \quad (12)$$

$$\begin{cases} \nabla \cdot (K^*(x) \nabla u^*(x)) = 0 & x \in \Omega \\ u^*(0, x_2) = 10, \quad u^*(1, x_2) = 1 & x \in \partial\Omega \\ K^* \frac{\partial u^*}{\partial \eta}(x_1, 0) = K^* \frac{\partial u^*}{\partial \eta}(x_1, 1) = 0 & x \in \partial\Omega \end{cases}$$

where $u(x)$ and $u^*(x)$ belong to $H^1(\Omega)$ and $K^*(x)$ is obtained from (11). In this example, the field $K(x)$ is a realization of a log-normal homogeneous stochastic process $Y(x, \omega) = \log(K(x, \omega))$, with expected value $E[Y(x, \omega)] = -1$ on a domain $\Omega = [0, 1]^2$. In this case, $Y(x, \omega)$ is a Gaussian process with covariance kernel given by:

$$R(x, y) = \sigma^2 \exp \left(-\frac{|x_1 - x_2|^2}{2L_1^2} - \frac{|y_1 - y_2|^2}{2L_2^2} \right) \quad (13)$$

The field is shown in Figure 6 (left), with standard deviation $\sigma = 4$ and correlation length in x -direction, $L_1 = 0.1$ and, $L_2 = 0.2$, the correlation in the y -direction. The minimum and maximum values of $K(x)$ are $4.1804e - 003$ and $2.3311e + 001$, respectively. The upscaled solutions were computed with 20×20 , 10×10 , 5×5 , upscaled tensors K^* , respectively. The results are illustrated in Figure 7 from left to right.

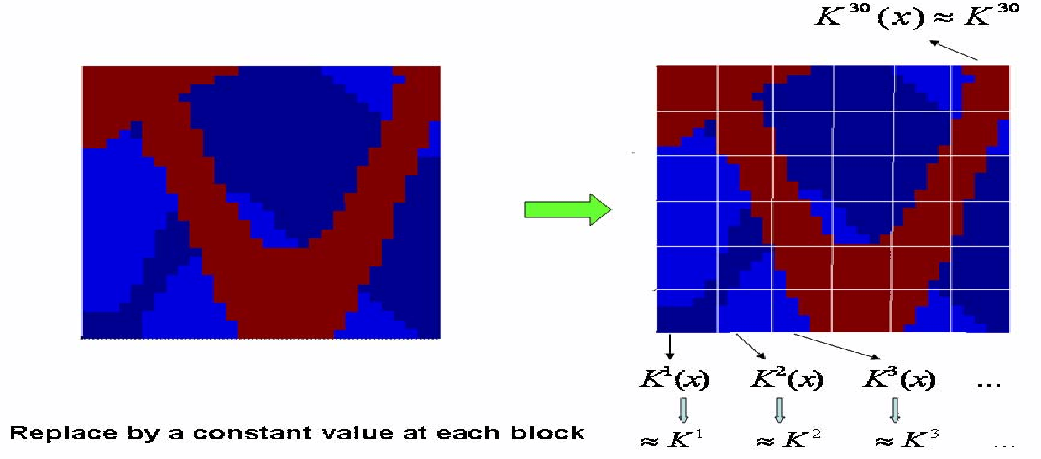


Figure 5: Example of a configuration where to apply the effective tensor on a 2-D computational grid, considering 6×6 upscaled tensors.

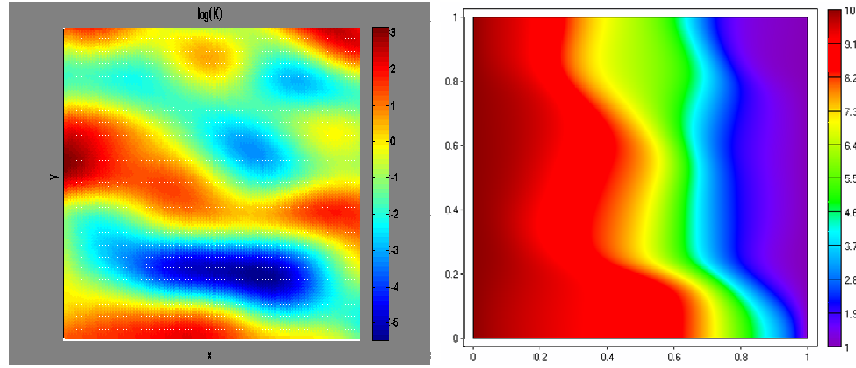


Figure 6: On the left, $\log(K(x, \omega))$ and respective heterogeneous solution of (12) in $\Omega = [0, 1]^2$.

2 Using the Approximations into Multilevel Numerical Methods

In this section, the coarse grid operator based on the analytical approximation to the homogenized tensor, K^* , is reviewed from [8]. The algorithm is an alternative to the

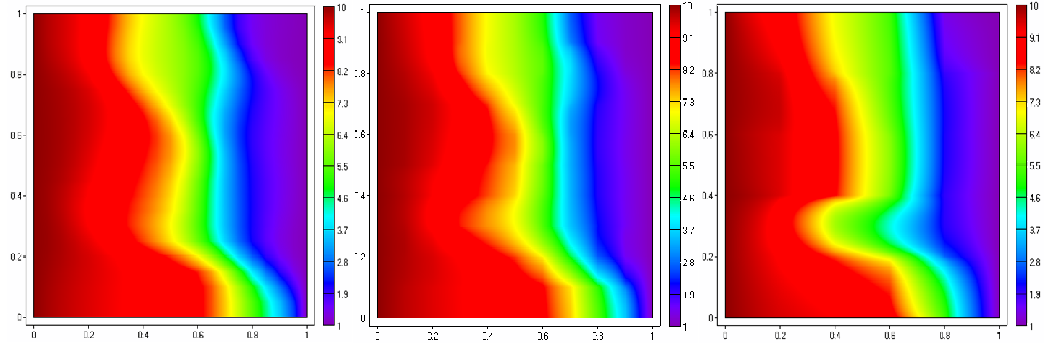


Figure 7: Results for Example 1 - From left to right the upscaled solutions using 20×20 , 10×10 , 5×5 , upscaled tensors K^* from left to right, respectively. Results for the error between these solutions and the heterogeneous from Figure 6 (right) are presented in Table 2. Note that the first graph approximates best the heterogeneous solution, as expected.

Number of Upscaled tensors	$\ u(x) - u^*(x)\ _2$	$\ \mathbf{v}(x) - \mathbf{v}^*(x)\ _2$
5×5	4.1785e-001	6.1118e+000
10×10	1.1949e-001	4.0393e+000
20×20	3.2306e-002	1.9502e+000

Table 2: Errors from refinement of the initial 5×5 upscaled tensors of the heterogeneous $K(x)$ illustrated on Figure 6 (left). Note that the rate at which the errors between the pressure solutions is decreasing is less than $r_u = 0.5$. The errors in the velocities are also decreasing at a rate less than $r_v = \sqrt{0.5}$.

classical geometrical multigrid applied to diffusion equations with variable coefficient such as eq. (8). The use of approximations of the upscaled coefficient, such as the arithmetic average and combination between arithmetic and harmonic averages are commonly used to define coarse grid operators in the literature. However, these averages are generally a rough approximation to the true upscaled coefficient, thus the use of a better one, such as K^* , comes as a natural application.

The algorithm follows by first defining a sequence of grids: $\Omega_0 \subset \Omega_1 \subset \dots \subset \Omega_h \subset \dots \subset \Omega$ together with the corresponding sequence of equations being discretized. The approximations K_0^*, K_1^*, \dots at each grid level leads to a sequence of linear operators from the coarse to fine level $L_0^* U_0 = f_0, \dots, L_H^* U_H = f_H, L_h U_h = f_h$, where a coarse-grid operator at a given level H , is:

$$(L_H^*)_{ij} = \int_{\Omega} \nabla \varphi_H^j K^* \nabla \psi_H^i dx \quad (14)$$

where $\{\varphi_H^j\}_{j=1}^{n_k}$ and $\{\psi_H^j\}_{j=1}^{n_k}$ are the test functions at that level.

Example 2- The goal is to show that the analytic coarse grid operator, ACO, derived using K^* , is a robust operator in the sense that it achieves better results than the widely used coarse operators derived using the arithmetic and/or harmonic averages, named here as ARCO and HCO respectively.

The case here was experiments presented were implemented to solve the left eq. (8) using rectangular finite elements (RFE) with size 63×63 , with 4 coarse subgrids and accuracy within $e = 09$. In this case, $K(x)$ has square inclusions such as illustrated on Figure (3) with the scale parameter $\varepsilon = \frac{1}{2}$ meaning that there are 2×2 square inclusions in the domain, $\varepsilon = \frac{1}{4}$ implies 4×4 inclusions, and so on. The number of Gauss-Siedel smoothing was fixed to be $\eta = 10$, obtained by simulating a comparable problem using numerical values. The intergrid operators are the standard full weight restriction and bilinear interpolation, like early works [1, 2].

Based on Table 3, the analytical ACO performed better than the arithmetic ARCO and harmonic HCO averages. The results also show that, unlike the other two, the ACO is nearly independent of ξ_1 and ε .

References

- [1] Alcouffe, R. E., Brandt, A., Dendy, J. E., Painter, J. W. *The Multi-grid Method for the Diffusion Equation with Stongly Discontinuous Coefficient*, SIAM J. Sci. Stat. Comput. (2), 4, pp. 430-454 (1981).
- [2] Enquist, B., Luo, E. *Convergence of a Multigrid Method Elliptic Equations with Highly Oscillatory Coefficients*, SIAM J. N. Anal. 34 (6), pp. 2254-2273 (1997).
- [3] Gilbarg, D., Trudinger, N.S. *Elliptic Partial Differential Equation of Second Order*, Springer Verlag (1983).

Sq. Inc	$\varepsilon = \frac{1}{2}$			$\varepsilon = \frac{1}{4}$			$\varepsilon = \frac{1}{8}$		
ξ_1	ACO	ARCO	HCO	ACO	ARCO	HCO	ACO	ARCO	HCO
$1E - 4$	13	15	\emptyset	14	19	\emptyset	15	21	\emptyset
$1E - 2$	13	15	\emptyset	14	18	\emptyset	15	21	\emptyset
$1E - 1$	14	15	14	18	21	14	15	19	25
$1e + 1$	17	26	20	17	28	15	17	34	14
$1E + 2$	18	113	17	24	128	47	22	220	19

Table 3: Comparison between the number of v-cycle iterations needed to solve eq. (8) (left). The sign \emptyset means that converge was not achieved with $\eta = 10$. The coefficient $K(x)$ has square inclusions occupying an area of $\frac{1}{4}$ of each cell and varying ξ_1 and fixed $\xi_2 = 1$. Observe how the analytical ACO performed better than the arithmetic ARCO and harmonic HCO averages. The results also show that, unlike the other two, the ACO is nearly independent of the contrast ratio and ε .

- [4] Sviercoski, R. F., Winter, C. L., Warrick, A.W. *Analytical Approximation for the Generalized Laplace's Equation with Step Function Coefficient*. SIAM Journal of Applied Mathematics vol. 68 (5) - pp. 1268-1281, (2008).
- [5] Sviercoski, R. F. , Travis, B. J., Hyman, J. M. *Analytical Effective Coefficient and First-Order Approximation for Linear Flow through Block Permeability Inclusions*. Comp. Math. Appl., 55, pp. 2118-2133, (2008).
- [6] Sviercoski, R. F., Popov, P., Travis, B. J., *A Zeroth and First-Order Homogenized Approximations to Nonlinear Diffusion through Block Inclusion by an Analytical Approach*. Comp. Meth. in Appl. Mechan. and Eng. DOI 10.1016/j.cma.2009.02.020 (2009).
- [7] Sviercoski, R. F. *An Analytical Effective Tensor for Flows through Generalized Composites*. Advances in Water Resources, 33(7), pp. 728-739, (2010).
- [8] Sviercoski et. al *Fast Multiscale Multigrid Methods - FastMM*, submitted.
- [9] Jikov, V. V., Kozlov, S.M., Oleinik, O.A. *Homogenization of Differential Operators and Integral Functionals*. Springer Verlag (1994).

APPLICATION OF FUZZY-NEURAL MODELING AND QUADRATIC PROGRAMMING FOR MODEL PREDICTIVE CONTROL

Yancho Todorov, Sevil Ahmed and Michail Petrov

Institute of Cryobiology and Food Technologies,
Agricultural Academy
53, Cherni Vrah blvd., 1407 Sofia, Bulgaria
Technical University-Sofia, branch Plovdiv,
25, Tsanko Dustabanov st., 4000 Plovdiv, Bulgaria
yancho.todorov@ikht.bg, sevil.ahmed@tu-plovdiv.bg,
mpetrov@tu-plovdiv.bg

1 Introduction

Model Predictive Control (MPC), refers to a class of algorithms which make explicit use of a process model to predict the future system state of a plant process and procedure to calculate an optimal control policy for the future system behavior, achieving a predefined goals by a cost function, while satisfying constraints. For more than 30 years, MPC has proved its success in many industrial applications due to the ease of constraints inclusion when formulate the controller algorithm.

This control technique, has reached great popularity in spite of the original lack of theoretical background concerning some crucial points such as stability and robustness. Originally, developed to cope with the control needs of power plants and petroleum refineries, it is currently successfully used in a wide range of applications, not only in the process industry but also other processes ranging from automotive to clinical anesthesia. Several recent publications provide a good introduction to theoretical and practical issues associated with the MPC technology [1-7]. The major reason for

the success of MPC algorithms consists in the intuitive way of addressing the control problem. Using the current states of the process as initials, at each sampling instant a finite horizon optimal control problem is solved over a prediction horizon.

A wide range of industrial processes is inherently nonlinear. For this purpose, several researchers have developed Nonlinear Model Predictive Control (NMPC) algorithms that work with different types of nonlinear models. A class of those models is based on empirical data, such as artificial Neural Networks (NN) and Fuzzy Logic (FL) models. Typical for this group is the precise description of the process by a set of linear sub-models. In this way the design of a MPC can be greatly simplified. Also, Fuzzy-Neural (FN) systems have been proved to be a promising approach to solve complex nonlinear control problems, which motivated many researchers to combine the advantages of NN and FL systems [8].

This contribution investigates the performances of a State-Space (SS) MPC based on FN models and implementations of optimization algorithms that realize *Quadratic Programming procedures*. The effectiveness of the proposed approaches is demonstrated by simulation experiments for process control of a pharmaceutical product lyophilization batch and an evaporator system.

2 Design of Fuzzy-Neural State Space models

As it is well known, the Takagi-Sugeno (TS) FN technique is suitable to model a class of nonlinear dynamic systems, which can be described in discrete time by a simple linear state-space model:

$$\left| \begin{array}{l} x(k+1) = f_x(x(k), u(k)) \\ y(k) = f_y(x(k), u(k)) \end{array} \right. \quad (1)$$

where $x(k)$, $u(k)$ and $y(k)$ are vectors of the state, the input and the output of the process and f_x and f_y are the nonlinear functions approximated by the TS type fuzzy rules.

The classical Hammerstein model consists of a series connection of a static nonlinearity and linear time invariant dynamics. Using the above mentioned TS technique and the ideas expressed in [9-10], we can obtain also a FN Hammerstein SS model by approximation of the static nonlinearity as a set of local linear simple systems in the following way:

$$\left| \begin{array}{l} x_1(k+1) = f_x(x_1(k), u(k)) \\ z(k) = f_z(x_1(k), u(k)) \end{array} \right. \quad (2)$$

where $x(k)$, $u(k)$ and $z(k)$ are vectors for the state, the input and the output of the nonlinear part of the model. Then the unknown nonlinear functions f_x and f_z are expressed as TS type fuzzy rules:

$$R^{(i)} : \text{if } r_1(k) \text{ is } M_1^{(i)} \text{ and } \dots r_p(k) \text{ is } M_p^{(i)} \text{ then } \left| \begin{array}{l} x_1(k+1) = A_1 x_1(k) + B_1 u(k) \\ z(k) = C_1 x_1(k) + D_1 u(k) + \vartheta \end{array} \right|^{(i)} \quad (3)$$

where R is the i -th rule of the rule base, r_p are the state regressors, M_i is a membership function of a fuzzy set, $A^{(i)}$, $B^{(i)}$, $C^{(i)}$ and $D^{(i)}$ are state-space matrices with dimensions: $A^{(i)} (n \times n)$, $B^{(i)} (n \times m)$, $C^{(i)} (q \times n)$ and $D^{(i)} (q \times m)$, where n is the number of system states, q is the number of the system outputs and system inputs for m , respectively. ϑ is a vector of free elements (offsets). The role of the model offsets is to compensate possible disturbances in the process [11]. In the same way this is done for the proposed general TS-SS model, where f_x and f_y represent the model structure. Afterwards, from a given input vector, the output of the FN Hammerstein model is inferred by computing the following equation:

$$\left| \begin{array}{l} x_1^{(i)}(k+1) = f_x^{(i)} g_u^{(i)} \\ z^{(i)}(k) = f_z^{(i)} g_u^{(i)} \end{array} \right| \quad \text{where } g_{ui} = \prod_{i=1}^N \mu_{ui} \quad (4)$$

where μ_{ui} are the degrees of fulfillment in notion to i -th activated fuzzy membership function. Thereafter, the linear part is flexibly introduced as:

$$\left| \begin{array}{l} x_2(k+1) = A_2 x_2(k) + B_2 z(k) \\ y(k) = C_2 x_2(k) + D_2 z(k) + \vartheta_1 \end{array} \right| \quad (5)$$

The same defuzzification manner can be used to infer the output of the general TS-SS model using the f_x and f_y functions.

Finally, the general Hammerstein model representation can be expressed as:

$$\left| \begin{array}{l} x_1(k+1) = \sum_{i=1}^N g_{ui} (A_1 x_1(k) + B_1 u(k)) \\ x_2(k+1) = \sum_{i=1}^N (A_2 x_2(k) + B_2 g_{ui} (C_1 x_1(k) + D_1 u(k) + \vartheta)) \\ y(k) = \sum_{i=1}^N (C_2 x_2(k) + D_2 g_{ui} (C_1 x_1(k) + D_1 u(k) + \vartheta) + \vartheta_1) \end{array} \right| \quad (6)$$

As well, for the used general TS State-Space model:

$$\left| \begin{array}{l} x(k+1) = \sum_{i=1}^N \bar{\mu}_{ui} (A x(k) + B u(k)) \\ y(k) = \sum_{i=1}^N \bar{\mu}_{ui} (C x(k) + D u(k) + \vartheta) \end{array} \right| \quad (7)$$

2.1 Learning algorithm for the designed models

The proposed learning algorithm lies on the minimization of an instant error measurement function $\Xi(k) = \varepsilon^2/2$ where $\varepsilon(k) = y(k) - \hat{y}(k)$, between the real plant output $y(k)$ and the model output $\hat{y}(k)$, calculated by the FN models. The algorithm performs two steps gradient learning procedure. Assuming that β_{si} is an adjustable s -th coefficient for the functions f into the i -th activated rule (3) as a connection in the output neuron, the general parameter learning rule for the consequent parameters is

$\beta_{si}(k+1)=\beta_{si}(k)+\eta(\partial\Xi/\partial\beta_i)$. After calculating the partial derivatives, the final recurrent predictions for each adjustable coefficient β_{si} ($a(i)$, $b(i)$, $c(i)$, $d(i)$ or $\vartheta(i)$) are obtained by the following equations: $\beta_{si}(k+1) = \beta_{si}(k) + \eta\varepsilon(k)\bar{g}_{ui}(k)r_p(k)$, $s = 1 \div \tilde{n} \times \tilde{n}$; $1 \div \tilde{n} \times \tilde{n}$; $1 \div \tilde{q} \times \tilde{n}$; $1 \div \tilde{q} \times \tilde{n}$ and $\vartheta_{si}(k+1) = \vartheta_{si}(k) + \eta\varepsilon(k)\bar{g}_{ui}(k)$, $s = 1 \div \tilde{q} \times \tilde{n}$. The output error Ξ can be used back directly to the input layer, where there are the premise (center - c_{pi} and the deviation - σ_{pi} of a Gaussian fuzzy set) adjustable parameters. The error Ξ is propagated through the links composed by the corresponded membership degrees where the link weights are unit. Hence, the learning rule for the second group adjustable parameters in the input layer can be expressed by the same learning rule:

$$\begin{aligned} c_{pi}(k+1) &= c_{pi}(k) + \eta\varepsilon(k)\bar{g}_{ui}(k)[f_y^{(i)}(k) - \hat{y}(k)] \frac{[r_p(k) - c_{pi}]}{\sigma_{pi}^2(k)} \\ \sigma_{pi}(k+1) &= \sigma_{pi}(k) + \eta\varepsilon(k)\bar{g}_{ui}(k)[f_y^{(i)}(k) - \hat{y}(k)] \frac{[r_p(k) - c_{pi}]^2}{\sigma_{pi}^3(k)} \end{aligned} \quad (8)$$

A similar learning procedure is applied to the general TS-SS model.

3 Model Predictive Control Strategy

Using the designed models, the optimization algorithm computes the future control actions at each sampling period, by minimizing the following cost function:

$$\begin{aligned} J(k) &= \sum_{i=N_1}^{N_2} \|\hat{y}(k) - r(k)\|^2 Q + \sum_{i=N_1}^{N_u} \|\Delta\hat{u}(k+1)\|^2 R \\ &\text{subject to } \Omega\Delta U \leq \gamma \end{aligned} \quad (9)$$

which can be expressed in vector form as: $J(k) = \|Y(k) - T(k)\|^2 Q + \|\Delta U(k)\|^2 R$, where Y is the matrix of the predicted plant output, T is the reference matrix, ΔU is the matrix of the predicted controls and Q and R are the matrices, penalizing the changes in error and control terms of the cost function. Taking into account the general prediction form of a linear state-space model (1), we can derive: $Y(k)=\Psi X(k)+\Upsilon u(k-1)+\Theta\Delta U(k)+\hat{\vartheta}$ where:

$$\Psi = \begin{bmatrix} \tilde{C} \\ \tilde{C}\tilde{A} \\ \tilde{C}\tilde{A}^2 \\ \vdots \\ \tilde{C}\tilde{A}^{N_2-1} \end{bmatrix} \quad \Upsilon = \begin{bmatrix} \tilde{D} \\ \tilde{C}\tilde{A} + \tilde{D} \\ \tilde{C}\tilde{A}^2 + \tilde{C}\tilde{A} + \tilde{D} \\ \vdots \\ \tilde{C}\sum_{i=N_1}^{N_2} \tilde{A}^i \tilde{B} + \tilde{D} \end{bmatrix} \quad (10)$$

$$\Theta = \begin{bmatrix} \tilde{D} & 0 & \dots & 0 \\ \tilde{C}\tilde{B} + \tilde{D} & \tilde{D} & & \vdots \\ \tilde{C}\tilde{A}\tilde{B} + \tilde{C}\tilde{B} + \tilde{D} & & \ddots & 0 \\ \vdots & & \ddots & \tilde{D} \\ \tilde{C}\sum_{i=1}^{N_2-2} \tilde{A}^i \tilde{B} + \tilde{D} & \dots & & 0 \\ \vdots & & \ddots & \vdots \\ \tilde{C}\sum_{i=1}^{N_2-1} \tilde{A}^i \tilde{B} + \tilde{D} & \dots & \tilde{C}\sum_{i=1}^{N_2-N_u-1} \tilde{A}^i \tilde{B} + \tilde{D} & \end{bmatrix} \quad (11)$$

Then we can define: $E(k) = T(k) - \Psi X(k) - \Upsilon u(k-1) - \vartheta$. This can be thought of as a tracking error, in sense of that it is the difference between the future target trajectory and the free response of the system, namely the response that would occur over the prediction horizon if no input changes were made - that is, if we set $\Delta U = 0$. Using the last notation, we can write: $J(k) = \Delta U^T H \Delta U + \Delta U^T \Phi + E^T Q E$, where $\Phi = 2\Theta^T Q E(k)$ and $H = \Theta^T Q \Theta + R$. Differentiating the gradient of J with respect to ΔU , gives the matrix of second order derivatives, or Hessian: $\partial^2 J(k) / \partial \Delta U^2(k) = 2H = 2(\Theta^T Q \Theta + R)$. If $Q(i) \geq 0$ for each i , this ensures that $\Theta^T Q \Theta \geq 0$. So, if $R \geq 0$ then the Hessian is certainly positive-definite, which is enough to guarantee that we have reached the minimum.

Linear constraints usually take place in the quadratic programming. Since, $U(k)$ and $Y(k)$ are not explicitly included in the optimization problem, the constraints can be expressed in terms of ΔU , as constraints on the amplitude of the control signal, on the output changes and on the rate change of the control signal.

3.1 Quadratic Programming

The problem of minimizing the cost function (10) is a quadratic programming problem. If H is positive definite, the problem is convex [11]. The solution is given by the closed form:

$$\Delta U = \frac{1}{2} H^{-1} \Phi \quad (12)$$

Therefore, the optimization problem can be rewritten as:

$$\begin{aligned} \min J(k) &= \Delta U^T H \Delta U - \Delta U^T \Phi + E^T Q E \\ \text{subject to } \Omega \Delta U &\leq \gamma \end{aligned} \quad (13)$$

The problem is still recognized as a QP problem, but in this formulation with linear inequality constraints (LICQP). Several of the most popular algorithms for constrained optimization are described in [12]. In the present study the active-set notation is used to solve the LICQP taking into account the above equations.

3.2 Hildreth Quadratic Programming

Solving an optimization problem in presence of inequality constraints requires the satisfaction of the KT conditions and evaluation the vector λ with the Lagrange multipliers. Using the active set notation the optimal solutions are based on primal decision variables which have to be identified along with the current active constraints. A major problem is the dimension of the set of constraints which impacts the computational load. To overcome this problem, a dual method is introduced in order to be identified constraints that are not active, so they can be eliminated in the solution. In this purpose a very simple programming procedure can be adopted for finding optimal solutions of constrained minimization problems [12]. The dual problem to the original primal problem is derived as follows. Assuming feasibility, the primal problem is equivalent to:

$$\begin{aligned} \max_{\lambda > 0} \min_{\Delta U} [\Delta U^T H \Delta U + \Delta U \Phi + E^T Q E + \lambda^T (\Omega \Delta U - \gamma)] \\ \Delta U = -H^{-1}(\Phi + \Omega^T \lambda) \end{aligned} \quad (14)$$

Substituting, the problem can be rewritten as:

$$\begin{aligned} \max_{\lambda > 0} (\lambda^T M \lambda - \lambda^T K + \Phi^T M^{-1} \Phi) \\ M = \Omega H^{-1} \Omega^T, K = \gamma + \Omega H^{-1} \Phi \end{aligned} \quad (15)$$

Thus, the dual is also a quadratic programming problem with λ as the decision variable:

$$\begin{aligned} \Delta U = -H^{-1} \Phi - H^{-1}(\Omega_{act} \lambda_{act}) \\ \min_{\lambda > 0} (\lambda^T M \lambda + \lambda^T K + \gamma^T M^{-1} \gamma) \end{aligned} \quad (16)$$

4 Case Studies

4.1 Lyophilization plant

On Fig. 1 a schematic diagram of the components of a lyophilization apparatus is shown. It consists of a drying chamber (1); temperature controlled shelves (2), a condenser (3) and a vacuum pump (4). The major purposes of the shelves are to cool/freeze or to supply heat to the product by the corresponding heating or refrigeration system (5). The product is placed on supportive product shelves (6) and the chamber is isolated from the condenser by the valve (7). The vacuum system is placed after condenser. The sublimation driving force pipes out the sublimed water from the product, which transforms back to ice on the condenser wall.

The product is loaded on the product shelves inside the chamber. When it is entirely frozen, the chamber is evacuated and the partial vapor water pressure difference increases between the frozen ice zone and the chamber, thus creating a natural driving force for the sublimation process. Then, the heating system starts to provide enthalpy to accelerate the sublimation, which occurs at the moving ice front and proceeds from the top of the frozen product downwards.

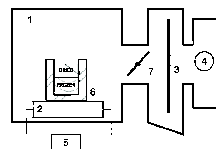


Figure 1: Schematic diagram of a lyophilization plant.

At the end of the primary stage of the process the major part of the water in the product has been removed and what remains is the portion of water constrained in the solution. At this point, the product can be unloaded, but the remaining water content is too high to be guaranteed its biological stability. For this purpose, to reduce the water content, the product is exposed at higher temperatures which induce the so called secondary drying stage of the freeze-drying process. In this study it is assumed

only the primary drying phase of a small scale apparatus, for drying 50 vials filled with glycine in water adjusted to pH 3, with hydrochloric acid [14].

4.2 Evaporator system

Fig. 2 presents a typical evaporation system. This kind of systems can be seen in industries like paper manufacturing and sugar production where evaporating solvent from a feed-stream is the main part of the production cycle. The main variable which needs to be controlled is the product composition X_2 , following the notation used in [15]. It is also necessary to operate the evaporator safely, and without damaging the installed equipment. This requires the pressure in the evaporator (P_2), and the level of liquid in the separator (L_2), to be controlled. There are three variables which we assume that can be adjusted in order to control the evaporator: the mass flow rate of the product being drawn off from the recirculating liquor (F_2), the pressure of the steam entering the evaporator (P_{100}) and the mass flow rate of the cooling water entering the condenser (F_{200}).

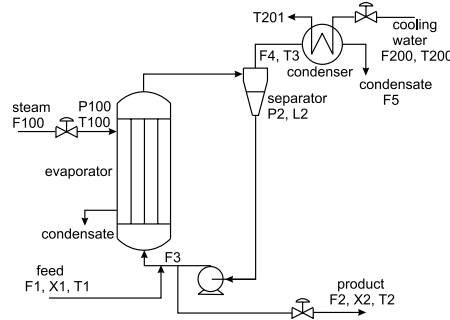


Figure 2: Schematic diagram of an Evaporator system.

These three variables will act as control inputs of the evaporator system. As it can be seen on (Fig. 2) there are several other variables which affect the evaporator performance (the feed flow rate (F_1), the circulating flow rate (F_3), the feed composition (X_1), the feed temperature (T_1), and the cooling water temperature (T_{200})). It is assumed that they are not under control and will act as measurable disturbances.

5 Discussion

5.1 Lyophilization plant control

Simulation experiments in Matlab/Simulink environments to control the heating shelves temperature in notion to temperature inside the frozen product layer, are made for a chosen value of the main diagonal of matrix R (Q is an identity matrix). In this case

the performance of a MPC algorithm based on FN-SS Hammerstein model and Hildreth Quadratic Programming procedure is investigated. *The following initial conditions for simulation experiments are assumed: $N_1=1$, $N_2=5$, $N_u=3$; system reference $r=255$ K; initial shelf temperature, before the start of the primary drying $T_{sin}=228$ K; initial thickness of the interface front $x=0.0023$ m; thickness of the product $L=0.003$ m.* In the primary drying stage it is required to maintain the shelf temperature about 298 K, until the product will be dried. This circumstance requires about 45 min of time for the primary drying stage of the process. *There are imposed the following constraints on the optimization problem:* on the amplitude of the control signal - the heating shelves temperature $228K < T_s < 298K$; on the output changes - product temperature $238K < T_2 < 256K$; and on the rate change of the control signal $0.5K < \dot{T}_s < 3K$. The temperature versus time profile of the product and heating shelf temperature for the representative vial is presented on Fig. 3. As it can be seen the process is driven as expected and the imposed constraints became active at certain point which guarantees the stability of the process and ensures the qualities of the product, without exceeding the physical and technological limitations for the assumed test product.

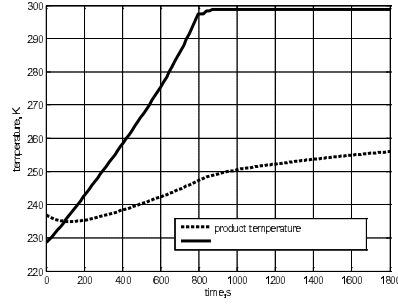


Figure 3: Product and heating shelves temperatures

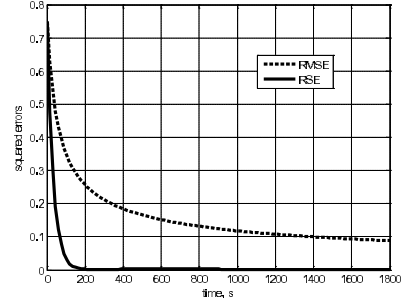


Figure 4: Root Squared Error and Root Mean Squared Error plots

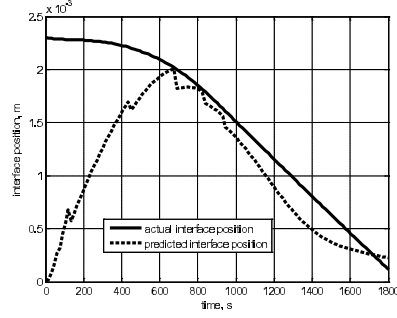


Figure 5: Interface position prediction x_1

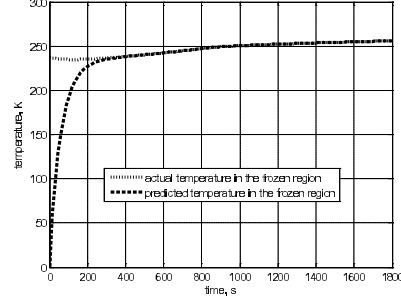


Figure 6: Frozen region temperature prediction x_2

On Fig. 5 is demonstrated the decrease of the frozen layer interface and its actual prediction by the model. The simulation results show good accordance between the predicted and the actual values with minimal error, which can be further reduced by additional experiments for selection of appropriate initial values of the rule consequent part coefficients. The prediction of the frozen region temperature is shown on Fig. 6. The presented results show a good prediction of this parameter which justifies its selection as process state used for product temperature prediction. The FN-SS Hammerstein model responses of the RMSE and RSE are shown on Fig. 4. The transient responses of the squared errors show the reliability of the chosen model structure in notion to its accuracy to predict the product temperature according to considered process states and limitations. They have a smooth nature and are successfully minimized during the learning process for the model. This circumstance proves again the proper operation of the predictive state space model and ensures a well driven lyophilization.

5.2 Evaporator system control

As well, in this case simulation experiments in the same computing environments are made with a MPC algorithm based on FN-SS Takagi-Sugeno model and Quadratic Programming procedure. The control system is configured with three manipulated variables u_1, u_2, u_3 : F2, P100 and F200; and three outputs y_1, y_2, y_3 : L2, X2 and P2 [16]. All manipulated variables are constrained as follows $0\text{ kg/min} \leq F2 \leq 4\text{ kg/min}$, $0\text{ kPa} \leq P100 \leq 400\text{ kPa}$ and $0\text{ kg/min} \leq F200 \leq 400\text{ kg/min}$. Simulation results with dynamic reference are shown on Fig. 7 and Fig. 8. The MPC tuning parameters used during the experiment are set to be as follow: $N_1=3$, $N_2=30$, $N_u=7$, weighting matrices $Q=\text{diag}(100, 0.1, 0.2)$ and $R=\text{diag}(10, 0.75, 0.1)$.

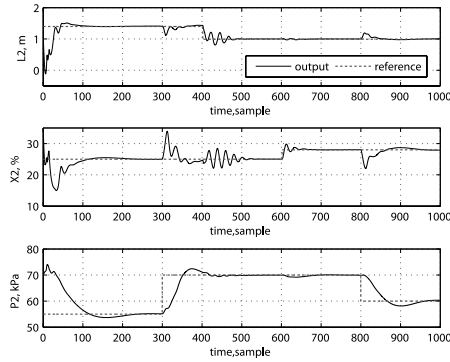


Figure 7: Outputs of the evaporator

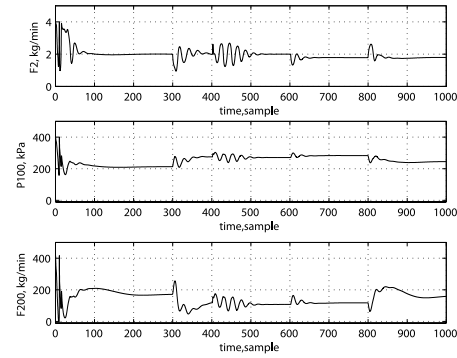


Figure 8: Inputs of the evaporator

It could be seen that the outputs of the system follow the changing setpoints without violating the constraints applied to the control inputs.

6 Conclusions

The simulation results show the efficiency of the proposed approaches, but its real time applicability has to be additionally studied taking into account some issues which cannot be considered in a simulation batch, as unmeasurable disturbances, possible system operation faults, type of the product and etc. Although, the State Space approach seems to be a promising solution for large scale plants, where the handling of the regime constraints is crucial and the system dynamic is relatively slow, which can accommodate with the computational procedures of the algorithms. A major advantage of the proposed control methodologies is the application of simple FN approach, which may impact the proper handling of some process uncertainties and disturbances.

References

- [1] J. Maciejowski, *Predictive Control with constraints*. Prentiss Hall (2002).
- [2] J. Rossiter, *Model based predictive control: A practical approach*. CRC Press (2003).
- [3] E. Camacho, C. Bordons, *Model Predictive Control*. Springer (2007).
- [4] D. Mayne, J. Rawlings, C. Rao, P. Scokaert, *Constrained model predictive control: Stability and Optimality*, Automatica, Vol. 36, No 4-5(2000), 789-814.
- [5] S. Qin, T. A. Badgwell, *A survey of industrial model predictive control technology*, Control Engineering Practice, Vol. 11, No. 7(2003), 733-764.

- [6] R. Findeisen, L. Imsland, F. Allgower, B.Foss, *State and output feedback nonlinear model predictive control: An overview*. European Journal of Control, Vol. 9, No. 2-3(2003), 190-206.
- [7] L. Magni, R. Scattolini, *Robustness and Robust Design of MPC for Nonlinear Discrete-Time Systems: Assessment and Future Directions*, Vol. 358, 239-254. Springer-Verlag Berlin Heidelberg (2007).
- [8] K. Passino, S.Yourkovic, *Fuzzy Control*. Adisson-Wesley (1998).
- [9] M. Terzyiska, Y. Todorov, M. Petrov, *Nonlinear Model Predictive Controller using a Fuzzy-Neural Hammerstein model*. In Proceedings of International conference Modern Trends in Control, Kosice, Slovakia (2006), 299-308.
- [10] Y. Todorov, M. Petrov, *Model Predictive Control of a Lyophilization plant: A simplified approach using Wiener and Hammerstein systems*. Journal of Control and Intelligent Systems, Vol. 39, No. 1(2011), 23-32.
- [11] V. Chitanov, M. Petrov, *Metavariable Fuzzy-Neural Model of Polymer Process*. The Berkeley Electronic Press, Chemical Product and Process Modeling, Vol. 4, No. 1(2009), article 10.
- [12] R. Fletcher. *Practical Methods of Optimization*, 2nd Edition, Wiley (2000).
- [13] L. Wang, *Model Predictive Control System Design and Implementation Using MATLAB*, Springer-Verlag, (2009).
- [14] M. Shoen, R. Jefferis III, *Simulation of a controlled freeze-drying process* International Journal of Modeling and Simulation, Vol. 20, No. 3(2000), pp. 255-263.
- [15] R. Newell, P. Lee, *Applied Process Control. A Case Study*, Prentice-Hall,(1989).
- [16] A. Taneva, M. Petrov, I. Ganchev. *Fuzzy Control of an Evaporator System*. 3rd International Symposium BIOINFO'07, Proceedings of International Conference Automatics and Informatics'07 Sofia, Bulgaria, Vol. III(2007), 61-64.

PART C:
LIST OF PARTICIPANTS

Gregory Agranovich

Dept. of Electrical and Electronic
Engineering,
Ariel University Center of Samaria,
44837 Ariel, Israel
agr@ariel.ac.il

Sevil Ahmed

Technical University-Sofia,
branch Plovdiv,
25, Tsanko Dustabanov st.,
4000 Plovdiv, Bulgaria
sevil.ahmed@tu-plovdiv.bg

Mary Aprahamian

School of Mathematics
Alan Turing Building
The University of Manchester
Manchester, M13 9 PL, UK
Mary.Aprahamian@
postgrad.manchester.ac.uk

Ana Avdzhieva

Department of Mathematics,
University of Sofia,
5 James Bourchier Boulevard,
1164 Sofia, Bulgaria
aavdzheva@fmi.uni-sofia.bg

Danail S. Brezov

University of Architecture,
Civil Engineering and Geodesy
1 Hristo Smirnenski Blvd.,
Sofia 1046, Bulgaria
e-mail: danail.brezov@gmail.com

Georgi Chobanov

Institute of Mathematics and
Informatics
Bulgarian Academy of Sciences
Sofia 1113, Bulgaria
chobanov@math.bas.bg

Stefka Dimova

Faculty of Mathematics and
Informatics
Sofia University
J.Baucher Blvd., 5
Sofia 1164, Bulgaria
dimova@fmi.uni-sofia.bg

Nina Dobrinkova

Institute for Parallel Processing, BAS
Acad. G. Bonchev str. bl.25A
1113 Sofia, Bulgaria

Assen Donchev

Department of Mathematics
University of Michigan
416 Fourth Street, 996-5250
USA
dontchev@umich.edu

Valentina Dyankova

Technical University Gabrovo
Gabrovo, Bulgaria

Stefka Fidanova

Institute for Parallel Processing, BAS
Acad. G. Bonchev str. bl.25A
1113 Sofia, Bulgaria
stefka@parallel.bas.bg

Krassimir Georgiev

Institute for Parallel Processing, BAS
Acad. G. Bonchev str. bl.25A
1113 Sofia, Bulgaria
georgiev@parallel.bas.bg

Vladimir Gerdjikov

Institute for Nuclear Research
and Nuclear Energy,
Bulgarian Academy of
Sciences,
72 Tzarigradsko chaussee,
1784 Sofia, Bulgaria

Todor Gramchev
Dipartimento di Matematica e
Informatica
Università di Cagliari
via Ospedale 72,
09124 Cagliari, Italy
todor@unica.it

Rossen Ivanov
School of Mathematical Sciences,
Dublin Institute of Technology,
Kevin Street, Dublin 8, IRELAND
Rossen.Ivanov@dit.ie

Stoyan Kapralov
Technical University of Gabrovo
Gabrovo, Bulgaria

Virginia Kiryakova
Institute of Mathematics and
Informatics
Bulgarian Academy of Sciences
Sofia 1113, Bulgaria
virginia@diogenes.bg

Jordanka Paneva-Konovska
Faculty of Applied Mathematics and
Informatics,
Technical University of Sofia,
8, Kliment Ohridski bul.,
1000 Sofia, Bulgaria
yorry77@mail.bg

Mihail Konstantinov
Department of Mathematics
University of Architecture, Civil
Engineering & Geodesy
1046 Sofia, Bulgaria
mmk_fte@uacg.bg

Nikolai Kutev
Institute of Mathematics and
Informatics

Bulgarian Academy of Sciences
Sofia 1113, Bulgaria
kutev@math.bas.bg

Nikodim Lazarov
Institute for Parallel Processing, BAS
Acad. G. Bonchev str. bl.25A
1113 Sofia, Bulgaria

Raicho Lazarov
Department of Mathematics, Texas A&M
University,
College Station, TX-77843, USA, and
Institute of Mathematics and Informatics,
Bulgarian Academy of Sciences,
Sofia, Bulgaria
lazarov@math.tamu.edu

Elena Litsyn
Department of Mathematics, Ben-Gurion
University of the Negev, Beer-Sheva, Is-
rael
elena.litsyn@weizmann.ac.il

Tony Lyons
School of Mathematical Sciences,
Dublin Institute of Technology,
Kevin Street, Dublin 8, IRELAND
Tony.Lyons@mydit.ie

Valentin Marinov
Institute for Parallel Processing, BAS
Acad. G. Bonchev str. bl.25A
1113 Sofia, Bulgaria

Pencho Marinov
Institute for Parallel Processing, BAS
Acad. G. Bonchev str. bl.25A
1113 Sofia, Bulgaria
pencho@parallel.bas.bg

Maya Markova
Department of Informatics

University of Russe
Russe 7000
maya.markova@gmail.com

Ivailo Mladenov
Institute of Biophysics,
Bulgarian Academy of Sciences
Acad. G. Bonchev Str., Bl. 21,
Sofia 1113, Bulgaria
mladenov@obzor.bio21.bas.bg

Clementina Mladenova
Institute of Mechanics,
Bulgarian Academy of Sciences
Acad. G. Bonchev Str., Bl. 4,
Sofia 1113, Bulgaria
clem@imbm.bas.bg

Geno Nikolov
Department of Mathematics,
University of Sofia,
5 James Bourchier Boulevard,
1164 Sofia, Bulgaria
geno@fmi.uni-sofia.bg

Mihail Petrov
Technical University-Sofia,
branch Plovdiv,
25, Tsanko Dustabanov st.,
4000 Plovdiv, Bulgaria
mpetrov@tu-plovdiv.bg

Petar Popivanov
Institute of Mathematics and
Informatics
Bulgarian Academy of Sciences
Sofia 1113, Bulgaria
popivano@math.bas.bg

Zarif Shapirov
Department of Mathematics,
University of Sofia,
5 James Bourchier Boulevard,

1164 Sofia, Bulgaria

Angela Slavova
Institute of Mathematics and
Informatics
Bulgarian Academy of Sciences
Sofia 1113, Bulgaria
slavova@math.bas.bg

Rosangela F. Sviercoski
Institute for Information and
Communication Technologies, BAS
Acad. G. Bontchev str., bl. 25A
1113 Sofia, Bulgaria
rosviercoski@parallel.bas.bg

Yancho Todorov
Institute of Cryobiology and
Food Technologies,
Agricultural Academy
53, Cherni Vrah blvd.,
1407 Sofia, Bulgaria
yancho.todorov@ikht.bg

Giorgia Tranquilli
Dipartimento di Matematica
e Informatica
Università di Cagliari
via Ospedale 72,
09124 Cagliari, Italy
tranquilli@unica.it

Vladimir Veliov
Institute of Mathematical Methods
in Economics,
Vienna University of Technology
Vienna, Austria
veliov@tuwien.ac.at